UNIVERSIDAD NACIONAL AUTÓNOMA DE MÉXICO

POSGRADO EN CIENCIAS BIOLÓGICAS

FACULTAD DE MEDICINA

ESTRUCTURA DEL GEN PARA LA SUPERÓXIDO DISMUTASA DE CU/ZN DE *Taenia solium* Y EL ANÁLISIS DE SU REGIÓN PROMOTORA

T E S I S

QUE PARA OBTENER EL GRADO ACADÉMICO DE

DOCTOR EN CIENCIAS

P R E S E N T A

JESUS RICARDO PARRA UNDA

TUTOR PRINCIPAL DE TESIS: DR ABRAHAM LANDA PIEDRA

COMITÉ TUTOR: DR JOSÉ PEDRAZA CHAVERRI

DR ROBERTO JOSÉ RAFAEL HERNANDEZ FERNANDEZ

MÉXICO, D.F. **MARZO, 2012**

UNAM
POSGRADO
Ciencias Biológicas

Dr. Isidro Ávila Martínez
Director General de Administración Escolar, UNAM
P r e s e n t e

Me permito informar a usted que en la reunión ordinaria del Comité Académico del Posgrado en Ciencias Biológicas, celebrada el día 28 de febrero de 2011, se aprobó el siguiente jurado para el examen de grado de **DOCTOR EN CIENCIAS** del alumno **PARRA UNDA JESÚS RICARDO** con número de cuenta 98552771 con la tesis titulada: : **"ESTRUCTURA DEL GEN PARA LA SUPEROXIDO DISMUTASA DE Cu/Zn DE *Taenia solium* Y EL ANÁLISIS DE SU REGIÓN PROMOTORA".** realizada bajo la dirección del**: DR. ABRAHAM LANDA PIEDRA**

Presidente:	DRA.	MARÍA IMELDA LÓPEZ VILLASEÑOR
Vocal:	DR.	ROBERTO JOSÉ RAFAEL HERNÁNDEZ FERNÁNDEZ
Secretario:	DRA.	BERTHA ESPINOZA GUTIÉRREZ
Suplente:	DR.	VÍCTOR MANUEL VALDÉS LÓPEZ
Suplente:	DR.	LUIS FELIPE JIMÉNEZ GARCÍA

Sin otro particular, me es grato enviarle un cordial saludo.

A T E N T A M E N T E
"POR MI RAZA HABLARA EL ESPIRITU"
Cd. Universitaria, D.F., a 07 de marzo de 2012

M. del Coro Arizmendi

DRA. MARIA DEL CORO ARIZMENDI ARRIAGA
COORDINADORA DEL PROGRAMA

Edif. de Posgrado P. B. (Costado Sur de la Torre II de Humanidades) Ciudad Universitaria C.P. 04510 México, D.F.
Tel. 5623-0173 Fax: 5623-0172 http://pcbiol.posgrado.unam.mx

Agradezco al Posgrado en Ciencias Biológicas, UNAM.

Asimismo, el autor de este trabajo recibió una beca para la realización de sus estudios de Doctorado del Programa de becas del CONACyT (Número de Becario: 169062), en el posgrado de Ciencias Biológicas de la Universidad Nacional Autónoma de México.

El proyecto fue apoyado por el Consejo Nacional de Ciencia y Tecnología (CONACyT) con el contrato 80134-M y por la Dirección General de Asuntos del Personal Académico.

Programa de apoyo a Proyectos de Investigación e Innovación Tecnológica (PAPIIT) con el contrato IN206708-3 y IN207507-3.

Esta tesis se realizó en el Laboratorio de Biología Molecular de *Taenia solium*. Depto. de Microbiología y Parasitología, Facultad de Medicina, Edificio A, 2do piso, Universidad Nacional Autónoma de México, Ciudad Universitaria, México D.F. 04510, México.

AGRADECIMIENTOS

Agradezco al Dr. Abraham Landa por la confianza depositada en mí para realizar todos los proyectos, por la amistad, empeño y dedicación de su tiempo y espacio personal para mi formación profesional. Aprendí de su pasión por la ciencia.

Agradezco al Dr. José Pedraza por asesoría científica, así como por sus consejos y apoyo personales. Su dedicación y forma de ejercer como científico, me sirven de inspiración y ejemplo.

Agradezco al Dr. Roberto Hernández, por su apoyo, observaciones y sugerencias, que enriquecieron mi aprendizaje. Su enseñanza es parte importante en mi formación académica y científica.

Agradezco mucho a los investigadores que leyeron esta tesis: Dra. María Imelda Lopéz Villaseñor, Dra. Bertha Espinoza Gutierrez, Dr. Victor Manuel Valdés López, Dr. Luis Felipe Jiménez García, Dr. Roberto Herneńdez Fernandez, Dr. José Pedraza Chaverrí y Dra. Kaethe Willms Manning. Sus sugerencias y comentarios fueron muy importantes en la etapa final de mi formación.

Agradezco a mis compañeros del laboratorio: Dr. Felipe Vaca Paniagua, C. a Dr. Victor Sanabria Ayala, Dra Anayetzin Torres, M. en C. Alicia Ochoa Sánchez, Dra. Lucía Jímenez, QFB. Oscar Rodriguez, M. en C. Aramis Roldán, Dra Gabriela Nava, Dr. Ponciano García. Gracias por compartir sus conocimientos, tristezas, gustos personales, secretos de laboratorio, momentos de amistad y alegría.

Agradezco a la Universidad Nacional Autónoma de México, por darme el privilegio de estudiar y tener acceso a excelentes académicos, científicos que nos ayudan a crecer y hacer crecer a nuestro país.

A Rosa María y Ricardo

A Adri, por apoyarme, entender y ser parte importante en este proyecto.

COMITÉ TUTORAL:

Dr. Abraham Landa Piedra

Dr. José Pedraza Chaverri

Dr. Roberto José Rafael Hernández Fernández

JURADO:

PRESIDENTE: Dra. María Imelda López Villaseñor

VOCAL: Dr. Roberto José Rafael Hernández Fernández

SECRETARIO: Dra. Bertha Espinoza Gutiérrez

SUPLENTE: Dr. Luis Felipe Jiménez García

SUPLENTE: Dr. Víctor Valdés López

CONTENIDO

LISTA DE ABREVIATURAS

°C	Grados centígrados
ABZ	Albendazol
ADN	Ácido Desoxiribo Nucleíco
cm	Centímetro (s)
Cu,Zn-SOD	Superóxido Dismutasa de Cu/Zn
DAB	Diaminobencidina
EOx	Estrés Oxidante
ER	Especies reactivas
EROs	Especies Reactivas de Oxígeno
FaDH2	Flavín mononucleótido en forma de quinona
FMNH2	Flavín mononucleótido en forma reducida
GST	Glutatión transferasa
H_2O_2	Peróxido de hidrógeno
$HO_2^{\cdot}$	Hidroperoxilo
IPTG	Isopropil-β-D-tiogalactosido
kDa	KiloDaltones
Kg	Kilogramos
LCR	Líquido Céfalo Raquídeo

m	Metro (s)
M	Molar
MBZ	Mebendazol
mg	Miligramos
min	Minutos
mL	Mililitros
mm	Milímetro (s)
mM	Milimolar
MTZ	Metronidazol
NADPH	Nicotinamida adenina dinucleótido fosfato
ng	Nanogramos
nm	Nanómetros
NO	Óxido nítrico
$O_2^{\cdot -}$	Anión superóxido
O_3	Ozono
$OH^{\cdot}$	Ión hidroxilo
$ONOO^-$	Peroxinitrito
PCR	Reacción en Cadena de la Polimerasa
pH	potencial de iones hidrógeno

PRX	Peroxiredixinas
PZQ	Prazicuantel
RM	Resonancia magnética
SSA	Solución Salina Amortiguadora
SDS	Dodecil sulfato de sodio
SOD	Superóxido Dismutasa
TC	Tomografía computarizada
Tris	Tris (hidroximetol) aminometano
U	Unidades
v/v	Volumen en Volumen
µg	Microgramos
µL	Microlitros
µm	Micrómetro
µM	Micromolar

ABSTRACT

Cytosolic Cu,Zn superoxide dismutase (Cu,Zn-SOD) catalyzes the dismutation of superoxide ($O_2^{\cdot-}$) to oxygen and hydrogen peroxide (H_2O_2) and plays an important role in the establishment and survival of helminthes in their hosts. In this work, we describe the *Taenia solium* cytosolic Cu,Zn-SOD gene (TsCu,Zn-SOD) and a *Taenia crassiceps* (TcCu,Zn-SOD) cDNA. TsCu,Zn-SOD gene spans 2.841 kb, and has three exons and two introns; the splicing junctions follow the GT-AG rule. Analysis *in silico* of the gene revealed that the 5´-flanking region has three putative TATA and CCAAT boxes, and transcription factor binding sites for NF1 and AP1. The transcription start site was a C, located 22 nucleotides upstream of the translation start codon (ATG). Southern blot analysis showed that TcCu,Zn-SOD and TsCu,Zn-SOD genes are single copy genes. The derivated amino acid sequences of TsCu,Zn-SOD gene and TcCu,Zn-SOD cDNA reveal an identity 98.47%, as well as the characteristic motives, including the catalytic site and β -barrel structure of the Cu,Zn-SOD.

Proteomic and immunohistochemical analysis indicated that Cu,Zn-SOD does not have isoforms, is distributed throughout the bladder wall and concentrated in the tegument of *T. solium* and *T. crassiceps* cysticerci. Expression analysis revealed that TcCu,Zn-SOD mRNA and protein levels do not change in cysticerci, even upon exposure to $O_2^{\cdot-}$ (0–3.8 nmol/min) and H_2O_2 (0–2 mM), suggesting that this gene is constitutively expressed in these parasites.

RESUMEN

La superóxido dismutasa citosólica de Cu,Zn (Cu,Zn-SOD) cataliza la dismutación de ($O_2^{\cdot-}$) a oxígeno y peróxido de hidrógeno (H_2O_2) y desempeña un papel importante en el establecimiento y sobrevivencia de helmintos en el hospedero. En este trabajo describimos el gen de Cu,Zn-SOD de *T. solium* (*TsCu,Zn-SOD*) y un ADN complementario de *T. crassiceps* (*TcCu,Zn-SOD*). El gen *TsCu,Zn-SOD* mide 2.841 Kb, contiene 3 exones y 2 intrones; las uniones de corte y empalme de los intrones cumplen con la regla GT-AG. El análisis *in sílico* reveló que la región 5´ que flanquea el gen presenta tres cajas TATA y CCAAT putativas, así como sitios de unión a los factores de transcripción NF1 y AP1. El sitio de inicio de la transcripción es C, localizado a 22 nucleótidos rio arriba del codón de inicio de la traducción (ATG). El análisis de Southern blot reveló que los genes *TcCu,Zn-SOD* y *TsCu,Zn-SOD* están codificados por un gen de copia única. La secuencia de aminoácidos de *TcCu,Zn-SOD;* derivada de la secuencia nucleótidica presentó un 98.47% de identidad con *TsCu,Zn-SOD*, y los motivos característicos de esta enzima, incluyendo el sitio catalítico y la estructura de barril–β de la Cu,Zn-SOD.

Los análisis proteómicos e inmunohistoquímicos indican que la TsCu,Zn-SOD no presenta isoformas; que está distribuida en toda la pared vesicular y concentrada en el tegumento de los cisticercos de *T. solium* y *T. crassiceps*. Los análisis de expresión revelaron que los niveles de ARN mensajero y proteína de TcCu,Zn-SOD no cambian en los cisticercos expuestos a $O_2^{\cdot-}$ (0-3.8 nmol/min) y H_2O_2 (0-2 mM), sugiriendo que este gen se expresa constitutivamente en estos parásitos.

JUSTIFICACIÓN

El parásito tiene una predisposición particular por afectar el sistema nervioso, produciendo la enfermedad denominada neurocisticercosis. Esta es la enfermedad parasitaria más frecuente del sistema nervioso central, representando una patología neurológica común, así como un serio problema de salud pública en diferentes países de América Latina, África y Asia [1,2,3].

Debido al pleomorfismo clínico de la neurocisticercosis, no es posible que un solo esquema de tratamiento sea útil en todos los casos. El tratamiento es sintomatológico y debe estar diseñado para cada paciente con antiepilépticos, analgésicos, corticosteroides o una combinación de ellos. Se utilizan de manera rutinaria antihelmínticos (prazicuantel y albendazol), en dosis específicas para el tratamiento.Por lo tanto, la caracterización precisa de la enfermedad, en lo que respecta a viabilidad y localización de las lesiones, es de fundamental importancia con el objeto de planificar un tratamiento adecuado [4].

Las medidas para el control de la cisticercosis/taeniosis, se han dividido en dos estrategias: las educativas y las de intervención. Las primeras han consistido en la realización de campañas educativas que se enfocan en la difusión de información que disminuye el contagio con el parásito, como son: hábitos higiene, cocimiento de la carne, identificación del la carne infectada, evitar fecalismo al aire libre. Sin embargo factores socioeconómicos y culturales han influido para que este tipo de campañas educativas no tengan el impacto esperado en la población. En cuanto a las medidas de intervención se ha propuesto una inspección más estricta en la carne, pero esto solo se da en rastros de las grandes ciudades, y no en las zonas rurales, que es donde existe

una mayor incidencia de cisticercosis [5]. Otra opción es el uso periódico de cestocidas (Prazicuantel, Flubendazol, niclosamida) en áreas de alta prevalencia, lo cual resulta costoso y no previene la reinfección, además de los efectos secundarios que pueden causar estos fármacos en el organismo [6].

Actualmente en helmintos el desarrollo de vacunas y fármacos específicos está siendo dirigido hacia la identificación de blancos enzimáticos indispensables para la supervivencia de los parásitos, o bien de moléculas relacionadas con los mecanismos de protección [7]. Un mecanismo de defensa que el huésped utiliza en contra de los parásitos, se da por la reacción del sistema inmune a través de macrófagos, eosinófilos y neutrófilos, los cuales responden en contra de los parásitos produciendo especies reactivas de oxígeno (EROs) primarios durante la explosión respiratoria. Las SODs tienen un papel muy importante en la defensa del parásito en la respuesta inmune del hospedero. La caracterización del gen nos permitirá conocer mejor la biología del parásito, su papel en el mecanismo de defensa y nos ayudará a desarrollar estrategias para poder eliminar el parásito.

ANTECEDENTES

En nuestro laboratorio estamos interesados en el análisis integral de enzimas del metabolismo de estrés oxidante de *T. solium* que pueden ser utilizadas como blancos farmacológicos o en el desarrollo de estrategias para dañar o eliminar al parásito.

En nuestro laboratorio se ha llevado a cabo un trabajo en colaboración con la UAM iztapalapa y el Instituto de Química de la UNAM, para poder usar a la superóxido dismutasa de Cu/Zn como blanco para causar daño al parásito. Los antecedentes directos de la realización de este trabajo se encuentran en las tesis *"Taenia solium*: superóxido dismutasa recombinante de Cu/Zn; su purificación y caracterización parcial" (Facultad de química UNAM), y "Variación de la expresión del gen para la Superóxido dismutasa Cu/Zn de *Taenia crassiceps* bajo condiciones de estrés oxidativo" (Facultad de Medicina UNAM, Posgrado en Ciencias Biológicas; Jesús Ricardo Parra Unda).

Previamente se clonó, purificó y caracterizó la enzima, y se observó que puede ser inhibida por antihelmínticos como el albendazol [8]. Con los métodos de expresión y purificación desarrollados en el laboratorio se obtuvo la enzima, y se realizaron ensayos de inhibición de la actividad enzimática con antihelmínticos y algunos derivados de bencimidazol. El disponer de la proteína recombinante pura, permitió conocer la estructura molecular de la Cu,Zn-SOD de *T. solium* por difracción de rayos X (cabe mencionar que es la primera estructura cristalográfica de una proteína de *T. solium*) [9]. Esto abrió la posibilidad de realizar un extenso estudio de simulación computacional de formación de complejos proteína-ligando (docking) entre la enzima y una base

de datos con aproximadamente 1`800`000 confórmeros estructurales, generados a partir de 50 mil compuestos químicos con potencial farmacológico. Los ensayos de inhibición de actividad de la enzima recombinante Cu,Zn-SOD de *T. solium*, mostraron inhibir parcial o totalmente la actividad de la enzima, a concentraciones de orden micromolar, con algunos de los compuestos que presentaron los mejores puntajes de formación de complejos proteína-ligando y selectividad de unión hacia algunos residuos no conservados en la secuencia de Cu,Zn-SOD de humano (*Homo sapiens*). Es importante mencionar que dicha inhibición no tiene efecto en la Cu,Zn-SOD de *Homo sapiens*.

1. INTRODUCCIÓN

GENERALIDADES DE CÉSTODOS

El ciclo de vida de los céstodos comprende tres estadios: huevo, larva y adulto.

HUEVO

Los parásitos en el estadio embrionario, oncósfera contienen una cubierta protectora o embrióforo compuesta por bloques de queratina unidos por una proteína cementante. Generalmente su coloración es blanquecina o ligeramente amarillenta aunque varía de acuerdo con los pigmentos que absorben en el intestino de los hospederos. El embrióforo recubre a la oncosfera o embrión hexacanto, nombrada así por que presenta 3 pares de ganchos, y tiene forma esférica con un tamaño de 30 - 40 µm (Figura 1) [10].

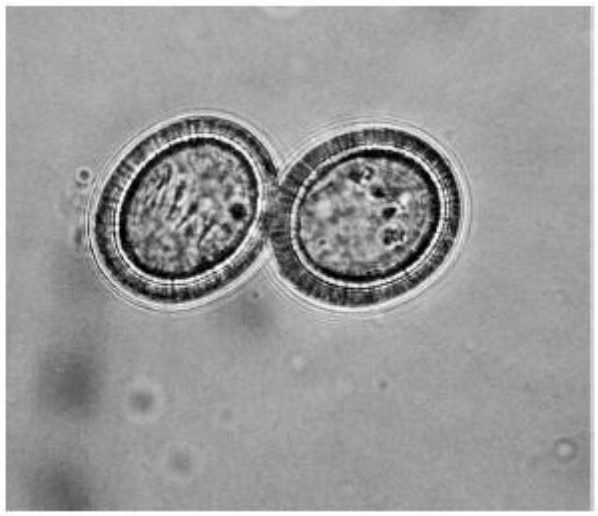

Figura 1. Micrografía de huevos de *Taenia sp*. Se observan a simple vista las estrías típicas del embrióforo y los ganchos en el huevo del lado izquierdo [10].

LARVA O CISTICERCO

La ultraestructura de la forma larvaria de un céstodo no difiere significativamente de lo descrito para otros taenidos [11]. Regularmente son descritos como una vesícula de 0.5 a 1.5 cm de diámetro, con un escólex invaginado, con cuatro ventosas y un róstelo armado con una doble corona de 22 a 28 ganchos que miden entre 0.110 y 0.180 mm de largo. Se observa como una vesícula opaca llena de líquido, cubierta por la pared vesicular. Microscópicamente, en la pared se pueden observar hacia el exterior microvellosidades cubiertas por una membrana plasmática, y un canal en espiral. La pared vesicular está formada por un tegumento y separado por una membrana basal del parénquima con varios tipos de celulares que colinda con el fluido vesicular; que constituye más del 90% del contenido de la larva (Figura 2).

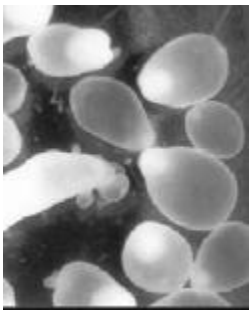

Figura 2. Imagen de larva de *T. crassiceps* en crecimiento obtenida de un hospedero intermediario [12].

ADULTO

El estadio adulto presenta un cuerpo alargado, con simetría bilateral, compuesto por proglótidos alargados y aplanados dorsoventralmente. El parásito adulto puede dividirse en 3 regiones:

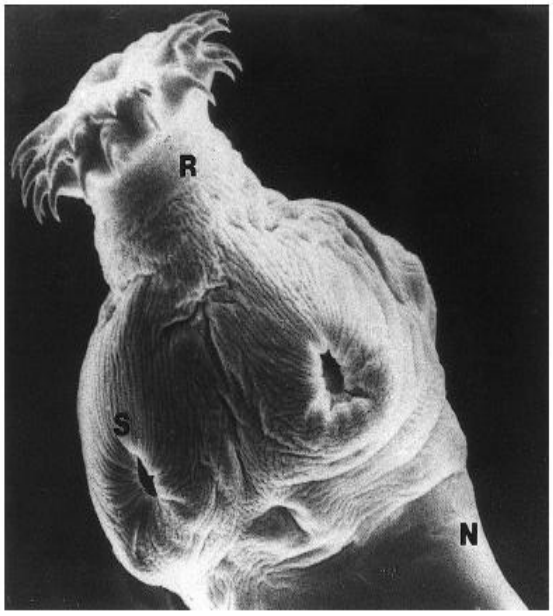

Figura 3. Micrografía electrónica de barrido de escólex de cisticerco *T. solium* evaginado. (R) Rostelum, (S) Ventosas, (N) Cuello [13].

Escólex: Órgano de fijación a la mucosa intestinal, redondeado con acetábulos redondos u ovales (ventosas), además de un róstelo armado como el ya descrito en la larva (Figura 3).

Cuello: Es la región de tejido de crecimiento (zona germinativa) indiferenciado situado inmediatamente abajo del escólex; Esta zona no es segmentada y produce por septación transversal los proglótidos, que componen el estróbilo; de ahí que la infección persista mientras el escólex y el cuello permanezcan unidos a la pared del intestino del hospedero (Figura 3).

Estróbilo: Está formado por un número variable de segmentos llamados proglótidos, que aumentan su grado de madurez a medida que se alejan del cuello. En el extremo proximal se encuentran los proglótidos inmaduros, seguido de los maduros y grávidos. En los proglótidos inmaduros, apenas se distinguen las estructuras celulares que originan los genitales masculinos y femeninos que alberga cada segmento, ya que este organismo es hermafrodita. Los proglótidos maduros, son de forma cuadrangular; en ellos se observan los órganos reproductores completamente desarrollados conteniendo entre 150 y 200 testículos (Figura 4 y 5). En la porción final del estróbilo se localizan los proglótidos grávidos de forma rectangular, ocupados casi en su totalidad por el útero que presenta entre siete y trece ramas uterinas, con los órganos sexuales atrofiados y llenos de huevos (Figura 5) [10,11,14].

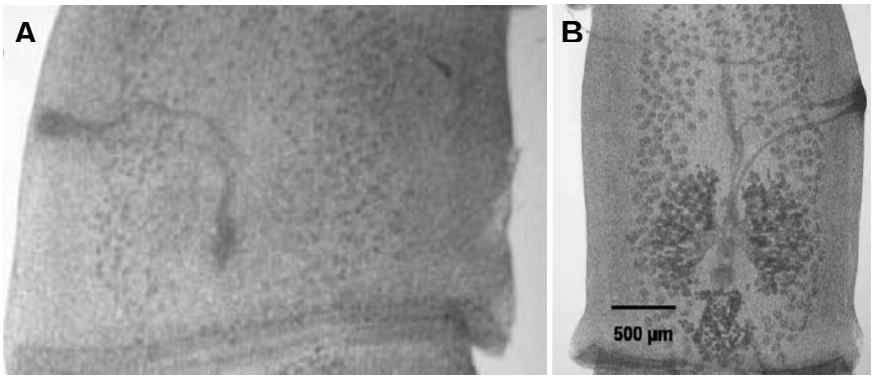

Figura 4. (A) Proglótido inmaduro de *T. crassiceps*. (B) Proglótido maduro de *T. crassiceps*, ambos recuperados de un hámster de 30 días de infección [12].

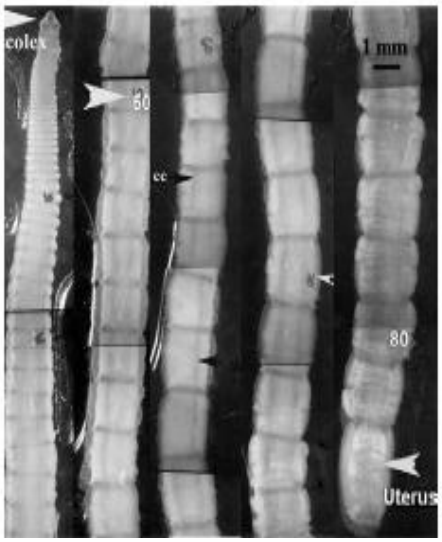

Figura 5. Segmentos de un gusano completo de *T. crassiceps.* Los números en blanco indican el número aproximando de proglótido [12].

Los céstodos carecen de sistema digestivo, en su lugar, poseen una superficie externa llamada tegumento que tiene actividad metabólica; a través de la cual se absorben y excretan selectivamente por difusión o por transporte activo las sustancias que requieren los céstodos para su deshecho, defensa y nutrición. La glucosa es la fuente de energía primaria en los céstodos, además de aminoácidos, purinas, pirimidinas y nucleótidos, que son absorbidos por esta superficie, y utilizados para sintetizar proteínas, vitaminas y ácidos nucleícos propios.

El tegumento, es el tejido que recubre al parásito; compuesto por la membrana tegumentaria y un sincicio anucleado cubierto de extensiones citoplásmicas (llamadas microtricas), mitocondrias y vacuolas de tamaños variables. El elemento más externo del tegumento es un glicocálix sobre la membrana tegumentaria, una cubierta con moléculas que inactivan algunas enzimas del hospedero y contiene amilasas utilizadas para degradar azúcares complejos (Figura 6 y 7).

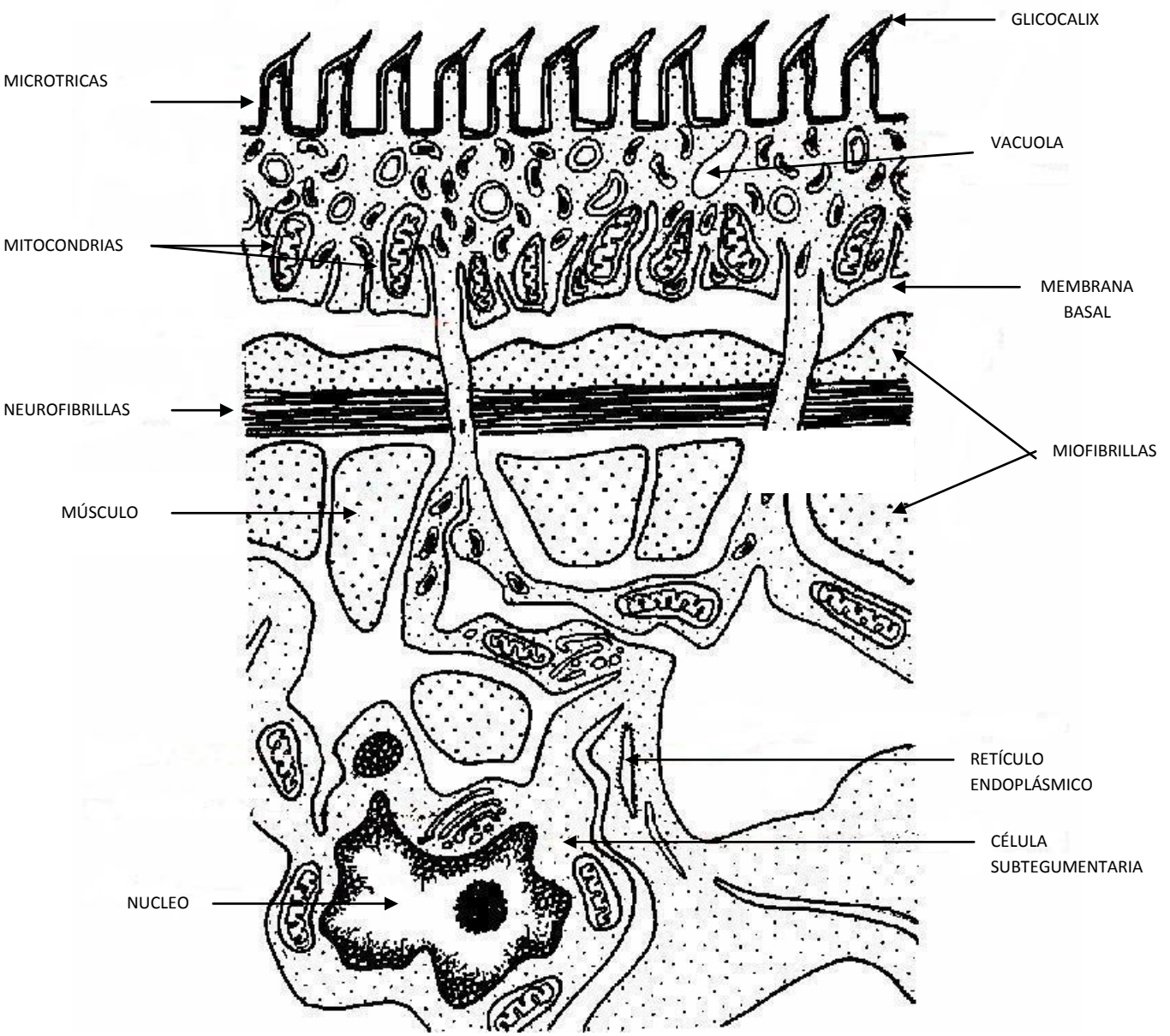

FIGURA 6. Esquema de la pared vesicular de un céstodo (Adaptado de BIODIDAC, University of Ottawa)

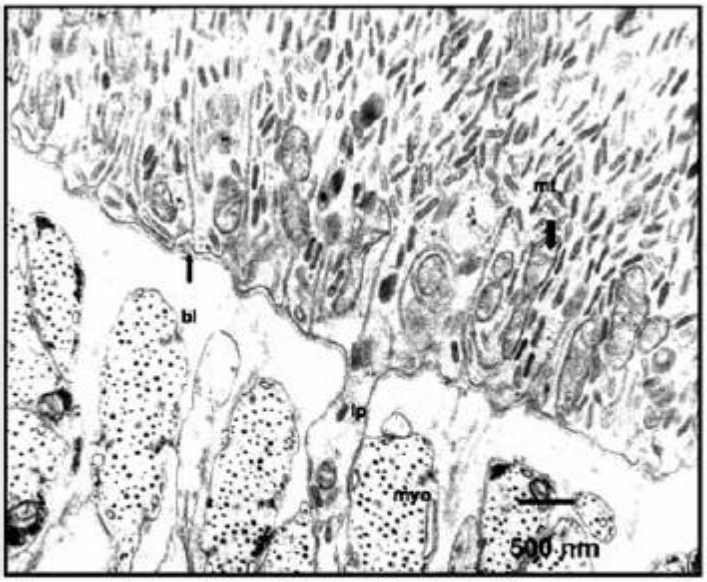

Figura 7. Micrografía electrónica del tegumento de gusano adulto, en flechas se muestra la matriz basal, células tegumentarias (ip), mitocondria tegumentaria (mt) y las miofibrillas (myo) [11].

El parénquima es delimitado por una membrana basal (colágena tipo IV) que tiene la función de sostén. Este también es considerado como centro de transporte y almacenamiento de glucógeno, es un tejido en el que se encuentran los sistemas de excreción, sistema nervioso, así como los paquetes de fibras musculares [15].

Taenia solium

En el ciclo biológico de *T. solium*, el estadio larvario se desarrolla en el humano (hospedero accidental) y en el cerdo (hospedero natural), mientras que los huevos se diseminan y se mantienen latentes en el medio ambiente. El humano es el único hospedero definitivo, ya que es la única especie que aloja a la forma adulta del parásito.

Cuando el hombre ingiere carne con cisticercos, las larvas evaginan en el intestino delgado; el escólex se adhiere a la pared intestinal y el cuerpo del parásito comienza a crecer y a formar proglótidos (Carpio [4]) (Flisser [16] 1979). El parásito adulto habita en el tubo digestivo del humano, en donde se mantiene adherido a la pared intestinal mediante ventosas y ganchos. Cada día, varios proglótidos grávidos se separan del extremo distal de la *Taenia* y son expulsados con las heces. Cada proglótido maduro diariamente libera miles de huevos en la materia fecal y pueden permanecer viables durante largo tiempo; con capacidad de infectar a humanos y cerdos [4]. En lugares en donde la eliminación de excretas es en un campo abierto, los cerdos se alimentan con heces humanas e ingieren los huevos de la *T. solium*. Una vez ingeridos por el cerdo, los huevos pierden su cubierta con la ayuda de enzimas proteolíticas y las sales biliares del tracto digestivo y se liberan las oncosferas (embriones hexacantos), atraviesan la pared intestinal y entran al torrente sanguíneo que los transporta a diversos tejidos del cerdo, principalmente músculos estriados y cerebro (causando cisticercosis y neurocisticercosis). En dichos tejidos, las oncosferas evolucionan y se transforman en larvas ó cisticercos. Por otra parte, el hombre puede convertirse en hospedero accidental de *T. solium* al ingerir huevos, y adquidir la cisticercosis humana. El mecanismo por el cual las

oncosferas entran al torrente sanguíneo y son distribuidos a los tejidos del hombre es similar al descrito en los cerdos.

La forma de contagio humano es por contaminación ano-mano-boca en individuos portadores del adulto de *T. solium* en el intestino, los que pueden auto-infectarse o infectar a otras personas, sobretodo a sus contactos domésticos al contaminar la comida con huevos de *T. solium*. La transmisión aérea de huevos y la regurgitación de proglótidos desde el intestino delgado hacia el estómago (auto-infección interna) no han sido adecuadamente demostrados como fuentes importantes de la enfermedad (Figura 8) [4,17].

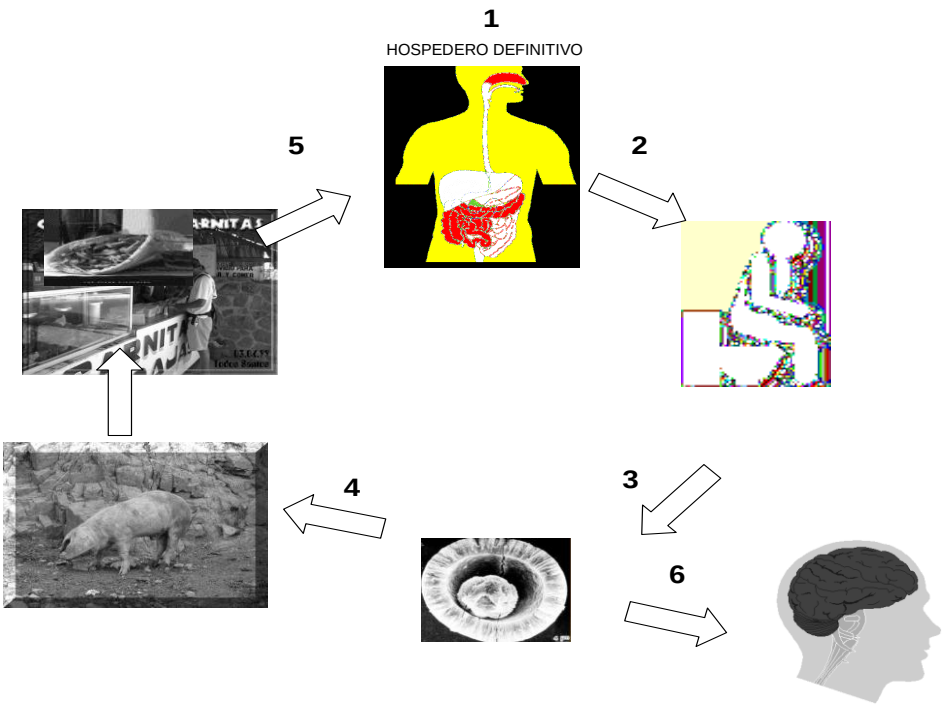

Figura 8. Ciclo de vida de *Taenia.solium* (1) El adulto habita el intestino delgado del humano (2) Liberación de huevos en heces (3) Diseminación de los huevos al medio ambiente (4) Infección de cerdos por ingesta de huevos (5) Infección en humanos por ingesta de carne de cerdo con cisticercos (6) Infección de humanos por ingesta de huevos.

T. solium es el agente etiológico de la taeniosis y la cisticercosis; que prevalecen en áreas rurales y urbanas, asociadas a prácticas tradicionales de crianza de cerdos, con malas condiciones higiénicas y sanitarias, ignorancia y pobreza; además se desarrolla en ciudades como resultado de una migración del campo a la ciudad [6,17] .

Taeniosis

La taeniosis generalmente es asintomática, ya que produce daño mínimo en la mucosa intestinal. El diagnóstico se realiza por la identificación de proglótidos expulsados en el excremento, los cuales deben ser observados al microscopio para la identificación de la especie, o bien, por el análisis de los huevos mediante técnicas coproparasitoscópicas de sedimentación y flotación, cuya sensibilidad no es mayor de 60% [18,19,20,21].

Actualmente se han desarrollado métodos de diagnóstico serológico como detección de anticuerpos y coproantígenos. El primero esta basado en la detección de anticuepos dirigidos contra antígenos de excresión y secresión (ES) de las formas inmaduras de *T. solium* obtenidas de hamsteres inmunosuprimidos. Está prueba presenta una sensibilidad de 95% y no presenta reacciones cruzadas con otras parasitosis como *T. saginata*. Además, la detección de coproantigenos se ha desarrollado en muestras de materia fecal del hospedero; para esto se utilizan anticuerpos obtenidos por hiperinmunización de conejos, con diferentes antígenos de proglótidos de *T. solium* y *T. saginata* homogenizados, antígenos de ES o fracciones de la superficie del parásito. Los resultados revelan que son género específicos y no presentan reacciones cruzadas con otros parásitos intestinales. El antígeno

puede ser detectado semanas después de tener evidencia de la infección y su detección es independiente de la expulsión de los huevos. Está técnica presenta una especificidad de 99% y detecta 2.4 veces más los casos de taeniosis que por métodos microscópicos [22].

Cisticerosis

La cisticercosis también es conocida como: grano, granillo, alfilerillo, fresilla, tomatillo, sapo, zahuate, liendrilla, granizo ó gusano vesiculoso de la carne del cerdo [15]. Se adquiere por la ingestión de huevos de *T. solium*, la cual se produce cuando el hombre se convierte, en forma accidental en el hospedero intermediario de dicho céstodo. Se localiza en diversas partes del cuerpo como: mucosas, ojo y músculo. El parásito tiene tendencia por instalarse en el sistema nervioso central, produciendo la enfermedad denominada neurocisticercosis. La gravedad de las lesiones que producen depende de su localización en las diversas partes del cuerpo, y no tanto de su número, pudiendo pasar inadvertida como en el caso de la cisticercosis muscular. También puede causar severos sintomas, desde dolor de cabeza, perdida del equilibrio y parálisis en uno o varios miembros, epilepsia, ceguera, hidrocefalia, demencia, déficit neurológico focal, e incluso la muerte en casos de neurocisticercosis [23,24] Esta última es es la enfermedad parasitaria más frecuente del sistema nervioso central, representando una patología neurológica común, así como un serio problema de salud pública en diferentes países de América Latina, África y Asia (Figura 9) [1,2,3].

Figura 9. Mapa mostrando las zonas endémicas de cisticercosis. Los países en negro representan los países en donde es endémica la cisticercosis, en gris los países en dónde se ha reportado [25].

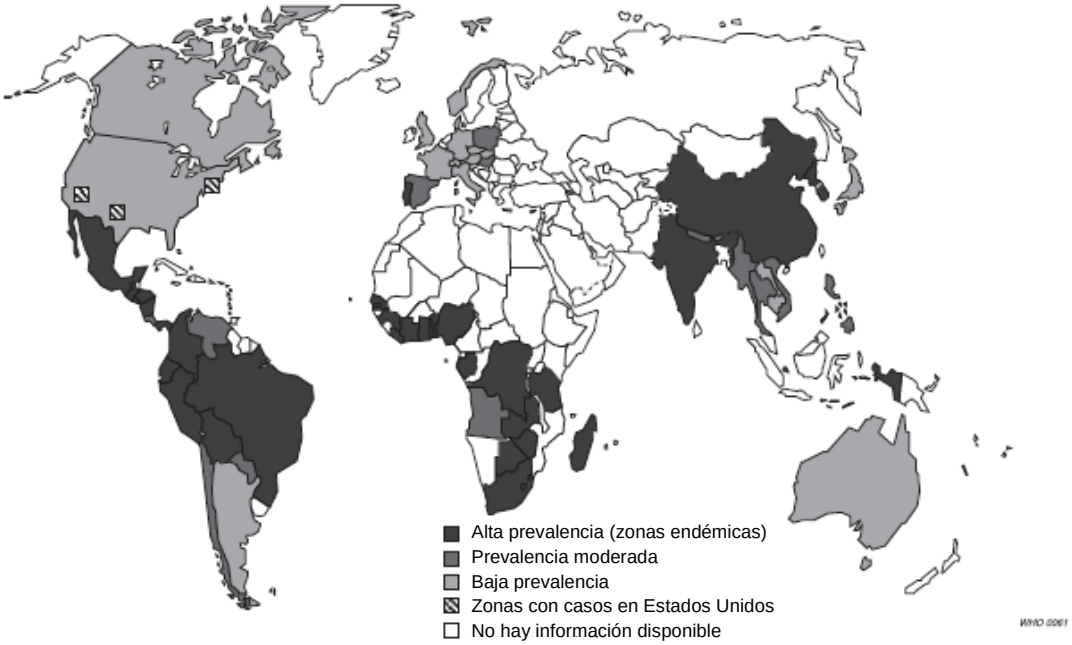

El tratamiento es sintomático y debe estar diseñado para cada paciente con antiepilépticos, analgésicos, corticosteroides o una combinación de ellos. Se utilizan de manera rutinaria antihelmínticos (prazicuantel y albendazol), para eliminar el parásito.

Debido al pleomorfismo clínico de la neurocisticercosis, no es posible que un solo esquema de tratamiento sea útil en todos los casos. Por lo tanto, la localización precisa del parásito, en lo que respecta a viabilidad y localización de las lesiones, es de fundamental importancia para diseñar un tratamiento adecuado [26,27,28].

Los antihelmínticos son fármacos que destruyen o expulsan a los helmintos. El tratamiento de la taeniosis, ha pasado por varias etapas: durante mucho tiempo se emplearon semillas de calabaza como vermífugos, los extractos de ciertas

plantas como el quenopodio (*Chenopodium ambrosioides*), el helecho macho (Dryopteris filix-mas), compuestos como mepacrina (2 – Metoxi – 6 – cloro – 9 - dietilaminopentilaminoacridina); pero las reacciones secundarias y la escasa acción antihelmíntica las hicieron caer en desuso. Para el tratamiento de la cisticercosis y la teniosis se utilizan fármacos sintéticos como el prazicuantel, el albendazol y la niclosamida [29][20].

Praziquantel: El mecanismo de acción no está completamente entendido, pero es generalmente aceptado que daña el tegumento del helminto y produce la paralisis del escolex [30]. Por último cabe señalar que el prazicuantel es el tratamiento de elección para cisticercosis recomendado por la OMS a una dosis única. 10 mg/kg (OMS, 2002). El tratamiento con prazicuantel (Figura 10) para la taeniosis, se administra a dosis de 5 o 10 mg/Kg, en una sola toma.

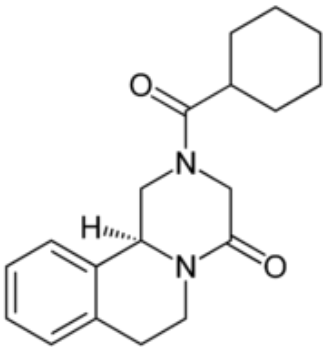

Figura 10. Praziquantel

Albendazol (Figura 11): Es un benzimidazol con potente efecto cestocida, altamente eficaz en la neurocisticercosis. Los benzimidazoles causan muchos cambios bioquímicos, por ejemplo la inhibición de la fumarato reductasa de las mitocondrias, disminución del transporte de glucosa, y desacoplamiento de la fosforilación oxidativa. En el caso de helmintos se ha observado que produce 50% de inhibición de la actividad de la Cu,Zn-SOD [8], lo que suguiere otro posible mecanismo de acción. Sin embargo, su principal acción es la inhibición de la polimerización de microtúbulos al unirse a β-tubulina. La toxicidad selectiva de estos compuestos depende de la actividad específica y muy ávida con la β-tubulina del parásito, se produce con concentraciones mucho menores que las necesarias para unirse a las proteínas de mamíferos. Después de administrarse, el albendazol es metabolizado en el hígado, hasta la forma de sulfóxido de albendazol, el cual tiene actividad antihelmíntica. El albenbazol ocasiona pocos efectos adversos si se utiliza por corto tiempo contra la helmintiasis gastrointestinal, destruye el 75% a 90% de los cisticercos y ha probado ser superior al praziquantel en diversos estudios comparativos [31,32], no solamente por su mejor porcentaje de destrucción sino también por su menor costo, aspectos importantes, ya que la cisticercosis usualmente afecta a personas de bajos recursos económicos. La dosis recomendada es de 15mg/kg/día por 1 mes [33].

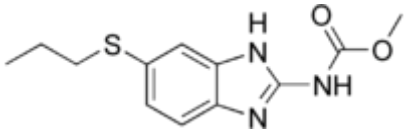

Figura 11. Albendazol

Taenia crassiceps

Taenia crassiceps (Zeder, 1800), es un céstodo cuyo estadio adulto infecta a zorros rojos (*Vulpes vulpes*), lobos (*Canis lupus baileyi*) y perros(*Canis lupus*). El estado larvario infecta de manera natural a topos, marmotas y ratones de campo. En ratones infectados, los cisticercos de *T. crassiceps* se localizan principalmente en tejidos subcutáneos y en las cavidades peritoneal y pleural (Figura 12) [12].

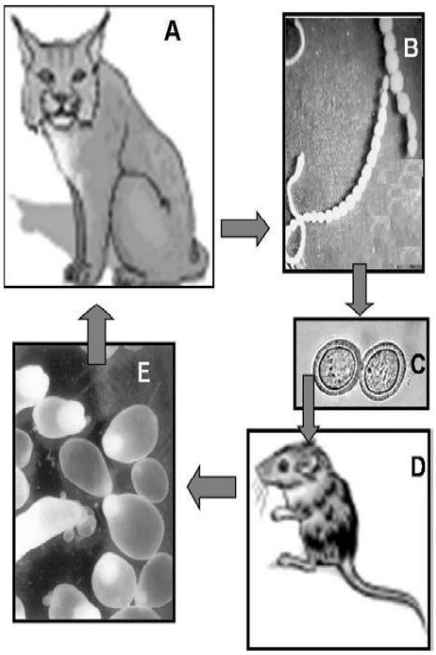

Figura 12. Ciclo de vida de *T. crassiceps* en la naturaleza. A) Hospedero definitivo; B) Adulto en intestino de hospedero; C) Huevos infectivos con heces; D) Ingestión de huevos por hospedero intermediario; E) Crecimiento de larva en hospedero intermediario, que es ingerido por un hospedero carnívoro; en el que los gusanos crecen en el duodeno [12].

Éste parásito se ha utilizado ampliamente como modelo experimental de cisticercosis; debido a que la reproducción asexual, de los cisticercos en el peritoneo por gemación, le permiten ser mantenido indefinidamente en la cavidad peritoneal de ratones, obteniendo así grandes cantidades del parásito. Se han aislado diversas cepas de *T. crassiceps* para propagar en el laboratorio, algunas son: HYG, KBS, Toi, la mutante ORF (carece de escólex) y la cepa WFU obtenida de la infección en un roedor silvestre en Norte América; adicionalmente se han aislado cepas en Alemania y Japón [12].

Algunas de la características que lo hacen un buen modelo son que la ultraestructura del estadio larvario y adulto de *T. crassiceps* no difieren significativamente de otros ténidos. Se han caracterizado varias enzimas de *T. solium* y *crassiceps* y se ha observado que presentan alta similitud entre ellas, incluso se han encontrado reacciones cruzadas entre antígenos. Su similitud y homología con *T. solium* son algunos de los atributos que lo hacen útil. Las propiedades bioquímicas, inmunológicas así como las características morfológicas y fisiológicas de este parásito son semejantes a *T. solium* [33,34,35,36]. Los estudios sobre estas cepas de *T. crassiceps*, en especial la ORF, han indicado que el balance hormonal y género del hospedero murino son de gran importancia para la velocidad de reproducción, ya que en ratones hembras se reproducen mejor [34].

ESTRÉS OXIDANTE

El estrés oxidante (EOx), se define como el desequilibrio bioquímico producido por la sintesis excesiva de especies reactivas (ER) que provocan daño oxidante en las biomoléculas y que no puede ser contrarrestado por los sistemas antioxidantes [35]. Las ER son especies químicas capaces de extraer electrones de las moléculas vecinas para completar su orbital, convirtiéndose en componentes altamente reactivos y en las principales sustancias oxidantes en los sistemas biológicos [35]; por ejemplo, el ión hidroxilo ($HO^{\cdot}$) y el peroxinitrito ($ONOO^{-}$). Las especies reactivas de oxígeno (ERO), se generan por la reducción incompleta del oxígeno durante la respiración en la mitocondria, como producto de reacciones metabólicas normales en la membrana citoplasmática, retículo endoplásmico, los peroxisomas y por macrófagos, neutrófilos y eosinófilos del hospedero [36,37]. Estas especies causan daño a toda clase de moléculas biológicas conduciendo a la oxidación, despolimerización de polisacáridos, modificaciones y ruptura de cadenas de ADN, daño a la membrana, lípidos, proteínas, carbohidratos. Además están involucradas en procesos de diferenciación celular, crecimiento, mutagénesis y carcinogénesis [38].

Estudios *in vitro* sugieren que los macrófagos son un buen mecanismo efector del humano contra los parásitos. Se ha demostrado que los fagocitos matan parásitos protozoarios intracelulares y extracelulares por medio de las ERO, a través del estallido respiratorio los fagocitos liberan H_2O_2 y $O_2^{\cdot -}$, el cual produce $OH^{\cdot}$ y el singulete ($^1O_2$) por medio de la reacción de Haber-Weiss.

ANIÓN SUPERÓXIDO

La reducción univalente del oxígeno, genera intermediarios reactivos en una serie de reacciones que involucra cuatro electrones, produciendo tres compuestos denominados (EROs), estos son el anión superóxido ($O_2^{\cdot -}$), el H_2O_2 y el radical $OH^{\cdot}$. El $O_2^{\cdot -}$ se produce en el organismo durante el proceso metabólico normal, radiación ionizante; y en respuesta a patógenos por medio de los leucocitos en el estallido respiratorio.

El $O_2^{\cdot -}$ no es extremadamente dañino, pero puede interactuar con el óxido nítrico y conducir a la formación de otras especies altamente oxidantes como los radicales $OH^{\cdot}$, $HO_2^{\cdot}$, y el $ONOO^{-}$ [39]. El $O_2^{\cdot -}$ es más selectivo en su reactividad y es potencialmente más dañino de esta forma; debido a que puede difundir una distancia considerable antes de encontrarse con un posible blanco. El $O_2^{\cdot -}$ es la base conjugada del radical oxidante hidroperoxilo ($HO_2^{\cdot}$).

El $O_2^{\cdot -}$, es inestable en solventes protonados como el agua; a pH neutro es suficientemente estable para oxidar compuestos como fenoles, tioles, ascorbato, catecolaminas, leucoflavinas, tetrahidropterinas, sulfito, con hierro libre o unido a algunas proteínas, por ejemplo los centros [Fe-S] y otros ERO como el óxido nítrico, los radicales fenoxi y el propio $O_2^{\cdot -}$. Además, este anión inhibe algunas enzimas como la deshidrogenasa 6-fosfogluconato, la aconitasa y la fumarasa o afecta la reducción del NAD^{+} y el metabolismo energético. También inhibe a la tercer enzima de la vía de síntesis de aminoácidos ramificados, la dehidratasa del dihidroxiácido, la reductasa del ribonucleótido que genera los difosfato de desoxiribonucleótidos para la síntesis del ADN y una fosfatasa de la proteína la calcineurina, importante en la transducción de señales [40].

Este $O_2^{\cdot-}$ se produce *in vivo* por enzimas como la NADPH en la fagocitosis. Algunas enzimas que reducen el O_2 y generan $O_2^{\cdot-}$; como las citocromo P450, peroxidasas, celubiosa oxidasas, nitropropano dioxigenasas, óxido nítrico sintasas, triptófano dioxigenasas, aldehído oxidasas y las indolamina dioxigenasas. Además biomoléculas como adrenalina, noradrenalina, dopamina, dihidroxifenilalanina (L-Dopa), FMNH2, FaDH2, gliceraldehído y algunas tetrahidropteridinas se pueden auto-oxidar y producir $O_2^{\cdot-}$. Cabe mencionar que las tetrahidropteridinas son cofactores de enzimas como las oxígenasas, fenilamina hidroxidasas y las tirosina hidroxilasas. De manera general las autooxidaciones son lentas, pero una vez formado un poco de $O_2^{\cdot-}$ continúan una reacción en cadena generando más $O_2^{\cdot-}$.

Algunos de los efectos del $O_2^{\cdot-}$ en el organismo son; la inactivación de proteínas por oxidación de grupos que contienen [4Fe-4S] en el sitio activo como la 6 fosfogluconato dehidratasa, la aconitasa y la fumarasa A y B.

Se ha observado que el $O_2^{\cdot-}$ está involucrado en procesos patológicos; como daño de isquemia-reperfusión, cáncer y procesos de envejecimiento. Participa en procesos de señalización en el crecimiento de bacterias, levaduras y diferentes tipos celulares por medio de la vía rac/ras-NAD(P)H oxidasa-MAPK; y la activación de la vía de ras/rac-Raf1-MAPK vía que puede conducir a una expresión defectuosa de genes [41]. El aumento en los niveles de $O_2^{\cdot-}$ se puede producir por diversos mecanismos, dando origen a diferentes efectos metabólicos. La inhibición de la enzima superóxido dismutasa incrementa y estimula la proliferación celular; por el contrario la sobre expresión de la superóxido dismutasa de Cu,Zn la inhibe. La regulación negativa de esta enzima con cebadores antisentido inhibe la apoptosis, y del mismo modo la

baja expresión de la SOD o la inhibición de NADPH oxidasa, incrementan la susceptibilidad a la apoptosis [41].

Los organismos tienen sistemas que los defienden del ataque de los ERO. Éstos se pueden clasificar en enzimático y no enzimático. Dentro de los mecanismos no enzimáticos se encuentran el β-caroteno, la vitamina A y ácido ascórbico entre otros. Los sistemas enzimáticos están conformados por enzimas como la catalasa, las peroxiredoxinas, glutatión peroxidasas, y las superóxido dismutasas.

PERÓXIDO DE HIDRÓGENO

El H_2O_2 es la forma menos reactiva de las ERO. Su importancia reside en que participa en numerosas reacciones que dan lugar a la generación de ERO secundarias. Atraviesa con gran facilidad por las membranas biológicas, con lo que puede dar lugar a reacciones de oxidación en puntos de la célula más alejados de su lugar de producción. Se puede originar a partir de diversas fuentes: Por reducción directa de una molécula de oxígeno por dos electrones ($O_2 + 2\ e^- + 2H^+ \rightarrow H_2O_2 + H_2O$), por dismutación del $O_2^{\cdot -}$ [42] o como producto de algunas reacciones por enzimas como glucosa oxidasa, uricasa, así como por reacciones químicas de autooxidación. Por otro lado, el H_2O_2 está implicado en la señalización y regulación de genes como los de la superóxido dismutasa de Mn (III), interleucina 2 (IL-2), factor de necrosis tumoral α (TNF-α), antígenos del complejo mayor de histocompatibilidad y c-fos, a través de NFκB y AP-1.

SISTEMAS ANTIOXIDANTES

Todos los organismos aerobios requieren mecanismos que limiten el daño molecular causado por las ERO como $O_2^{\cdot -}$, H_2O_2, y el $HO^{\cdot}$ que aumentan por exposición a la radiación, ciclización redox de xenobióticos o fagocitos estimulados del hospedero [43]. Las ERO formadas en el organismo pueden iniciar una serie de reacciones en cadena, que continúan hasta que éstos son eliminados tras diversas reacciones con otras ERO o por la acción de algún sistema antioxidante, el cual protege a los tejidos de los efectos que ellos producen. Un antioxidante es una entidad química que a bajas concentraciones, en comparación con el oxidante, retarda o previene la oxidación de sustratos como lípidos, proteínas, carbohidratos y ADN. Unos previenen la formación de nuevos ERO, convirtiéndolos en moléculas menos perjudiciales antes de que puedan reaccionar y formar nuevos ERO a partir de otras moléculas. Para detener este proceso destructivo, los organismos han desarrollado sistemas enzimáticos y no enzimáticos de protección del daño producido por las moléculas oxidantes [44]. Esta protección contra el daño oxidante puede ser por prevención, intercepción y reparación. En la figura 13 se esquematiza el ataque de las EROs.

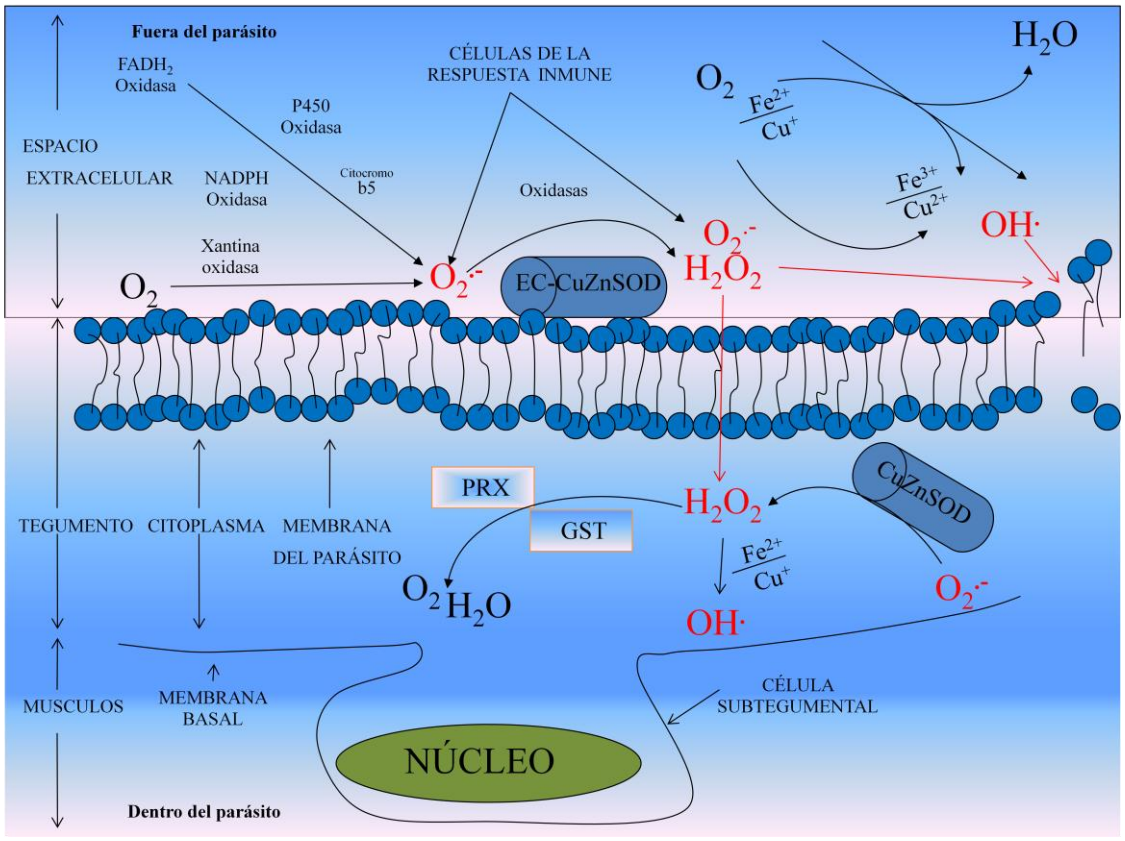

Figura 13. Esquema de daño de ER a la membrana parasitaria, el $O_2^{\cdot-}$ producido por la respuesta inmune (fagocitos) reacciona con la Cu,Zn-SOD extracelular generando H_2O_2 (molécula que puede cruzar la membrana) que a su vez genera radicales libres como $OH^{\cdot}$, que reaccionan con lípidos, proteínas de la membrana y ADN causando daño celular. Dentro del espacio celular, las enzimas como la glutatión transferasa, peroxiredixinas (PRX) y la Cu,Zn-SOD citosólica reaccionan con las ROS, participando en la defensa y regulación de los procesos fisiológicos, como señalización, diferenciación y crecimiento.

La prevención de la formación de ERO es la primera línea de defensa contra ellos. Esto incluye a proteínas como la ferritina, transferrina y la ceruloplasmina que se unen a iones metálicos (cobre y hierro) con el fin de secuestrarlos e impedir su oxidación o bien por utilización de pigmentos como la melanina que protegen de la radiación, impidiendo se generen nuevos ERO. La intercepción de los ERO, es el proceso de desactivación de los mismos, lo podemos dividir en dos clases enzimáticos y no enzimáticos. Los no enzimáticos que a su vez se subdividen en dos subclases: a) sustancias eliminadoras o secuestradoras que son pequeñas moléculas que limpian el plasma de oxiradicales (un ejemplo de esto son el α-tocoferol ácido ascórbico, carotenos y glutatión) y b) sustancias proteicas como la lactoferrina, la ceruloplasmina, la transferrina, y los sistemas enzimáticos, por ejemplo las tres principales enzimas antioxidantes, la superóxido dismutasa, la catalasa y la glutatión peroxidasa [38] .

SISTEMAS ANTIOXIDANTES NO ENZIMÁTICOS

Este sistema consiste en la formación de compuestos no radicales. Estos antioxidantes capturan a los ERO impidiendo reacciones en cadena, o la formación de ERO secundarios por medio de la unión a compuestos de alto peso molecular; algunos solubles en agua como el ácido ascórbico, tioles, urato y piruvato, así como algunos lípidos solubles como la vitamina E y el β-caroteno [45].

SISTEMAS ANTIOXIDANTES ENZIMÁTICOS

Los sistemas enzimáticos están conformados por una serie de enzimas antioxidantes esenciales en los parásitos. Las principales familias de enzimas antioxidantes en organismos eucariontes son las catalasas (CATs), las glutatión peroxidasas (GPXs) las peroxiredoxinas (PRXs). Las tres presentan actividad catalítica para descomponer H_2O_2 y producen agua y oxígeno molecular. También las GPXs, las PRXs y las glutatión transferasas pueden reducir hidroperóxidos lipídicos y carbonilos reactivos dando como producto final agua. Las superóxido dismutasas (SODs) son una familia de métaloenzimas las cuales catalizan la dismutación del $O_2^{\cdot-}$ a H_2O_2 y oxígeno molecular y son la primera línea de defensa que tienen los organismos [46]. El descubrimiento de estos sistemas enzimáticos representa un avance para entender cómo los parásitos se defienden del estrés oxidante interno y externo.

SUPERÓXIDO DISMUTASAS

Las SODs, (E.C 1.15.1.1) son una familia ubicua de métaloenzimas. Se clasifican de acuerdo con el metal que presentan en su sitio activo Mn, Fe, Ni y Cu,Zn. La enzima que contiene Cu,Zn presenta dos formas, la extracelular y la citosólica. Todas las SODs catalizan la misma reacción, son codificadas por diferentes genes y difieren en estructura, localización en la célula y son específicas para la remoción catalítica del $O_2^{\cdot-}$.

La Ni-SOD se ha reportado principalmente en cianobacterias y en algunas especies de *Streptomyces*. Son tetraméricas o hexaméricas con una masa relativa de 13 kDa por subunidad. Las Fe-SODs contienen uno o dos iones por dímero y se encuentran principalmente en plantas, algas tripanosomas y

bacterias. Estas enzimas presentan un peso de 22 kDa por dímero, aunque se han descrito algunas tetraméricas. La de Mn-SOD es homotetramérica y cada monómero maduro pesa de 32 a 40 kDa; está ampliamente distribuida en procariotes, eucariotes, animales y plantas. En todos los eucariontes se localiza en la mitocondria excepto en *Candida albicans*, que la expresa en el citoplasma en ciertas condiciones de crecimiento. Los organismos complejos contienen cuatro subunidades y tienen un ion de Mn por subunidad. La secuencia de aminoácidos de la Mn-SOD es homologa entre animales, plantas y bacterias; también es homologa a la de las Fe-SODs.

La SOD de Mn (III) o mitocondrial es una enzima tetramérica que es codificada en el núcleo como la de Mn^{2+}, sintetizada como un precursor con un péptido señal que le ayuda a ser transportada hacia la mitocondria, dónde pierde este péptido. La proteína precursora tiene un peso molecular de 25 kDa y la proteína madura dentro de la mitocondria un peso molecular de 22 kDa. Esta SOD de Mn (III) está localizada en la matriz de la mitocondria [47]. La SOD de Fe (III) es un tetrámero y se encuentra principalmente en organismos fotosintéticos ubicada en citoplasma, cloroplasto de algunas plantas, tiene un peso molecular de 22 kDa. Cabe mencionar que las SOD de Mn (III) y la de Fe (III) no se han descrito en helmintos.

1. La Cu,Zn-SOD extracelular protege a los organismos del daño que el $O_2^{\cdot-}$ pueda producir en la membrana; ya que el $O_2^{\cdot-}$ generado de fuentes extracelulares, como los leucocitos, xenobiótico y radiaciones, no puede cruzar la mayoría de las membranas biológicas [48]. Se encuentra en diversos organismos incluyendo parásitos como *Nocardia asteroids*, *Schistosoma mansoni*, *Onchocerca volvulus* [48]. Es una glicoproteína con peso molecular

de 135 kDa. En ocasiones se encuentra como dímero, sin embargo en la mayoría de las especies forma un tetrámero con subunidades de 30 kDa unidas por medio de puentes disulfuro. Esta enzima contiene un átomo de Cu y uno de Zn por subunidad, y es muy importante en parásitos [49,50]. Se ha obtenido la secuencia del gen en nemátodos como *Caenorhabditis elegans*, *Caenorhabditis briggsae* y *Haemonchus contortus*. La presencia de esta enzima parece ser un factor patogénico, ya que anticuerpos dirigidos a la SOD extracelular de *N. asteroides* aumentan el potencial de los leucocitos para matar a dicho organismo, en contraste inmunoglobulinas inespecíficas no tienen ningún efecto [51].

La SOD más descrita en helmintos es la Cu,Zn-SOD citosólica. Ésta enzima está presente en la mayoría de los eucariontes y en algunos procariontes. Es muy estable, en procesos de purificación resiste tratamientos con cloroformo, etanol, centrifugaciones, calentamiento, tratamiento con proteasas, dodecil sulfato de sodio y urea. Esta Cu,Zn-SOD se encuentra ampliamente distribuida en el citosol y el núcleo, pero está ausente en la mitocondria y compartimentos secretorios [47].

Esta enzima es un homodímero compuesto por subunidades o monómeros de 16 kDa, contiene un átomo de Cu y uno de Zn por subunidad. Se ha establecido que el Cu participa en la catálisis mientras que el Zn está involucrado en la estabilidad de la estructura (Figura 14 y 15).

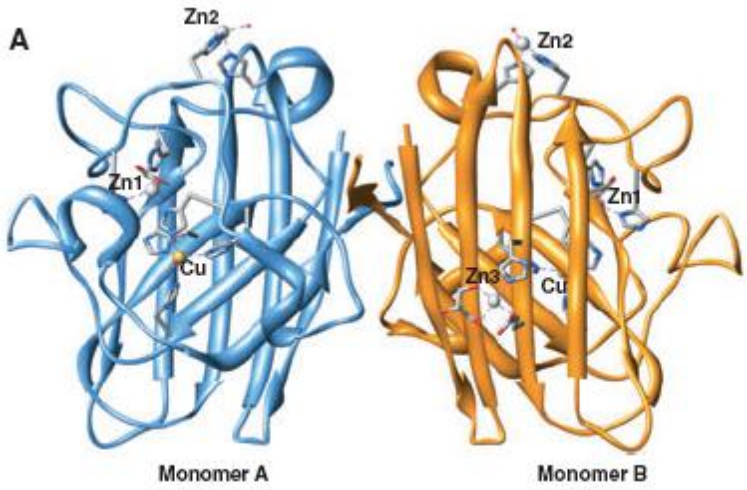

Figura 14. Estructura de la Cu,Zn-SOD. A) Representación Ribbon del diméro de la Cu,Zn-SOD, los metales se representan como esferas amarillas (cobre) y en gris (zinc) [9].

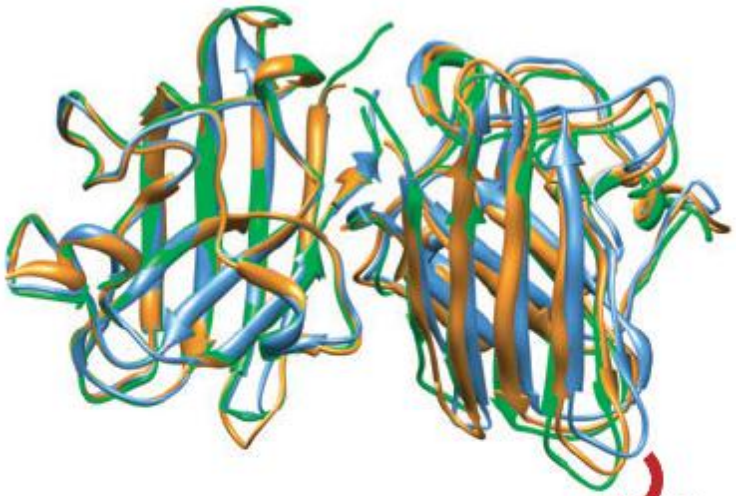

Figura 15. Alineamiento estructural de las superóxido dismutasas de *T. solium*(azul), *Schistosoma mansoni* [52] y *Homo sapiens* (verde).

La SOD citosólica y la extracelular tienen un 50% de identidad en la secuencia de aminoácidos, además contiene los residuos conservados requeridos para la actividad y unión a los metales, como los residuos de histidina, y el aspartato

involucrados en la unión al Zn y Cu, dos cisteínas envueltas en el puente disulfuro y la arginina en la entrada del sitio activo.

REGULACIÓN DE GENES DE CU,ZN-SOD

Se ha identificado el gen de la Cu,Zn-SOD en rata, ratón, bovino, y humano. En humano se localiza en el cromosoma 21q22 [53]. De manera general los genes de SOD en mamíferos están formados por cinco exones interrumpidos por cuatro intrones. Las regiones promotoras de los genes de Cu,Zn-SOD son célula y tejido específicos, pudiendo ser reguladas por factores mecánicos, químicos y biológicos como: temperatura, radiaciones X y UV tipo B, metales pesados, H_2O_2, O_3, NO, ácido araquidónico, entre otros [54].

En los análisis de los promotores proximales de Cu,Zn-SOD de mamíferos se han identificado regiones regulatorias como cajas TATA, sitios de unión para NF-KB, AP1, AP-2, Sp1, NF1, GRE, HSF, sitio de unión a proteína CCAAT (C/EBP) y regiones ricas en GC (Figura 16) [53]. En helmintos, se han encontrado potenciales regiones regulatorias como cajas TATA y CAAT, así como sitios AP-1 en el promotor del gen de calreticulina [55]. Adicionalmente se reportaron; un sitio para AP-1 y tres cajas TATA se reportaron en el promotor del gen de la glutatión transferasa de 28 kDa de *Schistosoma mansoni* [56]. En el caso de los promotores de *Cu,Zn-SOD*, se han descrito sitios de inicio de la transcripción (TSS del inglés Transcription Start Site), dos cajas CAAT, y tres regiones ricas en GC en *S. mansoni* [57,58], así como la presencia de sitios similares a elementos iniciadores en dos promotores de *Onchocerca volvulus* (*Ov-sod*-1 and *Ov-sod*-2) [59].

Estructura general de un gen de CuZnSOD de mamífero

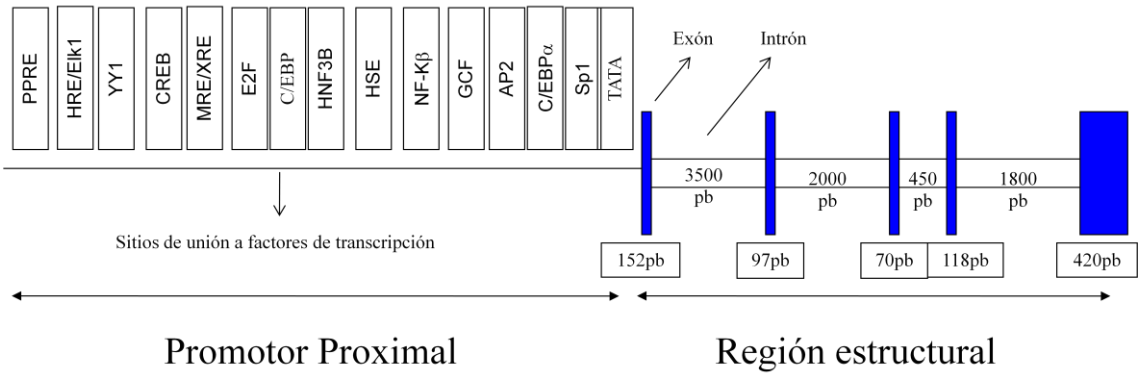

Figura 16. Estructura general de un gen de Cu,Zn-SOD de mamífero. Se muestran en cajas las siglas de los factores de transcripción que unen a la región promotora del gen, en rectángulos negros los exones y en blancos los intrones, con el número aproximando de bases que los componen.

En helmintos se sabe que la expresión de genes de *Cu,Zn-SOD* puede ser regulada por EROs, por ejemplo el $O_2^{\cdot-}$ aumenta los niveles de transcripción de la Cu,Zn-SOD en miracidios, esporocistos y cercarias de *S. mansoni* [54]; también aumenta los niveles de ARN mensajero de Mn-SOD y Cu,Zn-SODs en el estado larvario de *Caenorhabidits elegans* [60], así mismo, el H_2O_2 aumenta la transcripción de Cu,Zn-SOD en *S. mansoni* [61]. Además los niveles de actividad enzimática de la catalasa y Cu,Zn-SOD aumentan en gusanos hembras de *Heligmosomoides polygyrus* aisladas de ratones infectados con diferentes fenotipos de resistencia [62].

Cu,Zn-SOD EN HELMINTOS

Se ha encontrado actividad de Cu,Zn-SOD en diferentes estadios de desarrollo de algunos helmintos; dicha actividad varía dependiendo del estadio de desarrollo. Además se ha demostrado, que los estadios adultos son más susceptibles a daños por estrés que los juveniles. Se han purificado Cu,Zn-SODs de extractos de diversos helmintos como *T. taeniaeformis, Dirofilaria immitis* y *T. solium* [63,64,65]; además se han clonado las Cu,ZnSODs de *Onchocerca volvulus* (rOVSOD), *T. solium, Fasciola hepática* [8,50,66], así como las extracelular (SP-SOD) y la citosólica (CT-SOD) de *Schistosoma mansoni* y *Brugia pahangi* [49,57,67]. Todas las secuencias de estas enzimas contienen los motivos característicos y sitios conservados para las Cu,Zn-SOD.

Se han identificado diversas Cu,Zn-SOD en extractos proteicos y productos de excreción/secreción de helmintos. Todas las enzimas son codificadas por un gen de copia única, excepto en *Haemonchus contortus* [68]. Las Cu,Zn-SODs de céstodos presentan identidad de secuencia primaria entre un 47 hasta 96% con las de otros helmintos; en contraste las similitudes de estas con la secuencia de humano y bovino varían desde 53 a 63%. También, es notable el alto nivel de identidad que se presenta entre las enzimas de nematodos (*O. volvulus* y *Brugia malayi*, y *Dirofilaria immitis*) y trematodos (*Fasciola hepática, Clonorchis sinensis*), que por ejemplo presentan reacciones cruzadas entre las SODs de *O. volvulus* y *Brugia malayi* [43].

Se han realizado estudios en bacterias como *E.coli* que demuestran que las SODs participan en muchos procesos biológicos, en función del metabolismo bacteriano, condiciones ambientales y estado en el ciclo de vida. Los efectos de algunas bacterias mutantes con el gen nulo para SOD, presentan sensibilidad al estrés oxidante y a algunas ER, pérdida de la viabilidad, defectos en el ensamble de la esporulación y atenuación de la virulencia.

En el caso de la Mn-SOD, los ratones knockout $^{-/-}$, mueren pocos días después de nacer [69] y los organismos knockout (Cu,Zn-SOD$^{-/-}$) presentan disminución en el índice de crecimiento y un corto índice de vida [70].

En humanos la Cu,Zn-SOD está implicada en procesos de envejecimiento y fisiopatológicos como cáncer de intestino, riñón, hígado y leucemia; alergias (intolerancia a fármacos); daño cardiaco (isquemia y aterosclerosis); enfermedades infecciosas (por influenza y *Helicobacter pylori*); desorden genético (síndrome de Down), enfermedades neurodegenerativas (Alzheimer y esclerosis) y problemas oftalmológicos (cataratas), entre otros [71,72]. Los ratones “Knock outs” (que carecen de la Cu,Zn-SOD) parecen normales en su etapa juvenil, pero presentan problemas de fertilidad y un índice de vida más corto [70].

La Cu,Zn-SOD puede presentar un efecto pro-oxidante, en presencia de concentraciones mM de H_2O_2 y puede generar $OH^{\cdot}$ **.** La mezcla de SOD y H_2O_2 puede catalizar la oxidación de diversos sustratos *in vitro*, como azida, sales de urato, nitrato, triptófano e histidina incluyendo los del sitio activo de la SOD [35].

Debido a la presencia de la enzima y la importancia que esta representa en la protección al daño que se produce por los radicales libres muchos autores han

apuntado al uso de ésta como blanco de fármacos, así como para componente de una vacuna.

2. HIPÓTESIS

En helmintos se sabe que la expresión de genes de Cu,Zn-SOD puede ser regulada por especies reactivas de oxigeno; el objetivo es conocer la estructura completa del gen que codifica para la superóxido dismutasa de Cu,Zn de *Taenia solium* (TsCu,Zn-SOD), su región promotora y estructural, para entender como regula la expresión del gen.

3. OBJETIVO GENERAL

Clonar y caracterizar el gen (región del promotor y estructural) que codifica para la TsCu,Zn-SOD.

4. OBJETIVOS ESPECÍFICOS

1.- Caracterización del gen (promotor proximal y región estructural).

2.- Identificar los sitios de unión de proteínas en el promotor.

3.- Evaluar la expresión de gen de la Cu,Zn-SOD en cisticercos de

Taenia crassiceps bajo condiciones normales y de estrés oxidante.

MATERIAL Y MÉTODOS

MATERIAL BIOLÓGICO

Los cisticercos de *Taenia solium* y *T. crassiceps* (cepa WFU) se obtuvieron respectivamente de músculo de cerdos infectados y del peritoneo de ratones BALB/cAnN hembras con cinco meses de infección. Los cisticercos se lavaron con SSA estéril y almacenaron a -70°C, o se usaron para la inmunolocalización de la enzima y ensayos *in vitro.*

CLONACIÓN DEL GEN DE *Cu,Zn-SOD* DE *Taenia solium*

Para clonar el gen de la Cu,Zn-SOD de *T. solium* (TsCu,Zn-SOD), se tamizó una biblioteca de ADN genómico del parásito como se describió previamente [73]. Brevemente, se obtuvo ADN genómico de cisticercos de *T. solium*, extraídos de tejido muscular de un cerdo infectado. Los cisticercos se digirieron con proteinasa K y después se purificó al ADN por medio de una columna comercial de sílica (Quiagen). El ADN genómico se digirió con la endonucleasa de restricción *Eco*RI. El producto de la digestión se analizó en geles de agarosa, para después clonarse en el bacteriófago λ-ZAP (Stratagene, La Jolla, California). Posteriormente se infectaron bacterias XL1-Blue; las clonas se transfirieron a una membrana de nitro celulosa y se hibridaron con una sonda; que consiste en un fragmento de ADN complementario de la TsCu,Zn-SOD obtenido por RT-PCR con ARN mensajero, marcada con [α-^{32}P] dTCP. Posteriormente, las membranas se expusieron a una placa de auto radiografía. El tamizaje primario consistió en generar 120, 000 unidades formadoras de placa (UFP) en una caja de cultivo Luria solido, estas se transfirieron a una membrana de nitrocelulosa, para hibridarlas con la sonda marcada, 3 placas

fueron positivas. Éstas se volvieron a tamizar del mismo modo, para obtener 3 UFP positivas. Las placas positivas se caracterizaron por PCR y digestión con enzimas de restricción EcoRI, BamHI, HindIII, para determinar el tamaño y similitud de las placas. Las placas positivas se convirtieron a plásmidos pBluescript utilizando el fago cooperador ExAssist (Stratagene). Las colonias bacterianas transferidas con pBluescript crecieron toda la noche en medio Luria-Bertani (LB) con ampicilina 100 µg/mL. Se purificó el plásmido por el protocolo estándar de lisis alcalina y se secuenció en un secuenciador ABI prism 373 (Perkin-Elmer, Applied Biosystems). Se realizó el análisis de la secuencia primaria y se identificaron los sitios catalíticos, así como los motivos característicos utilizando el programa PCGENE. Para identificar los sitios de transcripción putativos, de las secuencias en la región 5´, se utilizó el programa PROMO: (http://alggen.lsi.upc.es/cgi-bin/promo_v3/promo/promoinit.cgi?dirDB=TF_8.3). Se reportan las secuencias de factores que obtuvieron 100% de identidad con los descritos e identificados por el programa.

CLONACIÓN DEL ADN COMPLEMENTARIO (ADNc) DE *Cu,Zn-SOD* DE *T. crassiceps*

El ADN complementario de la región codificante de Cu,Zn-SOD de *T. crassiceps* se obtuvo por una reacción en cadena de la polimerasa (PCR) usando 1 µg de ADN complementario de cisticercos y dos iniciadores diseñados a partir de los primeros seis y los últimos siete aminoácidos de la TsCu,Zn-SOD (SOD-X1: 5’-ATG-AAG-GCT-GTT-TGT-GTT-3’ y SOD-X2: 5’-ATT-GCT-AAG-AGC-GAG-TGA-3’), con el programa: 1 ciclo de 94°C por 30s,

55°C por 1 min, 72°C por 1 min; y una extensión final de 72°C 5 min. Todos los productos fueron clonados en pCRII (Invitrogen).

DETERMINACIÓN DEL SITIO DE INICIO DE LA TRANSCRIPCIÓN

Para determinar el sitio de inicio de la transcripción se utilizó la técnica de amplificación de regiones 5´ de ADN complementario (RACE, por sus siglas en inglés); empleando ARN total de *T. solium*, aislado con TRIzol (Invitrogen) que se usó como molde para la determinación de sito de inicio de la transcripción (TSS).

Brevemente, se homogenizaron 100-200 mg de cisticercos de *T. solium* con un politrón en un tubo sobre hielo, se adicionaron 200 µL de cloroformo, el homogenado se incubó 5 min a temperatura ambiente y se centrifugó a 12 000xg 15 min. Después de las extracciones con fenol y cloroformo, la fase acuosa se incubó con isopropanol por 10 min. El precipitado se resuspendió en etanol al 70% y nuevamente se centrifugó en las mismas condiciones. El precipitado, se resuspendió en H_2O con dietilpirocarbonato (DEPC), y se almacenó a -70°C, hasta su uso. La amplificación del extremo 5´no traducido de los transcritos se hizo con los estuches Smart RACE cDNA Amplification y 2 Polymerase Mix (Clontech), utilizando como cebador contrasentido Cu,Zn-SOD3R (5′-TGT-GTC-ACC-GAA-TTC-GTG-GAC-GTG-3′) diseñado a partir de la secuencia de ADN complementario del gen de Ts Cu,Zn-SOD; y el cebador antisentido SMARTII (5′-AAG-CAG-TGG-TAT-CAA-CGC-AGA-GTA-CGC-GGG-3′) para el gen de TsCu,Zn-SOD. El producto resultante de cada reacción se clonó en el vector pCRII para obtener su secuencia.

SOUTHERN BLOT

El Southern blot se realizó como se describió [74] utilizando 10 µg de ADN genómico (*T. solium* and *T. crassiceps*) digerido con *Hind* III, *Bam* HI, *Eco* RI. Las digestiones se cargaron en un gel de agarosa al 1% en TAE a 0.15V / cm, y los fragmentos transferidos a una membrana de nylon (Amersham). La membrana se lavó con una solución SCC durante 5 min a temperatura ambiente y el ADN fijado a una membrana con luz UV. La membrana se hibridó con la sonda marcada radioactivamente con de ADN que codifica para la Cu,Zn-SOD de *T. solium*. La hibridación se llevó a cabo a 60^{o}C, finalmente las membranas se secaron y expusieron en placas de autoradiografía durante 24 hrs.

INMUNOELECTROTRANSFERENCIA DE GELES DE DOBLE DIMENSIÓN (2D-WB)

Se utilizó la técnica descrita por O´farrell [75], para la preparación de extractos crudos se sonicaron (500 mg) de los parásitos cuatro veces a 40W por 1 min en 250 µL de un amortiguador de lisis, reposando 1 min en hielo entre cada pulso. La suspensión de los parásitos (100 µL) se procesó con el estuche 2-D Clean-Up Kit (Amersham) siguiendo las instrucciones del fabricante. El sobrenadante (300 µg) se utilizó para hidratar las tiras de 7 cm (pH 3-10 para gradiente linear) por 16h a temperatura ambiente. El electroenfoque comenzó a 300 V (1 h), aumentó a 1000 V por 30 min, y se mantuvo a 5000 V por 2 h en una cámara IPG-phor I (GE Healthcare). Las tiras se equilibraron por 20 min en un amortiguador de rehidratación, se corrieron en un gel SDS-PAGE y transferidas a una membrana de PVDF (Millipore). Las membranas primero se

incubaron con anticuerpos anti-TsCu,Zn-SOD de conejo producidos en nuestro laboratorio (1:500), se lavaron tres veces con SSA tween-20. Los anticuerpos en las membranas fueron detectados por un segundo anticuerpo conjugado con peroxidasa de cabra anti-IgG anti-conejo (1:2000) y una solución de diaminobencidina y H_2O_2. Las membranas fueron lavadas toda la noche, como se describió antes y posteriormente incubadas con anticuerpos anti-Triosa fosfato isomerasa de *T. solium* (TPI) (1:1,000), siguiendo el procedimiento de detección previamente descrito. Como control se usó una tira de la membrana con el extracto de cada *taenia* y se incubó con IgGs normales de conejo [76].

ENSAYOS DE INMUNOFLUORESCENCIA

Se realizó como se describió previamente para otras inmunolocalicaciones landa [77] . Se colocaron cisticercos completos de *T. solium y T. crassiceps* en Tissue-Tek (Miles Laboratories), y se almacenaron a -70^{o}C. Se prepararon cortes congelados de 6-8 µm de grosor en un portaobjeto de vidrio y se incubaron con 100 µL de anticuerpos anti-TsCu,Zn-SOD (0.4 mg/mL) en SSA con albúmina de bovino 1%, 0.05% Tween 20 (SSA-BT) durante toda la noche. Los cortes se lavaron tres veces con SSA y se incubaron por 60 min a temperatura ambiente con un anticuerpo anti-IgG de conejo hecho en cabra conjugado con isotiocianato de fluoresceína (Sigma) diluido 1:50 en SSA-BT. Como control se utilizó IgG normal de conejo a la misma dilución. Los cortes se lavaron como ya se describió, se montaron en una solución de SSA con glicerol (9:1), y se fotografiaron en un microscopio de epifluorescencia Nikon Optiphot.

ANIÓN SUPERÓXIDO PRODUCIDO POR EL SISTEMA XANTINA-XANTINA OXIDASA

Se utilizó el método descrito por McCord [78] , para producir $O_2^{\cdot-}$, se disolvió xantina (Sigma) a las concentraciones de 0.001 a 0.200 mM y se mezclaron con tres diferentes concentraciones de xantina oxidasa (30, 45, 56 mU) en un mL de amortiguador de 50 mM K_2HPO_4, 10 mM EDTA, pH 7.8, 0.019 mM citocromo C (Sigma). La producción de $O_2^{\cdot-}$ en cada mezcla fue medida por la reducción de citocromo C a $D.O._{550}$ nm por 2 min. (Tabla 1).

Tabla 1. Velocidades de producción de $O_2^{\cdot-}$ (nmol/min), usando el sistema xantina-xantina oxidasa. Se combinaron diferentes concentraciones de xantina (0.001 a 0.2 mM) con tres diferentes concentraciones de xantina oxidasa (30, 45 and 56 mU). Se presenta la desviación estándar junto a las velocidades.

mU XO	30	45	56
Xanthine (mM)	(nmol/min)	(nmol/min)	(nmol/min)
0.000	0.000	0.000	0.000
0.001	0.87+/-0.05	0.12 +/-0.07	1.16 +/-0.07
0.003	1.78 +/-0.09	1.81 +/-0.01	2.34 +/-0.17
0.005	2.22 +/-0.09	2.08 +/-0.2	2.86 +/-0.18
0.007	2.27 +/-0.08	2.63 +/-0.16	3.69 +/-0.22
0.010	2.36 +/-0.06	2.81 +/-0.16	4.46 +/-0.21
0.0150	2.67 +/-0.09	3.17 +/-0.17	4.43 +/-0.18
0.020	2.86 +/-0.08	3.4 +/-0.18	4.71 +/-0.21
0.030	2.8 +/-0.07	3.49 +/-0.21	5 +/-0.13
0.040	2.77 +/-0.07	3.57 +/-0.61	5.26 +/-0.18
0.060	2.91 +/-0.08	3.63 +/-0.2	5.57 +/-0.14
0.100	2.92 +/-0.07	3.63 +/-0.21	5.74 +/- 0.14
0.150	3.11 +/-0.08	3.6 +/-0.18	5.71 +/-0.15
0.200	2.90 +/-0.07	3.80 +/-0.23	5.83 +/-0.14

VIABILIDAD DE *Taenia crassiceps* Y EXPRESIÓN DE *Cu,Zn-SOD* BAJO CONDICIONES DE ESTRÉS OXIDANTE CON $O_2^{\cdot-}$ Y H_2O_2

Todos los cisticercos de *T. crassiceps* y se preincubaron en medio RPMI (Sigma) con CO_2 0.5% por 4 h a 37°C. Grupos de 20 cisticercos se incubaron en: 1) RPMI por 0, 1, 4 y 24 h. 2) con RPMI y $O_2^{\cdot-}$ (0, 1.9, 2.9, 3.8nmol/min) por 0.5, 1, 9 y 24 h; 3) con RPMI y H_2O_2 (0, 0.25, 0.5, 1 and 2 mM) por 0.5, 6 y 24 h. Finalizados estos tiempos los parásitos se incubaron por 1 h con bilis de cerdo diluida 1:3 en RPMI para evaluar la evaginación.

La viabilidad se determinó por tres parámetros: 1) Evaginación: la capacidad del escólex para evaginar. 2) Movilidad: determinada por movimiento de tipo contráctil y 3) Daño: por observación de la pared del cisticerco en un microscopio invertido (Nikon Eclipse TS100).

Se determinó la expresión del ARN mensajero de Cu,Zn-SOD y TPI en los tres grupos de cisticercos antes mencionados. Utilizamos el estuche One Step RT-PCR (Invitrogen), con 1 µg de ARN *T. crassiceps* total como molde y los iniciadores SOD-X1 y SOD-X2 para amplificar los transcritos de la TsCu,Zn-SOD, y para los de la TPI, los iniciadores TPI-10 (5'- TAC-CTG-AAG-TAT-GCT-CAG-G -3') y TPI-12 (5'-CGC-CAA-TGC-AAG-GAA-TGA-C-3') que codifican para los aminoácidos YLKYAQD y VIPCIGE. Se utilizó el programa 50°C por 30 min para la reacción de la transcriptasa reversa y el PCR se hizo con el programa anteriormente descrito. Para determinar la expresión de la proteína de Cu,Zn-SOD y TPI se utilizaron 15 µg de extracto de *T. crassiceps* por mm lineal se cargaron en un gel de poliacrilamida con SDS-PAGE al 12%, se transfirieron a membranas de fluoruro de polivinilideno (PVDF) y se incubaron

con anticuerpos anti-TsCu,Zn-SOD y anti-TPI, siguiendo el procedimiento ya descrito.

RESULTADOS

ANÁLISIS DE LAS SECUENCIAS QUE CODIFICAN PARA EL GEN Cu,Zn DE *T. solium* Y DEL ADN*c* DE *T. crassiceps*

Las secuencias completas de *TsCu,Zn-SOD* y *TcCu,Zn-SOD* ADN complementario se depositaron en el GenBank (1444642, 1444649). Las tres clonas aisladas de la biblioteca de ADN genómico de *T. solium* fueron idénticas en tamaño (~3000 pb) y secuencia de nucleótidos. Como se observa en la figura 17, el gen de *TsCu,Zn-SOD* mide 2841pb, presenta tres exones de 66, 279 y 111 nucleótidos, separados por 2 intrones de 286 y 1448pb con los sitios donador y aceptor NGT-AGN situados entre los codones 22, 23,115 y 116. Ambos intrones presentan una secuencia de reconocimiento putativa para U1 flanqueando el sitio donador (Primer intron ^{90}GTAGGT^{95}; segundo intron: ^{655}GTATGT^{660}, numerados desde el primer nucleótido transcrito, ver más adelante subrayado), y la región rica en pirimidina para el factor de unión asociado U2 (U2AF) (Primer intron ^{635}CTTTGATGTTATCTTTAG^{653}; segundo intron: ^{2083}TTCCCTTTCTTTGTCCAG^{2101}) posicionado en el sitio aceptor (subrayado). Se encontró un sitio de poliadenilación (^{2292}AATAAA^{2298}) al final de la secuencia.

La traducción de la secuencia primaria de *T. solium* y *T. crassiceps,* revelaron un 98.47% de identidad. Ambas secuencias primarias mantienen los residuos conservados H^{40}, H^{43}, H^{45}, H^{60} y H^{61}, H^{69}, D^{81} esenciales para la unión al Cu y Zn, respectivamente. Además, tienen la R^{140} conservada que estabiliza el cobre; en donde el $O_2^{\cdot -}$ se coordina para producir O_2. Las TsCu,Zn-SOD y TcCu,Zn-SOD están formadas por una estructura llamada barril β compuestas

de dos hojas β conservadas unidas con 4 láminas cada una [79].La primera hoja β está formada por los residuos K^{2}–G^{8}, G^{15}–A^{22}, A^{25}–E^{33} y A^{92}–D^{98} y la segunda hoja β por los residuos G^{38}–H^{45}, N^{83}–G^{87}, S^{113}–H^{117} y A^{142}–G^{145}. El canal que conduce al $O_2^{\cdot-}$ al sitio activo está formado por dos asas, uno con los residuos S^{56}-K^{66} y la segunda con los residuos H^{128}–G^{139}. Es notable que ambas secuencias carecen de triptófano. Interesantemente, se observa la presencia de los aminoácidos L^{130} y I^{133} que corresponden a L^{132} y V^{135} en la Cu,Zn-SOD de *S. mansoni* [80], importantes para conducir al $O_2^{\cdot-}$ hacia el sitio activo.

El sitio de inicio de la transcripción (TSS) en *TsCu,Zn-SOD*, se ubicó a -22 nucleótidos río arriba del codón de inicio de la traducción (ATG), en donde C es el primer nucleótido transcrito. El análisis *in sílico* de la región 5´ de *TsCu,Zn-SOD* (-542 pb antes de TSS) reveló tres cajas TATA putativas (a -404, -247 y -136), al igual que reveló sitios de unión para CCAAT (a -521 y 514), AP-1 (a -491 y -414), YY1 (a -426), y NF1 (a -179 y -99), no se encontraron regiones ricas de GC. En la tabla 2, se presenta un análisis comparativo buscando sitios de inicio de la transcripción y elementos regulatorios putativos en los promotores de genes de Cu,Zn-SOD *S. mansoni*, *H. sapiens*, *Drosophila melanogaster*, comparados con *T. solium*. *Schistosoma mansoni* presenta dos cajas TATA que podrían ser funcionales y tres regiones ricas en GC, pero carece de una caja TATA. En contraste, el humano presenta sitios TATA y CCAAT que pueden ser funcionales, además de otra caja CAAT lejana y tres regiones GC. Del mismo modo *D. melanogaster* presenta una caja TATA, una CCAT y una región GC. Notablemente el mismo análisis no reveló regiones putativas de unión a factores para NF-1, AP-1 y YY1 en el promotor de Cu,Zn-

SOD de *S. mansoni* y humano. En la tabla 2 se presenta la diferencia en número, tamaño y posición de los intrones en los genes analizados.

El southern blot que se realizó con ADN genómico de *T. solium* and *T. crassiceps* reveló un patrón de restricción similar, una banda al ser digeridos con las enzimas *Hind* III (~8 kb para *T. solium* y ~7.0 kb para *T. crassiceps*), *Bam* HI (~9 Kb), y dos bandas cuando se digieren con *Eco* RI (~6.5 y ~1.8 Kb, para *T. solium* y 6.7 y 1.8 para *T. crassiceps*), ver figura 18 A.

Tabla 2. Sitio de inicio de la transcripción, y potenciales sitios de unión de elementos regulatorios de regiones promotoras de genes de Cu,Zn-SOD de *S. mansoni, H. sapiens* y *T. solium*.

Organismo (Referencias)	TSS	Caja TATA	CCAAT	Región GC	Posición de intrones (nt) (Tamaño)
S. mansoni (Mei et al., 1995)	+1 (G)	0	−142, −195	−203, −334, −351	2 150, 435 (4600, 2700)
H. sapiens (Levanon et al., 1985)	+1 (G)	−29	−72, −131	−90, −135, −172	4 153, 522, 706, 1164 (273, 114, 340, 262)
T. solium	+1 (C)	−136, −247, −404	−421, −414	0	2 88, 367 (286, 1448)
D. melanogaster (Seto et al., 1987)	+1 (A)	−321	−137	−293	1 224 (725 bp)

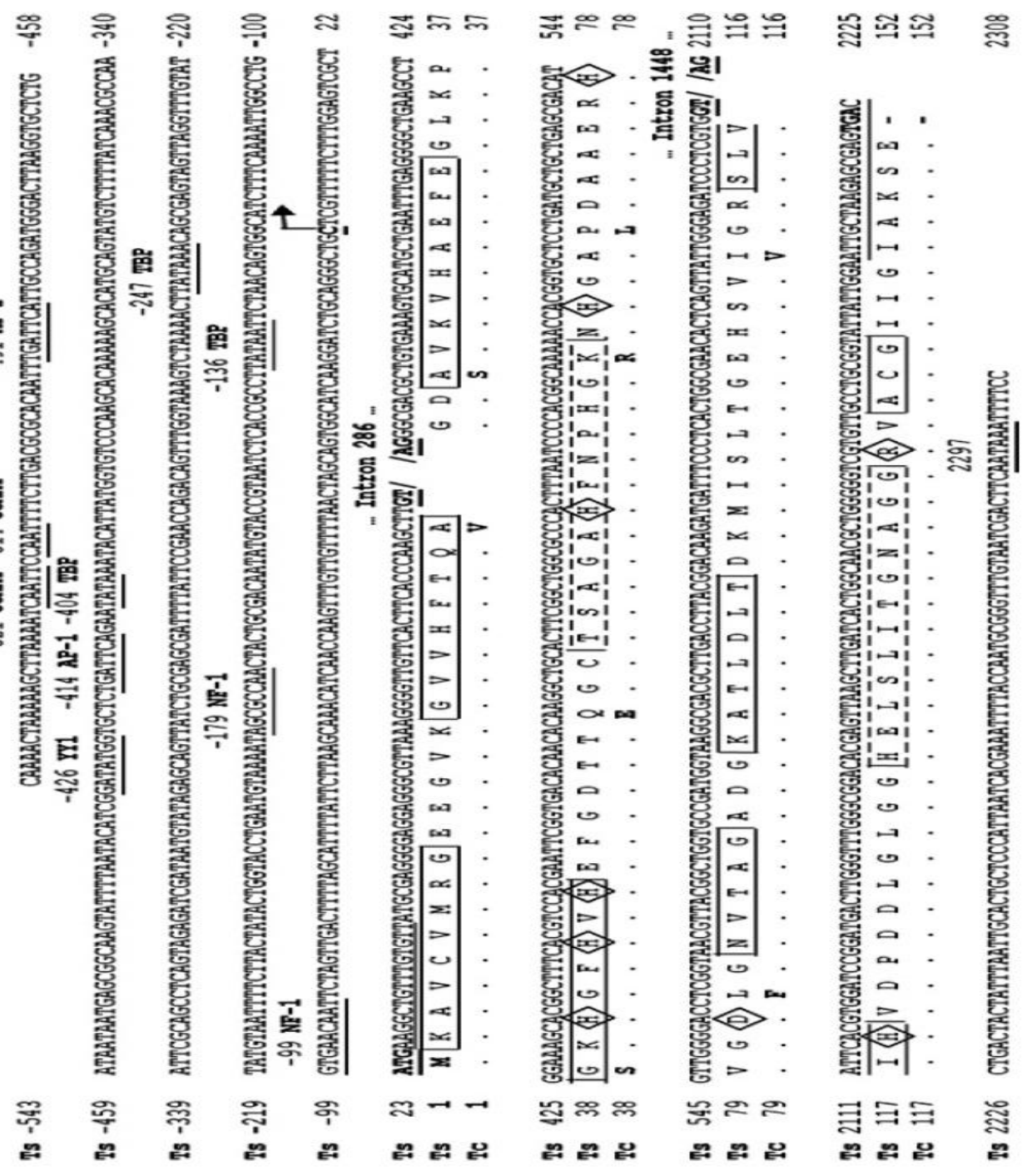

Figura 17. Secuencia de nucleótidos y aminoácidos del gen de *Cu,Zn-SOD* de *Taenia solium* (*TsCu,Zn-SOD*) y ADN complementario de *C*u,Zn-SOD *T. crassiceps* (TcCu,Zn-SOD). El sitio de inicio de la transcripción, corresponde a C marcada con una flecha. Tres cajas TATA putativas (en los sitios -404, -247 y -236), Los sitios de unión putativos para CCAAT (-491 y -414), AP1 (-491 y -414), YY1 (-426), NF1 (-179 y -99). Las secuencias aceptoras y donadoras de intrones (AG/GT), están subrayadas; los intrones están representados por // y el tamaño de cada uno está escrito arriba del signo //, y el sitio de poliadenilación está en negritas. Los aminoácidos característicos que forman en barril β de la enzima, están en cajas. Los aminoácidos que forman las asas del canal, están marcadas dentro de las cajas punteadas, los aminoácidos involucrados en la catálisis están marcados con ◊. Los codones de inicio (ATG) y de paro (TGA), la secuencia de los cebadores usados para amplificar la región codificante de la enzima están subrayados. Los diferentes aminoácidos entre *T. crassiceps* y *T. solium* están en negritas.

ANÁLISIS PROTÉOMICO Y LOCALIZACIÓN DE LA Cu,Zn-SOD DE CISTICERCOS DE *T. solium* y *T. crassiceps*

Para determinar el número de isoformas de Cu,Zn-SOD se separaron los extractos crudos de cisticercos de *T. solium* y *T. crassiceps* en geles de 2D-SDS con un intervalo de 10-100 kDa y se transfirieron a membranas de PVDF. Los anticuerpos anti-TsCu,Zn-SOD detectaron dos proteínas, una de ~32 kDa y otra de ~16 kDa en los extractos de ambas Taenias con un punto isoeléctrico cercano a 6. En contraste, se observaron dos proteínas de ~27 kDa con puntos isoeléctricos cercanos a 6.4 y 6.6 en los mismo extractos con los anticuerpos anti-TPI usados como control (En la Figura 18 B se observan únicamente los patrones de *T. crassiceps*).

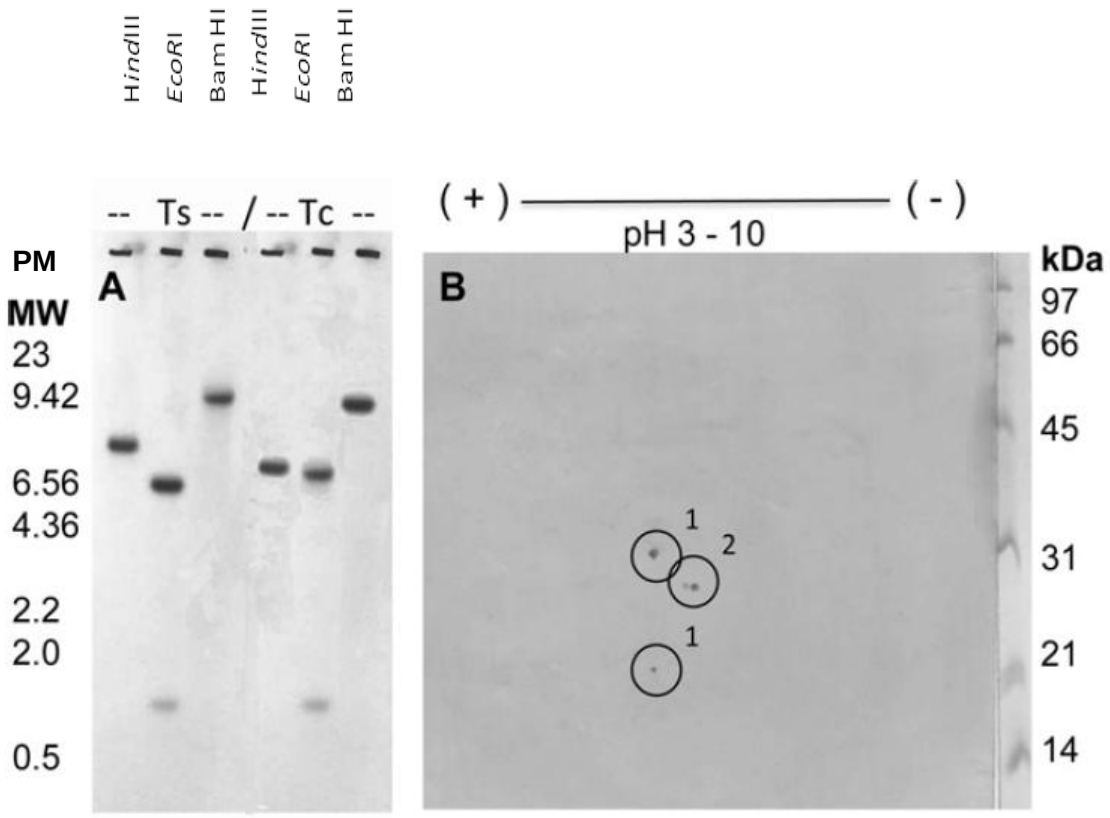

Figura 18. A) Southern blot de ADN de *Taenia solium* (Ts)S y *T. crassiceps* (Tc) digeridas con las enzimas *Hind* III, *Eco* RI y *Bam* HI. Los marcadores de peso molecular están ubicados a la izquierda. B) El western blot con extracto total de *T. crassiceps* con los anticuerpos anti-TsCu,Zn-SOD y anti-TPI. Las IgG aisladas de suero de conejo normal se usaron como control, dato no mostrado. Los marcadores de peso molecular (10-100 kDa), y punto isoeléctrico (pH 3-10) están ubicados a la derecha y sobre la figura respectivamente. Los círculos marcados con 1, representan la posición de la Cu, ZnSOD. El círculos marcado con 2 la posición de las isoformas de TPI.

Los anticuerpos anti-TsCu,Zn-SOD ubican a la enzima de manera abundante en el tegumento en el citoplasma de células subtegumentarias, células de músculo y células formadoras de canales, además está distribuida a través del parénquima y la pared de ambas Tenias (Figura 19 A y C). No se observa la tinción fluorescente en las secciones de cisticercos incubados con anticuerpos normales de conejo (Figura 19 B).

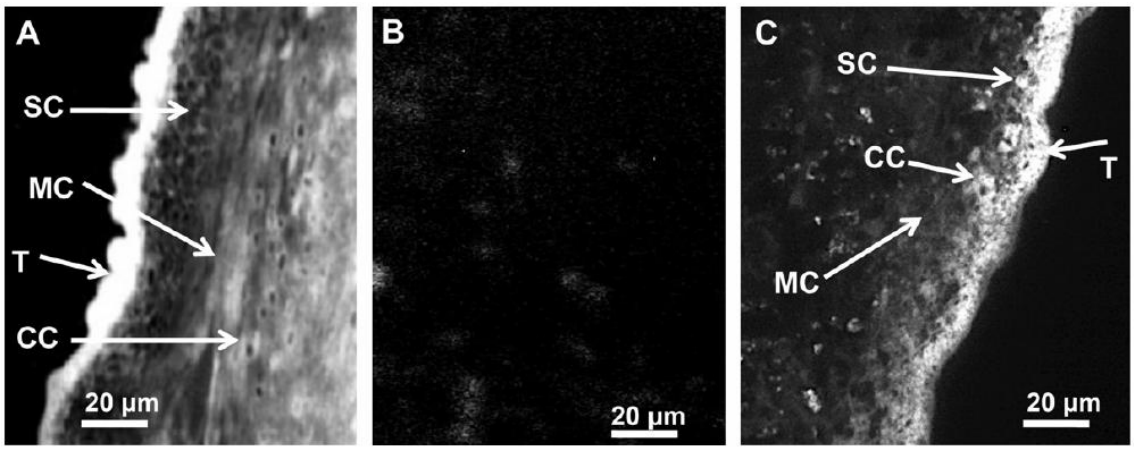

Figura 19. Localización de Cu,Zn-SOD por inmunofluorescencia indirecta sobre secciones de la pared de cisticercos de *T. solium* (A) y *T. crassiceps* (C) se expusieron a anticuerpos anti-*T. solium* Cu,Zn-SOD. Como control una sección de pared de *T. crassiceps* (B) se incubó con anticuerpos normales de conejo. Las letras y flechas muestran el tegumento (T), las células formadoras de canales (CC), los miocitos (MC), y células subtegumentarias (SC). Las barras representan una distancia =20µm.

PRODUCCIÓN DE $O_2^{\cdot -}$

El sistema de producción de $O_2^{\cdot -}$ consistió en combinar tres concentraciones de xantina oxidasa (30, 45 y 56 mU) con diferentes concentraciones de xantina (0.001 a 2.0 mM), para producir $O_2^{\cdot -}$ que es determinado por el método de xantina y xantina oxidasa con citocromo C. Los datos de la Tabla 1 revelan que las velocidades de producción de $O_2^{\cdot -}$ cuando la xantina oxidasa se mantiene constante a 30mU y mezcla con las diferentes concentraciones de xantina, se observa que la velocidad de producción de $O_2^{\cdot -}$ aumenta de 0.87 a 2.8 nmol/min, mientras que cuando la xantina oxidasa se mantiene constante a 45 ó 56mU y se mezcla con las mismas concentraciones de xantina, el aumento de las velocidades fue de 0.12 a 3.8 nmol/min; y de 1.16 a 5.83 nmol/min, respectivamente (Tabla 1, Figura 20).

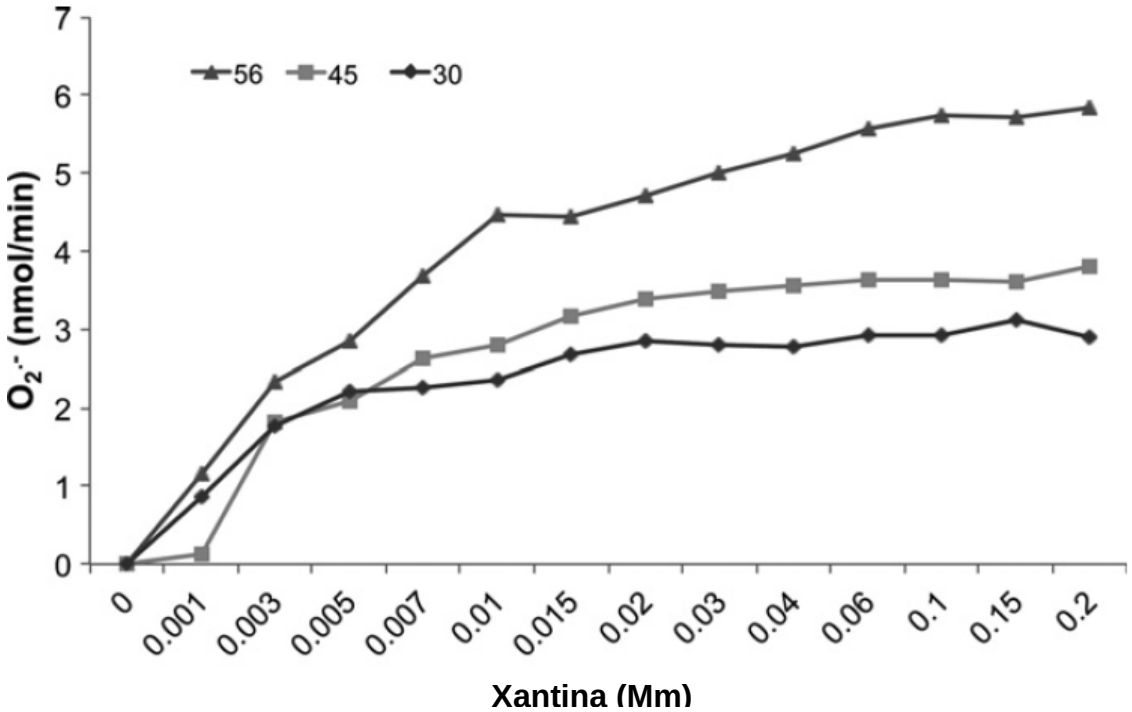

Figura 20. Las velocidades de producción de $O_2^{\cdot-}$ (nmol/min) generado con diferentes concentraciones de xantina (0.001-0.2mM) combinado con xantina oxidasa a diferentes concentraciones (30, 46 y 56mU).

EFECTO DE $O_2^{\cdot-}$ Y H_2O_2 EN CISTICERCOS DE *T. crassiceps*

La viabilidad de los cisticercos de *T. crassiceps* expuestos a concentraciones de 0, 1.9, 2.9 y 3.8 nmol/min de $O_2^{\cdot-}$ por 24 h no fue afectada en movimiento de contracción y relajamiento, evaginación y morfología. Todos los cisticercos evaginaron, mostrando movilidad normal y su morfología se mantuvo intacta al igual que en los cisticercos control (Tabla 3). No se expusieron a la máxima concentración de $O_2^{\cdot-}$ producida por el sistema (5.83 nmol/min), debido a que la xantina oxidasa fue tóxica para los cisticercos a concentraciones mayores a 45 mU.

Asimismo, cuando los cisticercos se incubaron con H_2O_2 1 y 2 mM por 24 h, permanecen sin daño aparente. En contraste, cuando los cisticercos se incubaron con H_2O_2 3 mM por 30 min, sólo evaginó el 40% los cisticercos, la movilidad, disminuyó hasta 60%, el color de los cisticercos cambió a opalescente, presentaron daño en la pared celular, determinado por la liberación de moléculas al medio. La incubación con más de 3 mM de H_2O_2 por más de 3 h destruyó completamente a los cisticercos. Los cisticercos usados como control incubados únicamente con RPMI presentaron 100% de viabilidad (Tabla 4).

Tabla 3. Efecto del $O_2^{\cdot-}$ (1.9, 2.9, y 3.8 nmol/min) en cisticercos de *Taenia crassiceps* incubados en medio RPMI a diferentes tiempos (30 min, 1, 9, and 24 h).

Tiempo (Horas)	CONTROL Solo RPMI	CONTROL Xantina oxidasa 45mU	CONTROL Xantina 0.2mM	1.9nm/min $O_2^{\cdot-}$	2.9nm/min $O_2^{\cdot-}$	3.8nm/min $O_2^{\cdot-}$
0.5	10/10 ++++ C	10/10 ++++ C	10/10 ++++ C	10/10 ++++ C	9.5/10 ++++ C	10/10 ++++ C
1	10/10 ++++ C	10/10 ++++ C	10/10 ++++ C	9.5/10 ++++ C	10/10 ++++ C	10/10 ++++ C
9	10/10 ++++ C	10/10 ++++ C	10/10 ++++ C	10/10 ++++ C	10/10 ++++ C	10/10 ++++ C
24	10/10 ++++ C	8/10 ++++ C	10/10 ++++ C	10/10 ++++ C	10/10 ++++ C	10/10 ++++ C

Se utilizaron como controles, cisticercos cultivados con xantina, xantina oxidasa y RPMI. La viabilidad se determinó por A) el % de cisticercos evaginados obtenido por: # parásitos evaginados/ total de parásitos cultivados. B) La Movilidad de los parásitos fue descrita como Alta ++++; Media +++; Moderada ++, y nula -. C) El daño en la pared del cisticerco fue descrita como: C= Cisticerco completo, M= Daño medio y N= Daño nulo.

Tabla 4. Efecto de H_2O_2 (1, 2, 3, 4, y 5 mM) en cisticercos de *Taenia crassiceps* cultivados a diferentes tiempos (0.5, 6, and 24 h).

Tiempo (Horas)	CONTROL	1.0mM	2.0mM	3.0mM	4.0mM	5.0mM
0.5	10/10 ++++ C	10/10 ++++ C	10/10 ++++ C	4/10 + M	0/10 - N	0/10 - N
6	10/10 ++++ C	10/10 ++++ C	10/10 ++++ C	0/10 - N	0/10 - N	0/10 - N
24	10/10 ++++ C	10/10 ++++ C	10/10 ++++ C	0/10 + N	0/10 - N	0/10 - N

Como control se utilizaron cisticercos cultivados en RPMI. La viabilidad fue determinada como se describió en la tabla 2.

EXPRESIÓN DE TcCu,Zn-SOD EN CONDICIONES OXIDANTES

Los niveles de expresión de ARN mensajero para la Cu,Zn-SOD y la TPI determinados por RT-PCR no cambiaron con respecto a los cisticercos controles en los ensayos realizados con cisticercos incubados solo con medio RPMI por 0, 1, 4 y 24 h (Figura 21 A), en los ensayos con cisticercos incubados con $O_2^{\cdot-}$ (2.9 y 3.8 nmol/min) por 30 minutos (Figura 21 B), ni en los ensayos donde se utilizó el H_2O_2 a las concentraciones de 0.25, 0.5,1 y 2 mM (Figura 21 C).

Por otro lado, el método de western blot con anticuerpos específicos determinó cualitativamente que los niveles de expresión a nivel de proteína de las enzimas Cu,Zn-SOD y TPI no cambiaron en los cisticercos de los ensayos donde se agregó RPMI solo o diferentes concentraciones de $O_2^{\cdot-}$, y H_2O_2 así como en los cisticercos controles (Figura 21 D).

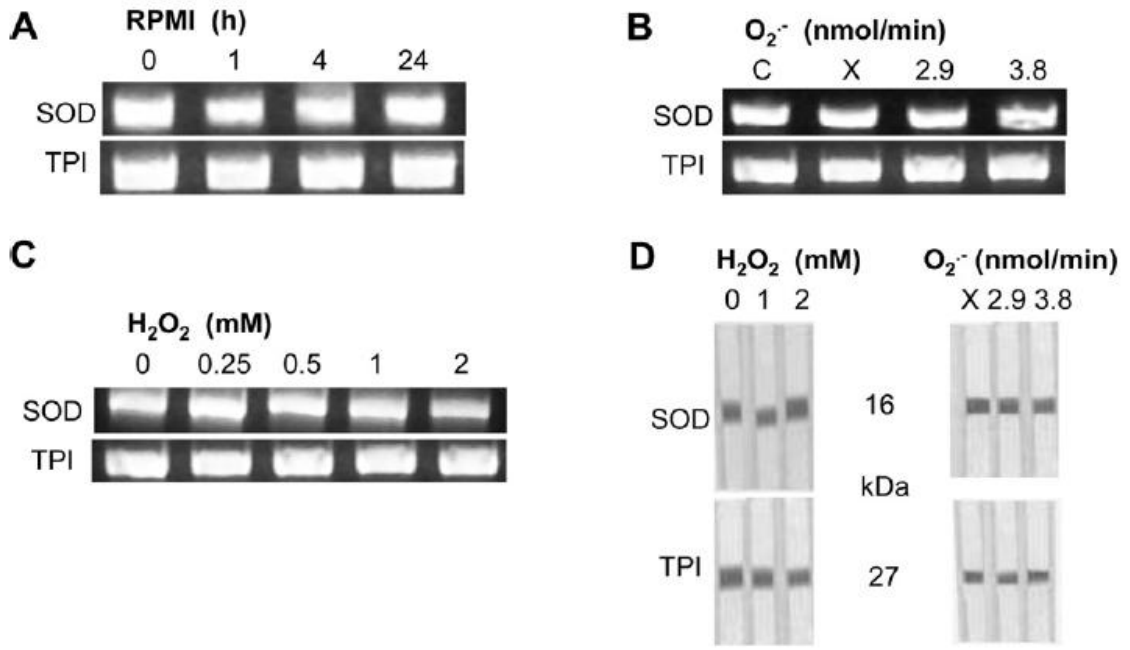

Figura 21. Expresión de Cu,Zn-SOD y TPI en cisticercos de *T. crassiceps* expuestos A) RPMI por 0, 1, 4 y 24 horas; B) RPMI^{-}, con xantina (X, 0.2mM), y RPMI con $O_2^{\cdot-}$ (2.9 y 3.8 nmol/min) por 30 minutos; C) RPMI y RPMI con H_2O_2 (0.25 a 2mM) por 30 minutos. D) Expresión de las proteínas Cu,Zn-SOD y TPI determinada por western blot, usando extractos de cisticercos incubados solo con RPMI, RPMI con $O_2^{\cdot-}$ (2.9 y 3.8 nmol/min) y RPMI con H_2O_2 (1 y 2 mM) por 30 min. Se utilizaron anticuerpos anti-Cu,Zn-SOD y anti-TPI de T. solium. Como control, 2 tiras con los extractos de cisticercos de *T. solium* and *T. crassiceps* se expusieron a una IgG purificada de suero normal de conejo, dato no mostrado.

DISCUSIÓN

En este trabajo, se clonaron el ADN genómico y el ADN complementario del gen de Cu, Zn-SOD de *T. solium* y *T. crassiceps*. Los análisis computacionales de la región promotora y estructural del gen de Cu,Zn-SOD revelaron que la estructura del gen de *TsCu,Zn-SOD* es diferente a otros genes de *Cu,Zn-SOD* en longitud, arreglo y posición de los intrones como se presenta en la tabla 2. El análisis computacional de la región 5´ de *TsCu,Zn-SOD* reveló sitios putativos de unión para la proteína de unión a la secuencia TBP y sitios CAAT, que participan en la transcripción. Cabe mencionar que los sitios que encontramos al parecer no están en una distancia apropiada para ser funcionales Figura 22 anexo. El mismo análisis reveló la presencia de sitios de unión putativos para NF1, AP-1 y YY1 que son reguladores redox positivos y negativos (es decir que aumentan ó disminuyen la expresión). Esos sitios de unión para factores de transcripción no están presentes en los genes de *Cu,Zn-SOD* de *S. mansoni* y de *Homo sapiens*. Es de hacer notar que, la región 5´del gen de *TsCu,Zn-SOD* (Céstodo) es diferente al promotor del gen de *Cu,Zn-SOD* de *S. mansoni* (Trematodo) en secuencia, y organización [56,57]; además ambos promotores son diferentes al de humano, indicando que los promotores proximales de los genes de *Cu,Zn-SOD* no están conservados (Tabla 2, figura 22), esto también sugiere que los genes de helmintos pueden ser regulados de forma diferente. Sin embargo, se deberán realizar análisis de tipo funcional para validar estas aseveraciones.

El análisis de la secuencia primaria de las enzimas de ambos parásitos reveló la presencia de los sitios característicos y de aminoácidos que participan en la catálisis de la enzima; además contienen los aminoácidos L^{130} y I^{133} similares a

(L^{132} y V^{135}) Cu,Zn-SOD de *S. mansoni*, y son diferentes de la enzima de humano. Se han sugerido éstos aminoácidos como blanco para el desarrollo de inhibidores para impedir el camino del $O_2^{\cdot-}$ al sitio activo de la Cu,Zn-SOD de parásitos [80]. El resultado de nuestro en este sentido, se describe más adelante.

El análisis de tipo southern blot sugiere que los genes que codifican para la *TsCu,Zn-SOD* y la *TcCu,Zn-SOD* son de copia única en los genomas de esos Tenidos, como se ha descrito para otros organismos [43].

En los ensayos de Western blot de una dimensión con *T. crassiceps*, la enzima es desnaturalizada con calor; en la presencia de SDS se observa una banda de 16 kDa; sin embargo los ensayos de 2D-WB se encontró el dímero 32 kDa y el monómero 16 kDa de la enzima. La no ruptura del dímero se debe a la alta resistencia a agentes desnaturalizantes como el SDS y la urea, descrita para otras Cu,Zn-SODs [43], así como a la mezcla compleja del extracto y una posible ruptura parcial de los puentes disulfuro de la proteina por parte de los agentes reductortes . Por otro lado, la Cu,Zn-SOD de *T. crassiceps*, no presenta isoformas. En cambio, encontramos que la TPI en ambos parásitos presenta dos isoformas, lo que concuerda con resultados obtenidos por Nguyen [81].

Por otro lado, los ensayos de inmunolocalización revelaron que la Cu,Zn-SOD está presente por toda la pared del cisticercos y en células subtegumentales, lo que sugiere que es sintetizada por estas, y distribuida en el parénquima de la pared, alcanzando la máxima concentración en el tegumento, lo que coincide con la localización de otras enzimas antioxidantes del parásito como las glutatión transferasas de 25 y 26 [82] y la 2-Cys peroxiredoxinas [77].

La sobre expresión de Cu,Zn-SOD y la catalasa, puede aumentar el índice de vida de *Drosophila melanogaster* [83]; la resistencia al estrés oxidante se ha asociado con la alta expresión y/o actividad de dichas enzimas antioxidantes. En el caso de los cisticercos de *T. crassiceps* pueden resistir 3.8 nmol/min de $O_2^{\cdot-}$ y 2 mM de H_2O_2 hasta por 24 horas. Notablemente, esas concentraciones son más altas que las que producen los leucocitos *in vivo* (1.03nmol $O_2^{\cdot-}$ /1x10^7 células) [84] y 0.01 nmol de H_2O_2/2.5x10^{-6} células [85]).

Los experimentos de expresión del ARN mensajero y proteína de la Cu,Zn-SOD con cisticercos de *T. cracciceps* expuestos y no expuestos a diferentes concentraciones de $O_2^{\cdot-}$ y H_2O_2 revelaron que los niveles del transcrito y proteína para la Cu,Zn-SOD son constantes, lo que indica que el gen se expresa constitutivamente. La no respuesta a los estímulos por $O_2^{\cdot-}$ y H_2O_2, puede deberse a que el promotor no contiene sitios que puedan ser regulados por estos compuestos manteniendo la expresión constante. Por otro lado los sistemas generadores empleados para producir $O_2^{\cdot-}$ en otros organismos, en donde si hay variación de la expresión de SODCu,Zn, requieren de acetaldehído, el cual mostró ser tóxico para *T. crassiceps*. Es posible ésta variación en los niveles de expresión de ARN mensajero en esos organismos, se deba a los sistemas generadores utilizados, así como a la toxicidad de los compuestos que se utilizan.

La estabilidad de la enzima, la alta eficiencia catalítica (~7 x 10^9 $M^{-1}s^{-1,}$ para $O_2^{\cdot-}$) [86]; la localización en el tegumento y la expresión constitutiva del gen en todas las células del cisticerco indica que la Cu,Zn-SOD juega un papel regulatorio y defensivo contra las EROs producidas por el metabolismo normal y las células inmunes del hospedero [43]. Es claro que las células deben

mantener un delicado balance entre las concentraciones de $O_2^{\cdot -}$ producido y que debe removerse, para mantener el metabolismo normal celular. Actualmente, hay poca información respecto a los mecanismos que controlan la expresión de los genes de SOD en los céstodos. Además, se deben realizar estudios para identificar las moléculas de señalización y factores que pueden ser importantes en la transcripción de Cu,Zn-SOD, así como entender el papel que este gen tiene en la relación hospedero-parásito.

Además de los resultados obtenidos en este proyecto, es importante resaltar el de nuestras colaboraciones, en donde una vez obtenida la estructura cristalográfica con apoyo del grupo de la Dra. Adela Rodríguez en el instituto de química de la UNAM [9], se realizaron análisis de docking en colaboración del Dr. Arturo Rojo en la UAM Iztapalapa [52]. De acuerdo a nuestros resultados, la búsqueda de fármacos se enfocó en compuestos que se unen a las diferencias que existen entre la SOD de *Homo sapiens* y la de *T. solium*. Se utilizó la biblioteca LeadQuest, que contiene las coordenadas bidimensionales de la estructura química de más de 50 mil compuestos orgánicos. Inicialmente se obtuvieron alrededor de 2,500,000 confórmeros. Se ensayaron y evaluaron 15 mil orientaciones de prueba en la colocación de cada uno de los ligandos sobre los dos sitios potenciales de unión localizados en el receptor, restringiendo la mayoría de la simulación del anclaje molecular a dos sitios ubicados en el canal. Bajo estas condiciones se observó unión por parte de los primeros 30 mil confórmeros de la base de datos a dichos sitios. Se hizo un refinamiento de los complejos para obtener mejores puntajes y lograr un reordenamiento de los mismos en función de la afinidad predicha. De los resultados obtenidos en esta última simulación del anclaje molecular, se seleccionaron los 500 mejores

puntajes (los mejores 500 complejos proteína-ligando simulados), posteriormente se seleccionaron de entre ellos a los mejores cien compuestos de acuerdo con criterios como: energía de interacción entre el ligando y la molécula receptora; número de enlaces tipo puente de hidrógeno formados con cadenas laterales de la molécula blanco ausentes en la SOD humana; complementariedad geométrica, hidrófobica y electrostática y peso molecular menor a 400 g/mol. Estos compuestos fueron ensayados como inhibidores de la actividad de la Cu,Zn-SOD de *T. solium* mediante experimentos directos con la enzima. Siete compuestos tuvieron actividad inhibitoria parcial y uno total, sin afectar la actividad de la SOD de *Homo sapiens*.

Es importante que los parásitos tengan mecanismos de defensa contra las EROs que se producen en la respuesta inmune. Existe poca información respecto a los mecanismos que controlan la expresión de los genes de SOD en los céstodos. Se deben hacer más estudios para identificar moléculas y factores que sean importantes en la transcripción de estos genes, para poder entender el papel de enzimas como la Cu, Zn-SOD en la relación huésped parásito.

CONCLUSIONES

Se describió la estructura y organización del gen que codifica para la TsCu,Zn-SOD.

La estructura del gen es diferente a otros genes de Cu,Zn-SOD.

Posiblemente el gen de la Cu,Zn-SOD, es una enzima de copia única y se expresa de manera constitutiva.

La enzima no presenta isoformas y es parcialmente resistente a agentes desnaturalizantes como el SDS y urea.

T. crassiceps resiste concentraciones de $O_2^{\cdot -}$ y H_2O_2 más altas a las producidas *in vivo* (1.03nmol $O_2^{\cdot -}$ /1x10^7 células) [84] y 0.01 nmol de H_2O_2/2.5x10^{-6} células [85]).

El conjunto de resultados obtenidos, abre la posibilidad de desarrollar un fármaco para causar daño a estos parásitos, utilizando a la Cu,Zn-SOD como blanco.

Figuras Anexas

Figura 22. Alineamiento múltiple de secuencias de promotor de Cu,Zn-SOD de *S. mansoni*, *H. sapiens*, *y T. solium*. Aquí se muestran los sitios regulatorios como: Regiones GC (Subrayadas), secuencias CAAT (Cajas en gris), Cajas TATA putativas, en negritas y subrayadas los sitios de inicio de transcripción de cada secuencia

```
S.mansoni       -571 CCGCGTGGCCAGTCCATGGAGTACGATTTATTTGTGCGCGTTGACTATCC  -520
H.sapiens       -701 -------CCAACTAGTTGCCGTTTGGTTATCTGTAGGGTTGTGGCCTTGC  -657
T.solium        -568 --------CAAAACTAAAAAGCTT-AAAATCAATTCCAATTTCTTGACG  -525
                             *.* :. ::. .* :  .:::: :  :  .   *     :

S.mansoni       -521 TTGACCTGGACAGGGACCAATGATCAGTTCGATATT-CAGTGACCCTACA  -471
H.sapiens       -658 CAAACAGG---AAAAATATAAAAGAATACCGAATT-CTG----CCAACC  -614
T.solium        -526 CGCACAAT---TTGATTCATTGCGCAAAACTAAAAAGCTT----AAAATC  -482
                       **.     : ..: .:::..  *.::* .:*:: *:     ..:* .

S.mansoni        -472 AGGTTCGGTGAACTGTTCGACATCCAGTGACCTAAGTGCCGGATGATTTG  -421
H.sapiens        -615 AAATAAGAAACTCTATACTAAGGACTAAGAAAATTGCAGGGGAAGAAAAG  -564
T.solium         -483 AATTCCAATTTCTTGACG-CGCACAATTGATTCATTGCTGGTGCTCTG  -433
                      *. * ...:  :**  :*  .. .*:.: : .:: .     *.:*.: :*

S.mansoni        -422 GCTAGGGCCCG---------GTGACATTTCACTAACCCTACAACAGTTCT  -380
H.sapiens        -565 GTAAGTCCCGGGATTGAGGTGTAGCGACTTTCTATACCCTCAG-AAAACT  -515
T.solium         -434 ATTCAGAATAT--------AAATACATTATGGTGTCCCAAGCACAAAAAG  -391
                      . :..  .            .: .*.: :   *.:.** : .. *.::.

S.mansoni        -381 AAACTACTTGATAATAAGTTTGCATCAGATATGTCCTCATTCTT------  -336
H.sapiens        -516 AAAAAACAAGACAAAAAAATGAAAACTACAAAAGCATCCATCTTGGGGCG  -465
T.solium         -392 CACATGCAGTATGTCTTTTATCAAACGCCAAATTCG-CAGCCT-------  -349
                      .*..:.*:  * .: :: ::  .*:*  .:*:  *  *.  **

S.mansoni        -337 --CCTGTT--TTAAAAACATGGAATTCACG-AGGACACTCTAAGAATGTT  -291
H.sapiens        -466 TCCCAATTGCTGAGTAACAAATGAGACGCTGTGGCCAAACTCAGTCATAA  -415
T.solium         -350 ---CAGTAGAGATCGATAATGTATAGAGCAGTTATCTGCGAGCGATTTTA  -302
                        *:.*:    :  *:.*:. .:  ..*  : . *:   : .*: : ::

S.mansoni        -292 CACAAGCCCGGAACAAATTACTTATCGTCTGACTGTCGAG----------  -251
H.sapiens        -416 CTAATGACATTTCTAGACAAAGTGACTTCAGATTTTCAAAGCGTACCCTG  -365
T.solium         -303 TTCCGAACCAGACAG--TTTGGTAAAGTCTAAAACTTATA----------  -264
                      :.. ..*.  :. .   ::  *.:. **:.* : * .:.

S.mansoni        -252 -------------------------TCATCAACGAATGGAACTCGTTAC  -227
H.sapiens        -366 TTTACATCATTTTGCCAATTTCGCGTACTGCAACCGGCGGGCCACGCCCC  -315
```

```
T.solium          -265 ----------------------------AACAGCGAGTAGTTAGG---TT  -245
                                                   : **.* .. .*  .

S.mansoni         -228 CTCAATATGTGG----TTGAATCTCCATCAGTGGACGCTCTAAAATAGAT  -181
H.sapiens         -316 CGTGAAAAGAAGGTTGTTTTCTCCACATTTCGGGGTTCTGGACGTTTCCC  -265
T.solium          -246 TGTATTATGTAA-----TTTTCTTACTATACTGGTACCTGAATGTAAAAT  -200
                              .::*:*:..     * :    .*:: :  **   **  * .::: .

S.mansoni         -182 GTTGGATTA----GCTGAGAGACCATCAG---TGCCCAAG-ACTAGCATA  -139
H.sapiens         -266 GGCTGCGGG----GCGGGGGGAGTCTCCGGCGCACGCGCC-CCTTGCCCC  -220
T.solium          -201 AGCGCCAACTACTGCGACAATATGTACCG-TAATCTCACCGCCTTATAAT  -151
                            .    .       ** . .. *   :*.*     * *..  .**:. .

S.mansoni         -140 AGCCACCCAGTCTCCTGTCCTTTCTCGTCTG--------------AAACT  -103
H.sapiens         -221 GCCCCCAGTCATTCCCGGCCACTCGCGACCCGAGGCTGCCGCAGGGGGCG  -170
T.solium          -152 TCTAACAGTGGCATCTTTCAAAATTGGCCTGG------------TGAACA  -113
                              ..*. :   : *   *.: :   * *               ...*

S.mansoni         -104 TAGTTAGGCCGTTCAAG--------------GTCGTAGAAAAAAACGCGG  -67
H.sapiens         -171 GGCTGAGCGCGTGCGAGGCGATTGGTTTGGGGCCAGAGTGGGCGAGGCGC  -120
T.solium          -114 ATTCTAGTTGACTTTTAG------------CATTTTATTCTTAAGCAAAC  -75
                                **   .    :.             .    * :   ... ...

S.mansoni         -68  TTGTTTCTG--------------------AAAGTGGTGTGGATTTTCGTC  -37
H.sapiens         -121 GGAGGTCTGGCCTATAAAGTAGTCGCGGAGACGGGGTGCTGGTTTGCGTC  -70
T.solium          -76  ATCAACCAAG-------------------TTTGTTGTTTTAACTAGCAGT  -44
                                *:.                    : *  **   .. *: *.

S.mansoni         -38  GTG-TCTCCT-------------------------------CAACCTATT  -21
H.sapiens         -71  GTAGTCTCCTGCAGCGTCTGGGGTTTCCTTGCAGTCCTCGGAACCAGGAC  -20
T.solium          -45  GGCATCAAGG------------------------------ATCTGCAGGGC  -23
                       *   **:.                                .: *. .

S.mansoni         -20  TTTTACAAAGTCATACGAGG----ATG +3
H.sapiens         -21  CTCGGCGTGGCCTAGCGAGTT---ATG +3
T.solium          -24  TGCTCGTTTTTCTTTGGAGTCGCTATG +3
                             :   *::  ***     ***
```

Figura 23. Alineamiento de secuencia primaria de SODs Cu, Zn de *T. crassiceps*, *T. solum*, *Bos taurus* y *Homo sapiens*.

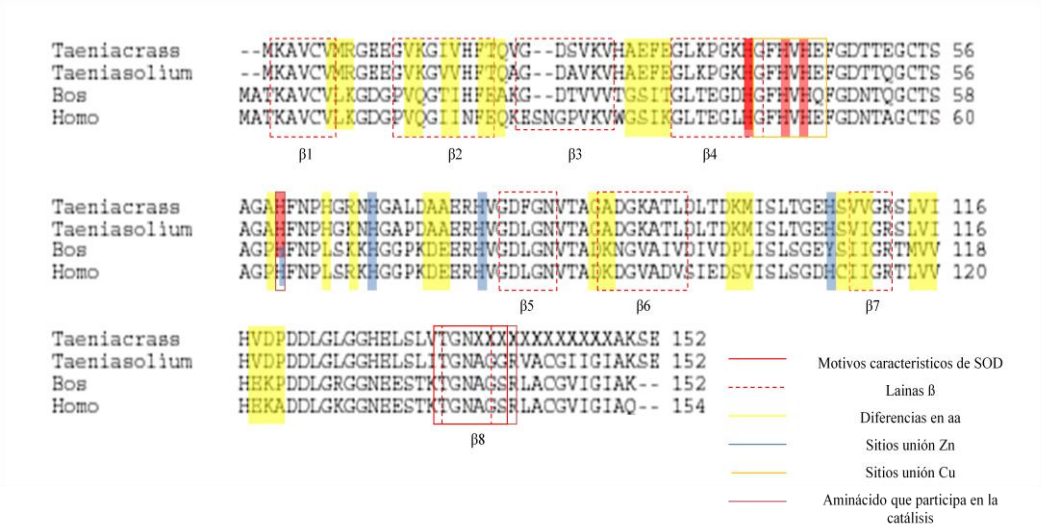

ANEXO REACTIVOS
Amortiguador de lisis 2D

Urea	8 M
CHAPS	0.5 M
Pepstatina	1 µM
Leupeptin	0.6 µM
Fenilmetanisulfonil fluoruro	0.2 mM
DTT	0.5 mM

Aforar a un litro

AMORTIGUADOR DE LISIS (Bacterias para ADN)

Tris	50mM
EDTA	0.1 mM
Sarcosil	0.5%

Ajustar pH 8.0 y aforar a un litro

Amortiguador de rehidratación

SDS	2%
Tris-HCl	50mM
Urea	6 M
Glicerol	30%
DTT	0.5%
Azul de bromofenol	0.002%
Ajustar pH 8.8	

Aforar a un litro

AMORTIGUADOR SALINO DE FOSFATOS (SSA Ó PBS 10X)

NaCl	137mM	80.0g
KCl	2.7mM	2.0g
$Na_2HPO_4 7H_2O$	4.3mM	11.5g

Ajustar a pH7.4 y aforar a un litro.

AMORTIGUADOR SALINO DE FOSFATOS pH 7.8

K_2HPO_4	50mM	6.80g

Ajustar a pH7.8 y aforar a un litro.

Amortiguador TE

Tris-HCl	10 mM
EDTA	1mM

Aforar a un litro

MEDIO DE CULTIVO LURIA BERTANI (LB)

NaCl	5.8g	
$MgSO_4\,7H_2O$	2.0g	
Tris-HCl pH 7.5	1M	50.0mL
Gelatina al 2%	5.0mL	

Todos los componentes del medio de cultivo se diluyen y aforan a 1L con agua desionizada. El pH del medio se ajusta a 7.0 y se esteriliza en autoclave durante 20min a 15Lb de presión en ciclo líquido.

PREPARACIÓN DE GEL DE AGAROSA AL 1.5 % + BROMURO DE ETIDIO

Para cuatro geles: Disolver 2.4 g de agarosa en 160 mL de TAE 1X, adicionar 36 µL de bromuro de etidio, mezclar bien y verter en los moldes. Dejar solidificando a 4 °C.

SSA-Tween 0.3% (AMORTIGUADOR SALINO DE FOSFATOS-TWEEN)

(SSA 10X)

NaCl	137mM	80.0g
KCl	2.7mM	2.0g
$Na_2HPO_47H_2O$	4.3mM	11.5g

Ajustar a pH7.4 y aforar a un litro. Hacer una dilución 1:10 con agua destilada y agregar: TWEEN-20 0.3%

SSC (Buffer de transferencia de ácidos nucleícos) (20x SSC)

Tris-citrato de sodio	88.23g
NaCl	175.32g

Agregar aproximadamente 800 mL de agua destilada. Mezclar. Verificar pH entre 7-8. Aforar a un litro.

TAE (Amortiguador de electroforesis de ADN) (50x)

Tris base	242 g
Ácido etilen diamino tetracético (EDTA)	18.6 g

Ajustar pH 8, con ácido acético glacial

Aforar a un litro

REFERENCIAS

[1] F. Diaz, H.H. Garcia, R.H. Gilman, A.E. Gonzales, M. Castro, V.C. Tsang, J.B. Pilcher, L.E. Vasquez, M. Lescano, C. Carcamo, et al., Epidemiology of taeniasis and cysticercosis in a Peruvian village. The Cysticercosis Working Group in Peru, Am J Epidemiol 135 (1992) 875-882.

[2] C. Mignard, D. Mignard, J.B. Dandelot, J.P. Polydor, J.P. Laporte, C. Bousquet, Y. Choucair, A. Michault, [Epidemiologic survey of the cysticercosis endemic on Reunion Island], Rev Neurol (Paris) 142 (1986) 635-637.

[3] M. Dumas, K. Grunitzky, M. Belo, F. Dabis, M. Deniau, B. Bouteille, Y. Kassankogno, G. Catanzano, M.P. Alexandre, [Cysticercosis and neurocysticercosis: epidemiological survey in North Togo], Bull Soc Pathol Exot 83 (1990) 263-274.

[4] A. Carpio, Neurocysticercosis: an update, Lancet Infect Dis 2 (2002) 751-762.

[5] E. Sarti, V. Rajshekhar, Measures for the prevention and control of Taenia solium taeniosis and cysticercosis, Acta Trop 87 (2003) 137-143.

[6] E. Sarti, P.M. Schantz, A. Plancarte, M. Wilson, I.O. Gutierrez, A.S. Lopez, J. Roberts, A. Flisser, Prevalence and risk factors for Taenia solium taeniasis and cysticercosis in humans and pigs in a village in Morelos, Mexico, Am J Trop Med Hyg 46 (1992) 677-685.

[7] N. Vibanco-Perez, L. Jimenez, M.T. Merchant, A. Landa, Characterization of glutathione S-transferase of Taenia solium, J Parasitol 85 (1999) 448-453.

[8] A. Castellanos-Gonzalez, L. Jimenez, A. Landa, Cloning, production and characterisation of a recombinant Cu/Zn superoxide dismutase from Taenia solium, Int J Parasitol 32 (2002) 1175-1182.

[9] A. Hernandez-Santoyo, A. Landa, E. Gonzalez-Mondragon, M. Pedraza-Escalona, R. Parra-Unda, A. Rodriguez-Romero, Crystal structure of Cu / Zn superoxide dismutase from Taenia solium reveals metal-mediated self-assembly, FEBS J 278 (2011) 3308-3318.

[10] R. Zurabian, L. Aguilar, J.A. Jimenez, L. Robert, K. Willms, Evagination and infectivity of Taenia crassiceps cysticerci in experimental animals, J Parasitol 94 (2008) 1-6.

[11] K. Willms, Morphology and biochemistry of the pork tapeworm, Taenia solium, Curr Top Med Chem 8 (2008) 375-382.

[12] K. Willms, R. Zurabian, Taenia crassiceps: in vivo and in vitro models, Parasitology 137 (2010) 335-346.

[13] E. Sciutto, G. Fragoso, A. Fleury, J.P. Laclette, J. Sotelo, A. Aluja, L. Vargas, C. Larralde, Taenia solium disease in humans and pigs: an ancient parasitosis disease rooted in developing countries and emerging as a major health problem of global dimensions, Microbes Infect 2 (2000) 1875-1890.

[14] A. Landa, L. Jimenez, K. Willms, L.F. Jimenez-Garcia, R. Lara-Martinez, L. Robert, O. Cirioni, W. Baranska-Rybak, W. Kamysz, Antimicrobial peptides (Temporin A and Iseganan IB-367): effect on the cysticerci of Taenia crassiceps, Mol Biochem Parasitol 164 (2009) 126-130.

[15] R. Lamothe-Argumedo, et al. , Helmintiasis del hombre en México. Tratamiento y profilaxis, AGT editor, México, 1988.
[16] A. Flisser, R. Perez-Montfort, C. Larralde, The immunology of human and animal cysticercosis: a review, Bull World Health Organ 57 (1979) 839-856.
[17] E. Sarti Gutierrez, P.M. Schantz, J. Aguilera, A. Lopez, Epidemiologic observations on porcine cysticercosis in a rural community of Michoacan State, Mexico, Vet Parasitol 41 (1992) 195-201.
[18] P.M. Schantz, E. Sarti-Gutierrez, Diagnostic methods and epidemiologic surveillance of Taenia solium infection, Acta Leiden 57 (1989) 153-163.
[19] E. Sarti, P.M. Schantz, A. Plancarte, M. Wilson, O.I. Gutierrez, J. Aguilera, J. Roberts, A. Flisser, Epidemiological investigation of Taenia solium taeniasis and cysticercosis in a rural village of Michoacan state, Mexico, Trans R Soc Trop Med Hyg 88 (1994) 49-52.
[20] J.H. Theis, R.S. Goldsmith, A. Flisser, J. Koss, C. Chioino, A. Plancarte, A. Segura, D. Widjana, P. Sutisna, Detection by immunoblot assay of antibodies to Taenia solium cysticerci in sera from residents of rural communities and from epileptic patients in Bali, Indonesia, Southeast Asian J Trop Med Public Health 25 (1994) 464-468.
[21] A. Plancarte, M. Fexas, A. Flisser, Reactivity in ELISA and dot blot of purified GP24, an immunodominant antigen of Taenia solium, for the diagnosis of human neurocysticercosis, Int J Parasitol 24 (1994) 733-738.
[22] N. Deckers, P. Dorny, Immunodiagnosis of Taenia solium taeniosis/cysticercosis, Trends Parasitol 26 (2010) 137-144.
[23] M. Barry, L.C. Kaldjian, Neurocysticercosis, Semin Neurol 13 (1993) 131-143.
[24] J. Sotelo, P. Penagos, F. Escobedo, O.H. Del Brutto, Short course of albendazole therapy for neurocysticercosis, Arch Neurol 45 (1988) 1130-1133.
[25] G. Roman, J. Sotelo, O. Del Brutto, A. Flisser, M. Dumas, N. Wadia, D. Botero, M. Cruz, H. Garcia, P.R. de Bittencourt, L. Trelles, C. Arriagada, P. Lorenzana, T.E. Nash, A. Spina-Franca, A proposal to declare neurocysticercosis an international reportable disease, Bull World Health Organ 78 (2000) 399-406.
[26] O.H. Del Brutto, Medical management of neurocycticercosis, Int J Antimicrob Agents 3 (1993) 133-137.
[27] J. Sotelo, O.H. Del Brutto, Therapy of neurocysticercosis, Childs Nerv Syst 3 (1987) 208-211.
[28] O.H. Del Brutto, The use of albendazole in patients with single lesions enhanced on contrast CT, N Engl J Med 328 (1993) 356-357.
[29] P.M. Schantz, M. Cruz, E. Sarti, Z. Pawlowski, Potential eradicability of taeniasis and cysticercosis, Bull Pan Am Health Organ 27 (1993) 397-403.
[30] J.S. O. H. Del Brutto, and G. C. Roman, Neurocysticercosis: A Clinical Handbook, Swets & Zeitlinger, The Netherlands, 1998.
[31] M. Cruz, I. Cruz, J. Horton, Clinical evaluation of albendazole and praziquantel in the treatment of cerebral cysticercosis, Southeast Asian J Trop Med Public Health 22 Suppl (1991) 279-283.

[32] M. Cruz, I. Cruz, J. Horton, Albendazole versus praziquantel in the treatment of cerebral cysticercosis: clinical evaluation, Trans R Soc Trop Med Hyg 85 (1991) 244-247.
[33] O.H. Del Brutto, [Neurocysticercosis: up-dating in diagnosis and treatment], Neurologia 20 (2005) 412-418.
[34] M.C. Romano, R.A. Valdez, A.L. Cartas, Y. Gomez, C. Larralde, Steroid hormone production by parasites: the case of Taenia crassiceps and Taenia solium cysticerci, J Steroid Biochem Mol Biol 85 (2003) 221-225.
[35] B. Halliwell, Reactive oxygen species and the central nervous system, J Neurochem 59 (1992) 1609-1623.
[36] P.A. Southorn, G. Powis, Free radicals in medicine. II. Involvement in human disease, Mayo Clin Proc 63 (1988) 390-408.
[37] P.A. Southorn, G. Powis, Free radicals in medicine. I. Chemical nature and biologic reactions, Mayo Clin Proc 63 (1988) 381-389.
[38] H. Sies, Strategies of antioxidant defense, Eur J Biochem 215 (1993) 213-219.
[39] G.M. Rosen, S. Pou, C.L. Ramos, M.S. Cohen, B.E. Britigan, Free radicals and phagocytic cells, FASEB J 9 (1995) 200-209.
[40] H.J. Forman, M. Torres, Reactive oxygen species and cell signaling: respiratory burst in macrophage signaling, Am J Respir Crit Care Med 166 (2002) S4-8.
[41] T.M. Buetler, A. Krauskopf, U.T. Ruegg, Role of superoxide as a signaling molecule, News Physiol Sci 19 (2004) 120-123.
[42] K.H. Cheeseman, T.F. Slater, An introduction to free radical biochemistry, Br Med Bull 49 (1993) 481-493.
[43] K. Henkle-Duhrsen, A. Kampkotter, Antioxidant enzyme families in parasitic nematodes, Mol Biochem Parasitol 114 (2001) 129-142.
[44] H.L. Callahan, R.K. Crouch, E.R. James, Helminth anti-oxidant enzymes: a protective mechanism against host oxidants?, Parasitol Today 4 (1988) 218-225.
[45] P.M. Brophy, D.I. Pritchard, Immunity to helminths: Ready to tip the biochemical balance?, Parasitol Today 8 (1992) 419-422.
[46] S. McGonigle, G.P. Curley, J.P. Dalton, Cloning of peroxiredoxin, a novel antioxidant enzyme, from the helminth parasite Fasciola hepatica, Parasitology 115 (Pt 1) (1997) 101-104.
[47] J.D. Crapo, T. Oury, C. Rabouille, J.W. Slot, L.Y. Chang, Copper,zinc superoxide dismutase is primarily a cytosolic protein in human cells, Proc Natl Acad Sci U S A 89 (1992) 10405-10409.
[48] I. Fridovich, Superoxide radical and superoxide dismutases, Annu Rev Biochem 64 (1995) 97-112.
[49] L. Tang, X. Ou, K. Henkle-Duhrsen, M.E. Selkirk, Extracellular and cytoplasmic CuZn superoxide dismutases from Brugia lymphatic filarial nematode parasites, Infect Immun 62 (1994) 961-967.
[50] E.R. James, D.C. McLean, Jr., F. Perler, Molecular cloning of an Onchocerca volvulus extracellular Cu-Zn superoxide dismutase, Infect Immun 62 (1994) 713-716.
[51] B.L. Beaman, C.M. Black, F. Doughty, L. Beaman, Role of superoxide dismutase and catalase as determinants of pathogenicity of Nocardia asteroides: importance in resistance to microbicidal activities of human polymorphonuclear neutrophils, Infect Immun 47 (1985) 135-141.

[52] P. Garcia-Gutierrez, A. Landa-Piedra, A. Rodriguez-Romero, R. Parra-Unda, A. Rojo-Dominguez, Novel inhibitors to Taenia solium Cu/Zn superoxide dismutase identified by virtual screening, J Comput Aided Mol Des 25 (2011) 1135-1145.
[53] L. Miao, D.K. St Clair, Regulation of superoxide dismutase genes: implications in disease, Free Radic Biol Med 47 (2009) 344-356.
[54] I.N. Zelko, T.J. Mariani, R.J. Folz, Superoxide dismutase multigene family: a comparison of the CuZn-SOD (SOD1), Mn-SOD (SOD2), and EC-SOD (SOD3) gene structures, evolution, and expression, Free Radic Biol Med 33 (2002) 337-349.
[55] J. Khalife, C. Godin, A. Capron, Transcriptional regulation of Schistosoma mansoni calreticulin: possible role of AP-1, Parasitology 111 (Pt 4) (1995) 469-475.
[56] E. Serra, K. Zemzoumi, J. Trolet, A. Capron, C. Dissous, Functional analysis of the Schistosoma mansoni 28 kDa glutathione S-transferase gene promoter: involvement of SMNF-Y transcription factor in multimeric complexes, Mol Biochem Parasitol 83 (1996) 69-80.
[57] H. Mei, H. Hirai, M. Tanaka, Z. Hong, D. Rekosh, P.T. LoVerde, Schistosoma mansoni: cloning and characterization of a gene encoding cytosolic Cu/Zn superoxide dismutase, Exp Parasitol 80 (1995) 250-259.
[58] H. Mei, P.T. LoVerde, Schistosoma mansoni: cloning the gene encoding glutathione peroxidase, Exp Parasitol 80 (1995) 319-322.
[59] W. Tawe, R.D. Walter, K. Henkle-Duhrsen, Onchocerca volvulus superoxide dismutase genes: identification of functional promoters for pre-mRNA transcripts which undergo trans-splicing, Exp Parasitol 94 (2000) 172-179.
[60] W.N. Tawe, M.L. Eschbach, R.D. Walter, K. Henkle-Duhrsen, Identification of stress-responsive genes in Caenorhabditis elegans using RT-PCR differential display, Nucleic Acids Res 26 (1998) 1621-1627.
[61] U.E. Zelck, B. Von Janowsky, Antioxidant enzymes in intramolluscan Schistosoma mansoni and ROS-induced changes in expression, Parasitology 128 (2004) 493-501.
[62] A. Ben-Smith, D.A. Lammas, J.M. Behnke, Effect of oxygen radicals and differential expression of catalase and superoxide dismutase in adult Heligmosomoides polygyrus during primary infections in mice with differing response phenotypes, Parasite Immunol 24 (2002) 119-129.
[63] R.W. Leid, C.M. Suquet, A superoxide dismutase of metacestodes of Taenia taeniaeformis, Mol Biochem Parasitol 18 (1986) 301-311.
[64] H.L. Callahan, R.K. Crouch, E.R. James, Dirofilaria immitis superoxide dismutase: purification and characterization, Mol Biochem Parasitol 49 (1991) 245-251.
[65] R. Gonzalez, G. Mendoza-Hernandez, A. Plancarte, Purification of Taenia solium cysticerci superoxide dismutase and myoglobin copurification, Parasitol Res 88 (2002) 881-887.
[66] T.S. Kim, Y. Jung, B.K. Na, K.S. Kim, P.R. Chung, Molecular cloning and expression of Cu/Zn-containing superoxide dismutase from Fasciola hepatica, Infect Immun 68 (2000) 3941-3948.
[67] H. Mei, P.T. LoVerde, Schistosoma mansoni: the developmental regulation and immunolocalization of antioxidant enzymes, Exp Parasitol 86 (1997) 69-78.

[68] S. Liddell, D.P. Knox, Extracellular and cytoplasmic Cu/Zn superoxide dismutases from Haemonchus contortus, Parasitology 116 (Pt 4) (1998) 383-394.
[69] Y. Li, T.T. Huang, E.J. Carlson, S. Melov, P.C. Ursell, J.L. Olson, L.J. Noble, M.P. Yoshimura, C. Berger, P.H. Chan, D.C. Wallace, C.J. Epstein, Dilated cardiomyopathy and neonatal lethality in mutant mice lacking manganese superoxide dismutase, Nat Genet 11 (1995) 376-381.
[70] Y.S. Ho, M. Gargano, J. Cao, R.T. Bronson, I. Heimler, R.J. Hutz, Reduced fertility in female mice lacking copper-zinc superoxide dismutase, J Biol Chem 273 (1998) 7765-7769.
[71] J.M. Mates, C. Perez-Gomez, I. Nunez de Castro, Antioxidant enzymes and human diseases, Clin Biochem 32 (1999) 595-603.
[72] J.M. Mates, F. Sanchez-Jimenez, Antioxidant enzymes and their implications in pathophysiologic processes, Front Biosci 4 (1999) D339-345.
[73] F. Vaca-Paniagua, R. Parra-Unda, A. Landa, Characterization of one typical 2-Cys peroxiredoxin gene of Taenia solium and Taenia crassiceps, Parasitol Res 105 (2009) 781-787.
[74] E.M. Southern, Detection of specific sequences among DNA fragments separated by gel electrophoresis, J Mol Biol 98 (1975) 503-517.
[75] P.H. O'Farrell, High resolution two-dimensional electrophoresis of proteins, J Biol Chem 250 (1975) 4007-4021.
[76] H. Towbin, T. Staehelin, J. Gordon, Electrophoretic transfer of proteins from polyacrylamide gels to nitrocellulose sheets: procedure and some applications, Proc Natl Acad Sci U S A 76 (1979) 4350-4354.
[77] J. Molina-Lopez, L. Jimenez, A. Ochoa-Sanchez, A. Landa, Molecular cloning and characterization of a 2-Cys peroxiredoxin from Taenia solium, J Parasitol 92 (2006) 796-802.
[78] J.M. McCord, I. Fridovich, Superoxide dismutase. An enzymic function for erythrocuprein (hemocuprein), J Biol Chem 244 (1969) 6049-6055.
[79] J.A. Tainer, E.D. Getzoff, K.M. Beem, J.S. Richardson, D.C. Richardson, Determination and analysis of the 2 A-structure of copper, zinc superoxide dismutase, J Mol Biol 160 (1982) 181-217.
[80] R.M. Cardoso, C.H. Silva, A.P. Ulian de Araujo, T. Tanaka, M. Tanaka, R.C. Garratt, Structure of the cytosolic Cu,Zn superoxide dismutase from Schistosoma mansoni, Acta Crystallogr D Biol Crystallogr 60 (2004) 1569-1578.
[81] H.A. Nguyen, Y.A. Bae, E.G. Lee, S.H. Kim, S.P. Diaz-Camacho, Y. Nawa, I. Kang, Y. Kong, A novel sigma-like glutathione transferase of Taenia solium metacestode, Int J Parasitol 40 (2010) 1097-1106.
[82] N. Vibanco-Perez, L. Jimenez, G. Mendoza-Hernandez, A. Landa, Characterization of a recombinant mu-class glutathione S-transferase from Taenia solium, Parasitol Res 88 (2002) 398-404.
[83] W.C. Orr, R.S. Sohal, Extension of life-span by overexpression of superoxide dismutase and catalase in Drosophila melanogaster, Science 263 (1994) 1128-1130.
[84] B.M. Babior, R.S. Kipnes, J.T. Curnutte, Biological defense mechanisms. The production by leukocytes of superoxide, a potential bactericidal agent, J Clin Invest 52 (1973) 741-744.

[85] R.K. Root, J. Metcalf, N. Oshino, B. Chance, H2O2 release from human granulocytes during phagocytosis. I. Documentation, quantitation, and some regulating factors, J Clin Invest 55 (1975) 945-955.
[86] P. Heinrich, Georg, L., Petro, E.P, Biochemie und Pathobiochemie (2006).

ARTICLE IN PRESS

Experimental Parasitology xxx (2011) xxx–xxx

Contents lists available at SciVerse ScienceDirect

Experimental Parasitology

journal homepage: www.elsevier.com/locate/yexpr

Cu,Zn superoxide dismutase: Cloning and analysis of the *Taenia solium* gene and *Taenia crassiceps* cDNA

Parra-Unda Ricardo, Vaca-Paniagua Felipe, Jiménez Lucia, Landa Abraham *

Departamento de Microbiología y Parasitología, Facultad de Medicina, Universidad Nacional Autónoma de México, Edificio A, 2do Piso, Ciudad Universitaria, México D.F. 04510, Mexico

ARTICLE INFO

Article history:
Received 20 April 2011
Received in revised form 25 July 2011
Accepted 3 October 2011
Available online xxxx

Keywords:
Taenia solium
Taenia crassiceps
Cu,Zn superoxide dismutase
Superoxide
Gene

ABSTRACT

Cytosolic Cu,Zn superoxide dismutase (Cu,Zn-SOD) catalyzes the dismutation of superoxide (O_2^-) to oxygen and hydrogen peroxide (H_2O_2) and plays an important role in the establishment and survival of helminthes in their hosts. In this work, we describe the *Taenia solium Cu,Zn-SOD* gene (*TsCu,Zn-SOD*) and a *Taenia crassiceps* (*TcCu,Zn-SOD*) cDNA. *TsCu,Zn-SOD* gene that spans 2.841 kb, and has three exons and two introns; the splicing junctions follow the GT-AG rule. Analysis *in silico* of the gene revealed that the 5′-flanking region has three putative *TATA* and *CCAAT* boxes, and transcription factor binding sites for *NF1* and *AP1*. The transcription start site was a C, located at 22 nucleotides upstream of the translation start codon (ATG). Southern blot analysis showed that *TcCu,Zn-SOD* and *TsCu,Zn-SOD* genes are encoded by a single copy. The deduced amino acid sequences of *TsCu,Zn-SOD* gene and *TcCu,Zn-SOD* cDNA reveal 98.47% of identity, and the characteristic motives, including the catalytic site and β-barrel structure of the Cu,Zn-SOD.

Proteomic and immunohistochemical analysis indicated that Cu,Zn-SOD does not have isoforms, is distributed throughout the bladder wall and is concentrated in the tegument of *T. solium* and *T. crassiceps* cysticerci. Expression analysis revealed that *TcCu,Zn-SOD* mRNA and protein expression levels do not change in cysticerci, even upon exposure to O_2^- (0–3.8 nmol/min) and H_2O_2 (0–2 mM), suggesting that this gene is constitutively expressed in these parasites.

1. Introduction

Superoxide dismutase (SOD) catalyzes the dismutation of superoxide anion (O_2^-) to oxygen and hydrogen peroxide (H_2O_2); therefore, it is a key enzyme in the production of reactive oxygen species (ROS) in cells (Winterbourn, 1993). Eukaryotic organisms have three genes coding for superoxide dismutase: a MnSOD located in mitochondria, one in the cytosol (Cu,Zn-SOD) and one extracellular (ECCu,Zn-SOD) (Fridovich, 1995). Knockout mice for Mn-SOD$^{-/-}$ die a few days after birth (Li et al., 1995), and knockout organisms (Cu,Zn-SOD$^{-/-}$) exhibit a decreased growth rate and shortened life span (Phillips et al., 1989; Reveillaud et al., 1994).

Analysis of Cu,Zn-SOD proximal promoters in mammals have identified regulatory regions like GC-rich, TATA box, and binding sites for NF-KB, AP1, AP-2, Sp1, NF1, GRE, HSF as well as CCAAT-enhancer binding protein (C/EBP) (Miao and St Clair, 2009). By using mammalian cell transformation systems in helminthes, potential regulatory regions such as TATA and CCAAT boxes and AP-1 sites have been found in the core promoter of the calreticulin gene (Khalife et al., 1995). Additionally, an AP-1 site and three CCAAT boxes were reported in the glutathione transferase (GST) of the 28 kDa gene promoter of *Schistosoma mansoni* (Serra et al., 1996). In the case of *Cu,Zn-SOD* promoters, a transcription start site (TSS), two CAAT boxes, and three GC-rich regions in *S. mansoni* (Mei et al., 1995), and the presence of Inr-like elements in two *Onchocerca volvulus* promoters (*Ov-sod-1* and *Ov-sod-2*) have been described (Tawe et al., 2000).

Cu,Zn-SOD gene expression is regulated by physical, chemical, and biological stimuli, such as temperature, X-ray and UVB radiations, heavy metals, phagocytosis, O_2^-, H_2O_2, O_3, and NO_2 (Zelko et al., 2002). For example, it is known that O_2^- increases transcription levels of Cu,Zn-SOD in *S. mansoni* miracidia, sporocyst and cercaria (Zelck and Von Janowsky, 2004); likewise, it increases mRNA levels of Mn-SOD and Cu,Zn-SODs in *Caenorhabditis elegans* larval stage (Tawe et al., 1998). Moreover, H_2O_2 augments Cu,Zn-SOD transcription expression levels in *S. mansoni* (Zelck and Von Janowsky, 2004). In addition, catalase and Cu,Zn-SOD enzymatic activity levels increase in *Heligmosomoides polygyrus* female worms isolated from infected mice with different resistance phenotypes (Ben-Smith et al., 2002).

Previously, we characterized a complementary DNA (cDNA) from *Taenia solium* superoxide dismutase (TsCu,Zn-SOD) and its recombinant product (Castellanos-Gonzalez et al., 2002). In this

* Corresponding author. Fax: +52 55 56232358.
E-mail address: landa@servidor.unam.mx (A. Landa).

0014-4894/$ - see front matter © 2011 Published by Elsevier Inc.
doi:10.1016/j.exppara.2011.10.002

Please cite this article in press as: Parra-Unda, R., et al. Cu,Zn superoxide dismutase: Cloning and analysis of the Taenia solium gene and Taenia crassiceps cDNA. Exp. Parasitol. (2011), doi:10.1016/j.exppara.2011.10.002

work, we describe and analyze the *TsCu,Zn-SOD* gene and compare its primary sequence with a cDNA coding for Taenia crassiceps superoxide dismutase (TcCu,Zn-SOD). Furthermore, we determined the mRNA and protein level expression in *Taenia crassiceps* cysticerci exposed to O_2^- and H_2O_2 *in vitro*.

2. Materials and methods

2.1. Biological materials

T. solium and *T. crassiceps* (WFU strain) cysticerci were obtained from infected pork muscle and from the peritoneum of BALB/cAnN female mice at 5 months of infection. Cysticerci were washed with sterile PBS and stored at −70 °C, or used for immunolocalization and *in vitro* assays.

2.2. *T. solium* Cu,Zn-SOD gene and *T. crassiceps* cDNA cloning

Preparation of the *T. solium* genomic DNA and screening of 100,000 clones from a ZAPII genomic DNA library of *T. solium* cysticerci were carried out as previously described (Campos et al., 1990), using a probe of full length cDNA encoding for TsCu,Zn-SOD. Two genomic clones of ~3000 bp were obtained and sequenced on an automated DNA sequencer ABI Prism model 373 (Perkin-Elmer, Applied Biosystems).

T. crassiceps Cu,Zn-SOD cDNA coding region was obtained by polymerase chain reaction (PCR) using 1 μg of cDNA from cysticerci and primers designed for the first six and last seven amino acids of TsCu,Zn-SOD (forward SOD–X1: 5′-ATG–AAG–GCT–GTT–TGT–GTT-3′ and reverse SOD–X2: 5′-ATT-GCT–AAG–AGC–GAG–TGA-3′) running the following cycles: 1 at 94 °C for 3 min, 30 at 94 °C for 30 s, at 55 °C for 1 min, at 72 °C for 1 min; and a final extension at 72 °C for 5 min. All PCR products were cloned into pCRII (Invitrogen) and the plasmid was prepared and sequenced as before. The sequences were analyzed using the program PROMO: (http://alggen.lsi.upc.es/cgi-bin/promo_v3/promo/promoinit.cgi?dirDB=TF_8.3). Only putative transcription factor binding sites with a 100% score were selected.

2.3. Transcription start site determination

T. solium and *T. crassiceps* total RNA were prepared with TRIzol (Invitrogen) and used as template for transcription start site (TSS) determination, using Smart RACE cDNA Amplification Kit (Clontech). 5′-RACE fragments amplified with reverse primer Cu,Zn-SOD3R (5′-TGT-GTC-ACC-GAA-TTC-GTG-GAC-GTG-3′) and forward primer SMARTII (5′-AAG-CAG–TGG-TAT-CAA-CGC–AGA–GTA-CGC-GGG-3′) were cloned and sequenced.

2.4. Southern blot

Southern blot was performed using 10 μg of genomic DNA (*T. solium* and *T. crassiceps*) digested with *Hind* III, *Bam* HI, *Eco* RI, resolved on a 1% agarose gel and blotted on a nylon membrane (Amersham). Prehybridization and hybridization were performed according to Sambrook et al. (1989) and the same probe was used for the screening of *T. solium* DNA library.

2.5. Western blot of 2-dimension gels (2D–WB)

Crude extracts of parasites (500 mg) were sonicated four times at 40 W (1 min) in 250 μL of buffer (8 M urea, 0.5 M CHAPS, 1 μM pepstatin, 0.6 μM leupeptin, 0.2 mM phenylmethanesulfonyl fluoride, 0.5 mM DTT), leaving 1 min on ice between each pulse. Parasite suspension (100 μL) was processed with 2D Clean-Up Kit (Amersham) following manufacturer's instructions. The supernatant (300 μg) was applied on 7-cm strips (pH 3–10 linear gradient) for 16 h at room temperature for rehydration. Focusing started at 300 V (1 h), increased to 1000 V for 30 min, and maintained at 5000 V for 2 h in an IPG-phor I unit (GE Healthcare). Strips were equilibrated 20 min in 1X Laemmli sample loading buffer (63 mM Tris–HCl, pH 6.8, 2% SDS, 30% glycerol, 1% 2-mercaptoethanol, and 0.002% bromophenol blue), run in a 12% SDS–PAGE and transferred to PVDF membrane (Millipore). Membranes were incubated first with anti-TsCu,Zn-SOD (1:500) antibodies for 1 h and then washed three times with PBS Tween-20 (0.3%). Antibodies in membranes were detected by a second antibody peroxidase-conjugated goat anti-rabbit IgG (1:2000) and a solution of diaminobenzidine and H_2O_2. Membranes that reacted with anti-TsCu,Zn-SOD were washed overnight as described before, and incubated with anti-*T. solium* triose phosphate isomerase antibodies (TTPI) (1:1000), following the procedure of detection described before. A membrane strip of each Taeniid extract was incubated with normal rabbit IgG as control (Towbin et al., 1979).

2.6. Immunofluorescence assays

T. crassiceps and *T. solium* cysticerci were embedded in Tissue-Tek (Miles Laboratories), frozen in liquid nitrogen, and stored at −70 °C. Frozen sections of 6–8 μm thick were prepared and incubated overnight with 100 μL of anti-TsCu,Zn-SOD (0.4 mg/mL) antibodies in PBS with 1% BSA, 0.05% Tween 20 (PBS-BT) overnight. Sections were rinsed three times with PBS and incubated 60 min at room temperature with FITC-conjugated goat anti-rabbit IgG (Sigma) diluted 1:50 in PBS-BT. Normal rabbit IgG was used as control at the same concentration of first antibody. Sections were rinsed, as before, mounted on a glycerol–PBS solution (9:1), and photographed in a Nikon Optiphot epifluorescence microscope.

2.7. Superoxide anion produced by xanthine-xanthine oxidase system

To produce O_2^-, xanthine (Sigma) was dissolved at concentrations from 0.001 to 0.200 mM and mixed with three different concentrations of xanthine oxidase (30, 45, and 56 mU) in 1 mL of 50 mM K_2HPO_4, 10 mM EDTA, pH 7.8, 0.019 mM cytochrome C (Sigma). The production of O_2^- in each mixture was measured by reduction of cytochrome C at $OD_{550\,nm}$ for 2 min (McCord and Fridovich, 1969).

2.8. *T. crassiceps* viability and Cu,Zn-SOD expression under oxidative conditions with O_2^- and H_2O_2

Groups of 20 *T. crassiceps* cysticerci were incubated either in: (1) RPMI (Sigma) plus 0.5% CO_2 at 37 °C for 0, 1, 4, and 24 h; and for next assays the cysticerci were preincubated 4 h in RPMI, before being exposed to: (2) RPMI with O_2^- (0, 1.9, 2.9, and 3.8 nmol/min) for 0.5, 1, 9, and 24 h; 3) RPMI with H_2O_2 (0, 0.25, 0.5, 1, and 2 mM) for 0.5, 6, and 24 h. Parasites were further incubated for 1 h in pig bile diluted 1:3 with RPMI to measure evagination. Viability was estimated by: (1) evagination, i.e., capacity of the scolex to evaginate. (2) Contractile movements. (3) Damage in the cysticerci bladder wall, observing in an inverted microscope (Nikon Eclipse TS100).

Messenger RNA expression of Cu,Zn-SOD and TPI were determined in the same groups of cysticerci described before. To detect messenger RNA, we used the One Step RT-PCR kit (Invitrogen), with 1 μg of *T. crassiceps* total RNA as template and primers SOD–X1 and SOD–X2; for TPI, primers were TPI–30 (5′-TAC-CTG–AAG-TAT-GCT-CAG-G-3′) and TR–12 (5′-CGC-CAA-TGC-AAG-GAA-TGA-C-3′) coding for YLKYAQD and VIPCIGE amino acids of TTPI. The program used for reverse transcriptase reaction was at 50 °C for 30 min; and for PCR the program described above. To determine Cu,Zn-SOD protein expression a western blot method was

Please cite this article in press as: Parra-Unda, R., et al. Cu,Zn superoxide dismutase: Cloning and analysis of the Taenia solium gene and Taenia crassiceps cDNA. Exp. Parasitol. (2011), doi:10.1016/j.exppara.2011.10.002

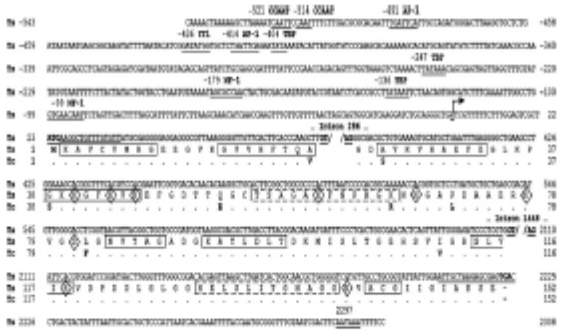

Fig. 1. Sequence of nucleotides and amino acids of Taenia solium Cu,Zn-SOD (TsCu,Zn-SOD) gene and a T. crassiceps Cu,Zn-SOD (TcCu,Zn-SOD) cDNA. Transcription start site (TSS) corresponds to a C marked with an arrow. Three putative TATA boxes, the putative binding sites for CCAAT C/EBP, AP1, YY1, NF1 are numbered, underlined and labeled under the sequence. Acceptor and donor intron sequences (AC/CT) are underlined, intron sizes are represented by //, and it in bold. Characteristic amino acids that form the β-barrel of enzyme are in boxes, amino acids that form the loops of the channel are marked inside the dotted box, and amino acids involved in the catalysis are marked with ◇. Start (ATG) and stop (TGA) codons, polyadenylation signal, and sequence of primers used to amplify coding region of enzyme are underlined. The differences in amino acids between T. crassiceps and T. solium are marked in bold.

used. Around 15 μg/lane of *T. crassiceps* cysticerci extract were boiled for 5 min with 2-mercaptoethanol and loaded in a 12% SDS–PAGE, and transferred to PVDF membranes. Membranes were incubated with anti-TsCu,Zn-SOD and anti-TTPI antibodies, following the procedure before described (Laemmli, 1970).

3. Results

3.1. Nucleotide sequence analysis of *T. solium Cu,Zn-SOD* gene and *T. crassiceps* cDNA

Sequences of *TsCu,Zn-SOD* gene and TcCu,Zn-SOD cDNA were deposited in GeneBank with the ID numbers: 1445298 and 1445306, respectively. The two genomic clones isolated from the *TsCu,Zn-SOD* gene were identical in size (~3000 pb) and nucleotide sequence. As seen in Fig. 1, the *TsCu,Zn-SOD* gene spans 2841 bp and has three exons of 66, 279, and 111 nt, separated by two introns of 286 and 1448 pb that present NGT-AGN donor–acceptor sites placed between codons 22 and 23, and 115 and 116. Both introns showed a putative U1 recognition sequence (first intron: ^{90}GTAGGT^{95}; second intron and: ^{655}GTATGT^{660}, showing the donor site underlined), and a pyrimidine-rich tract for U2 Associated Factor (U2AF) binding (first intron ^{655}CTTTGATGTTATCTTTAG^{674}; second intron: and ^{2083}TTCCCTTTCTTTGTGCAG^{2101}) positioned in the acceptor site (underlined). At the end of the sequence a conserved polyadenylation site (^{2287}AATAAA^{2292}) was found.

The predicted primary sequence from *T. solium* and *T. crassiceps* showed 98.47% identity, and both maintain the conserved residues (H^{46}, H^{48}, H^{63}, H^{80}) and (H^{61}, H^{69}, H^{78}, and D^{81}) essential for Cu and Zn binding, respectively. The sequences also have the conserved R^{140} that stabilizes the Cu; where O_2^- is coordinated to produce O_2. Likewise, the TsCu,Zn-SOD and TcCu,Zn-SOD proteins form a β-barrel structure composed of two conserved β sheets with four strands each (Tainer et al., 1982). The first β sheet is formed by residues K^2 to D^{16}, and the second β sheet by residues G^{36} to G^{45}. The channel that leads the O_2^- to the catalytic center is formed by two loops, one with residues S^{38} to K^{46} and the second with residues H^{120} to G^{139}. Interestingly, we observed in the second loop the presence of the amino acids L^{130} and I^{133} that correspond to L^{132} and V^{135} in *S. mansoni* Cu,Zn-SOD (Cardoso et al., 2004).

The transcription start site (TSS) in *TsCu,Zn-SOD* gene was mapped at −22 nucleotides upstream from the translation start codon (ATG), where a C is the first nucleotide transcribed. In these experiments we did not find any splice leader sequence in the *TsCu,Zn-SOD* transcript. Analysis *in silico* of the 5′-flanking region corresponding to −542 bp before the TSS of *TsCu,Zn-SOD* gene revealed three putative TATA boxes (−404, −247, and −136 respective to TSS), putative binding sites for CCAAT (−521, −514), AP-1 (−491, −414), YY1 (−426), and NF1 (−179, −99), and no GC-rich hexanucleotide elements were found. Table 1 shows a comparison analysis looking for TSS, and putative transcription regulatory elements in the 5′-flanking region of Cu,Zn-SOD genes from *S. mansoni*, *H. sapiens*, *Drosophila melanogaster* with *T. solium*. Schistosoma shows two CCAAT boxes and three copies of the GC-rich hexanucleotide, but lack of a TATA box. In contrast, human present a TATA and a CCAAT sites that could be functional, and other CAAT box and three GC-rich hexanucleotide sequences. Likewise, *D. melinogaster* presents a TATA, a CCAT boxes and one GC-rich hexanucleotide. Noteworthy, the same analysis did not find putative transcription factor binding sites for NF1, AP-1, and YY1 in the 5′-flanking region of the *S. mansoni* and human *Cu,Zn-SOD* genes. The same Table 1 shows the difference in number, size and position of introns in the Cu,Zn-SOD genes analyzed. The Southern blot using genomic DNA from *T. solium* and *T. crassiceps* displayed a similar restriction pattern; one band when they are digested with the enzymes *Hind* III, and *Bam* HI, and two bands when digested with *Eco* RI, see Fig. 2A.

3.2. *Cu,Zn-SOD proteomic analysis and localization in T. solium and T. crassiceps cysticerci*

To determine the number of Cu,Zn-SOD isoforms, we resolved *T. solium* and *T. crassiceps* cysticerci crude extracts in 2D-SDS gels with a range of 10–100 kDa and transferred them to PVDF membranes. Anti-TsCu,Zn-SOD antibodies detected two spots (one strong ~32 kDa and one weak ~16 kDa) in both Taeniid extracts with a pI close to six. In contrast, two spots of ~27 kDa with pI of 6.4 and 6.6 were observed in the same membranes in a second blot when anti-TTPI antibodies were used as positive control

Please cite this article in press as: Parra-Unda, R., et al. Cu,Zn superoxide dismutase: Cloning and analysis of the Taenia solium gene and Taenia crassiceps cDNA. Exp. Parasitol. (2011), doi:10.1016/j.exppara.2011.10.002

Table 1
Transcription start site (TSS) and potential regulatory elements from *S. mansoni*, *H. sapiens*, and *T. solium* Cu,Zn-SOD gene promoter sequences.

Organism (References)	TSS	TATA box	CCAAT	GC-rich hexanucleotide	Introns position (nt) (size bp)
S. mansoni (Mei et al., 1995)	+1 (C)	0	−142, −195	−203, −334, −351	2 1 50, 435 (4600, 2700)
H. sapiens (Levanon et al., 1985)	+1 (C)	−29	−72, −131	−90, −135, −172	4 1 53, 522, 706, 1164 (273, 114, 340, 262)
T. solium	+1 (C)	−136, −247, −404	−421, −614	0	2 818, 367 (286, 1448)
D. melanogaster (Seto et al., 1987)	+1 (A)	−321	−137	−293	1 2.24 (72.5 bp)

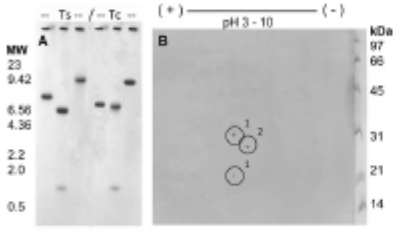

Fig. 2. (A) Southern blot of DNA of *Taenia solium* (Ts) and *T. crassiceps* (Tc) digested with enzymes *Hind* III, *Eco* RI and *Bam* HI. Size DNA markers are shown on the left. (B) 2D-western blot of *T. crassiceps* total extract with antibodies anti-TcCu,Zn-SOD and anti-TTPI. The IgG isolated from normal rabbit serum was used as control. Molecular weight protein (10–100 KDa) and isoelectric point (pH 3–10) markers are written on the right and top of the figure, respectively.

(Fig. 2B shows only the *T. crassiceps* patterns). No spots reacted with normal rabbit IgG used as negative control.

Anti-TcCu,Zn-SOD antibodies located the enzyme abundantly in the cytoplasm of tegumentary cytons, muscle and channel forming cells and distributed through the parenchyma of the bladder wall in both Taeniids (Fig. 3A and C). No fluorescent staining was observed in control sections of cysticerci incubated with normal rabbit serum (Fig. 3B).

3.3. O_2^- anion production

Fig. 4 shows the velocity of production of O_2^-, when xanthine oxidase was maintained constant at 30 mU and mixed with the different concentrations of xanthine (0.001–2.0 mM). The production of O_2^- increased from 0.87 to 2.8 nmol/min. Conversely, when xanthine oxidase was maintained constant at 45 or 56 mU and mixed with the same concentrations of xanthine described above, the production increased from 0.12 to 3.8 nmol/min; and from 1.95 to 5.83 nmol/min, respectively. The system was used to generate the quantity required of O_2^- used in the assays.

3.4. Effect of O_2^- and H_2O_2 on *T. crassiceps* cysticerci

T. crassiceps cysticerci exposed to 0, 1.9, 2.8, and 3.8 nmol/min of O_2^- remained unaffected up to 24 h. All cysticerci evaginated, had normal motility, and their morphology remained intact when compared with control cysticerci (data no shown). We did not use the highest concentration of O_2^- (5.83 nmol/min) produced by the system, because xanthine oxidase alone at 56 mU was toxic for cysticerci.

Additionally, cysticerci incubated with H_2O_2 (1 and 2 mM) for 24 h remained unaffected. In contrast, the cysticerci incubated with H_2O_2 (3 mM) for 30 min, exhibited 40% of evagination and their mobility decreased ~75%; also they became opalescent, presented wall damage, and released tissue into the medium. Cysticerci exposed to more than 3 mM H_2O_2, and after 6 h, were completely destroyed. Control cysticerci cultivated in RPMI presented 100% viability (Table 2).

3.5. *TcCu,Zn-SOD expression under oxidant conditions*

The Cu,Zn-SOD and TPI mRNA expression levels determined by RT-PCR did not change in any of the assays with cysticerci incubated only with RPMI medium for 0, 1, 4, and 24 h (Fig. 5A), cysticerci incubated for 30 min with O_2^- (2.9 and 3.8 nmol/min) (Fig. 5B), and cysticerci exposed to H_2O_2 at concentrations of 0.25, 0.5, 1, and 2 mM (Fig. 5C). Additionally, we observed that

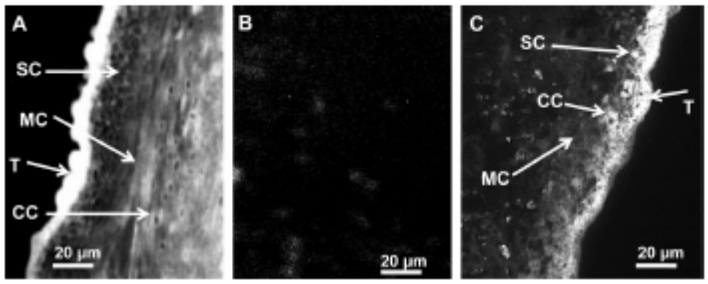

Fig. 3. Localization of Cu,Zn-SOD by indirect immunofluorescence on cysticerci wall from *T. solium* and *T. crassiceps*. Section of *T. solium* (A) and *T. crassiceps* (C) were exposed to anti-*T. solium* Cu,Zn-SOD antibodies, whereas section of *T. crassiceps* (B) was incubated with normal rabbit serum as control. Arrows and letters show labeled tegument (T), channel forming cells (CC), myocytons (MC), and subtegumental cytons (SC). Bars = 20 µm.

Please cite this article in press as: Parra-Unda, R., et al. Cu,Zn superoxide dismutase: Cloning and analysis of the *Taenia solium* gene and *Taenia crassiceps* cDNA. Exp. Parasitol. (2011), doi:10.1016/j.exppara.2011.10.002

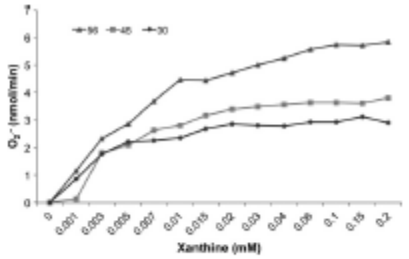

Fig. 4. Velocities of O_2^- production (nmol/min) generated with different concentrations of xanthine (0.001–0.2 mM) combined with each concentration of xanthine oxidase (30, 45, and 56 mU).

Table 2
Effect of H_2O_2 (1, 2, 3, 4, and 5 mM) on *Taenia crassiceps* cysticerci cultured in RPMI at different times (0.5, 6, and 24 h). Cysticerci cultured in RPM were used as control.

Time (h)	Control	1.0 mM	2.0 mM	3.0 mM	4.0 mM
0.5					
[E]	100%	100%	100%	40%	0%
[M]	****	****	****	+	–
[D]	C	C	C	I	N
6					
[E]	100%	100%	100%	0%	0%
[M]	****	****	****	–	–
[D]	C	C	C	N	N
24					
[E]	100%	100%	100%	0%	0%
[M]	****	****	****	+	–
[D]	C	C	C	N	N

Viability was determined by:
[E] % of cysticerci evaginated: # parasites evaginated/total of parasites cultured.
[M] Mobility of parasites: high, ****; medium, **, and null –.
[D] Damage on the cysticerci wall: C, complete, M medium, and N null damage.

CuZn-SOD and TPI protein expression determined by western blot did not change in the same cysticerci (Fig. 5D).

4. Discussion

Computational analysis of the 5′-flanking region from *TsCuZn-SOD* gene revealed putative sites for TATA-binding protein and CCAAT sites that participate in transcription. However, these sites are not in the correct position to be functional. The same analysis showed the presence of putative transcription factors sites for NF1 (Satoh et al., 2005), AP-1 and YY1, which are redox positive or negative regulators (Chang et al., 2002).

Our results show that the 5′-flanking region of *TsCuZn-SOD* gene (Cestoda) is different in sequence and organization from the *S. mansoni* (Trematoda) *CuZn-SOD* promoter (Mei et al., 1995); and both are different from the human and *D. melanogaster* promoters, indicating that proximal promoters of *CuZn-SOD* genes are not conserved, and also suggesting that these helminthes genes could be regulated differently. However, functional assays must be carried out to validate these assertions. Moreover, the *TsCuZn-SOD* gene differs from other *CuZn-SOD* genes in number, length, and position of introns and exons (Levanon et al., 1985; Mei et al., 1995; Seto et al., 1987), but appear most similar to *S. mansoni* (Mei et al., 1995). Southern blot analysis suggests that *TsCuZn-SOD* and *TcCuZn-SOD* genes are represented as single copies in these Taeniid genomes, as reported in other organisms (Henkle-Duhrsen and Kampkotter, 2001).

On the other hand, the *T. solium* enzyme has the amino acids L^{130} and I^{133} positioned similarly to the *S. mansoni* (L^{132} and V^{135}) CuZn-SOD enzyme, both different from the equivalent residues found in the human enzyme. Thus, they have been suggested as targets to develop inhibitors to block the O_2^- pathway towards the active site in parasite enzymes (Cardoso et al., 2004).

Anti-TsCuZn-SOD antibodies in the 2D-WB assays showed a dimer of ~32 kDa and a monomer of ~16 kDa. No complete disruption of the dimer could be due to the strip not being boiled for 3 min and for the high resistance to denaturing agents such as SDS and urea, as has been reported for others CuZn-SODs (Gutteridge, 2007). On the other hand, CuZn-SOD in *T. crassiceps*

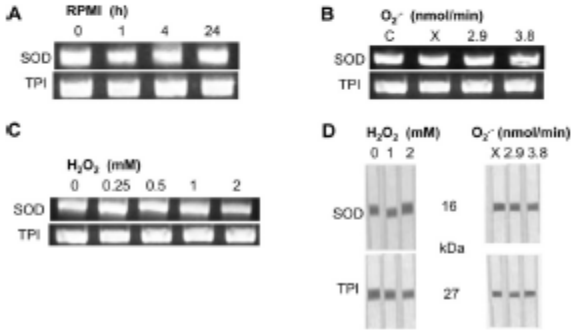

Fig. 5. Cu,Zn-SOD and TPI gene expression in *T. crassiceps* cysticerci exposed to O_2^- and H_2O_2. *T. crassiceps* were cultured in: (A) RPMI for 0, 1, 4, and 24 h; (B) RPMI without O_2^-, with xanthine (shown as X, 0.2 mM), and O_2^- (2.9 and 3.8 nmol/min) for 30 min; (C) RPMI without H_2O_2 and with H_2O_2 (0.25–2 mM) for 30 min. (D) CuZn-SOD and TPI protein expression determined by western blot using extracts from cysticerci incubated with RPMI alone, O_2^- (2.9 and 3.8 nmol/min) and H_2O_2 (1 and 2 mM) for 30 min, enfronted with anti-CuZn-SOD and TPI antibodies. As control, two membrane strips with *T. solium* and *T. crassiceps* cysticerci extracts were exposed to IgG from rabbit normal sera.

Please cite this article in press as: Parra-Unda, R., et al. Cu,Zn superoxide dismutase: Cloning and analysis of the Taenia solium gene and Taenia crassiceps cDNA. Exp. Parasitol. (2011), doi:10.1016/j.exppara.2011.10.002

and *T. solium* do not have isoforms. Conversely, we found that TR has two isoforms, which is in agreement with Nguyen's observations (Nguyen et al., 2010). Localization of the Cu,Zn-SOD in cysticerci tissue suggests that it is synthesized by parasite and distributed throughout the bladder wall, with maximum concentration in the tegument.

Overexpression of Cu,Zn-SOD and catalase increase the lifespan of *D. melanogaster* (Orr and Sohal, 1994), and their resistance to oxidative stress an observation which has been associated with higher expression and/or activity of antioxidant enzymes. *T. crassiceps* cysticerci can resist 3.8 nmol/min of O_2^- and 2 mM of H_2O_2 for 24 h. Remarkably, these concentrations are higher than those produced *in vivo* by leukocytes (1.08 nmol O_2^-/1 × 10^7 cells (Babior et al., 1973), and less than 0.01 nmol of H_2O_2/2.5 × 10^{-6} cells (Root et al., 1975).

Different systems to produce O_2^- has been used to demonstrate damage on helminthes (Fridovich, 1995). However, these reports do not mention how much O_2^- is produced (Mkoji et al., 1988; Piedrafita et al., 2000; Zelck and Von Janowsky, 2004). Here, we report a system method to quantify this radical produced by the xanthine–xanthine oxidase system.

On the other hand, Cu,Zn-SOD mRNA and protein expression experiments with *T. crassiceps* cysticerci exposed or not to different concentrations of O_2^- and H_2O_2 showed constant levels of transcript and protein, which indicates that this gene is expressed constitutively, as is other antioxidant enzyme of this parasite (Vaca-Paniagua et al., 2009).

Like other antioxidant enzymes, Cu,Zn-SOD is localized in the tegument, much as are glutathione transferases (Vibanco-Perez et al., 2002), and 2-Cys peroxiredoxins (Molina-Lopez et al., 2006). Therefore, its stability, high catalytic efficiency for O_2^- (~7×10^9 $M^{-1}s^{-1}$) (Heinisch et al., 2006), its localization in the tegument, and the constitutive expression of the gene in all cells of cysticerci could indicate that Cu,Zn-SOD plays a regulating and defensive role against ROS produced by normal mammalian metabolism and immune cells (Henkle-Duhrsen and Kampkotter, 2001).

It is clear that living cells must maintain a delicate balance between the rates of O_2^- generation and removal to maintain normal cell metabolism. To date, little information exists about the mechanisms controlling the expression of SOD genes in Cestoda. Therefore, studies should be carried out to identify the signal molecules and factors that could be important in the transcription of this *TsCu,Zn-SOD* gene, in order to understand the role of this antioxidant enzyme in the host-parasite relationship.

Acknowledgments

This work was supported by CONACyT (80134-M) and DGAPA-PAPIIT (IN207507-3 and IN206708). Authors declare that the experiments comply with the current laws for animal use and care (NOM-062-ZOO-1999) of Mexico. We thank M.D. Alicia Ochoa Sánchez for technical help.

References

Babior, B.M., Kipnes, R.S., Curnutte, J.T., 1973. Biological defense mechanisms. The production by leukocytes of superoxide, a potential bactericidal agent. J. Clin. Invest. 52, 741–744.

Ben-Smith, A., Lammas, D.A., Behnke, J.M., 2002. Effect of oxygen radicals and differential expression of catalase and superoxide dismutase in adult *Heligmosomoides polygyrus* during primary infections in mice with differing response phenotypes. Parasite Immunol. 24, 119–129.

Campos, A., Bernard, P., Rauconnier, A., Landa, A., Gomez, E., Hernandez, R., Willms, K., Ludeña, J.P., 1998. Cloning and sequencing of two actin genes from Taenia solium (Cestoda). Mol. Biochem. Parasitol. 40, 87–93.

Cardoso, R.M., Silva, C.H., Ulian de Araujo, A.P., Tanaka, T., Tanaka, M., Garratt, R.C., 2004. Structure of the cytosolic Cu,Zn superoxide dismutase from *Schistosoma mansoni*. Acta Crystallogr. D Biol. Crystallogr. 60, 1569–1578.

Castellanos-Gonzalez, A., Jimenez, L., Landa, A., 2002. Cloning, production and characterization of a recombinant Cu/Zn superoxide dismutase from Taenia solium. Int. J. Parasitol. 32, 1175–1182.

Chang, M.S., Yoo, H.Y., Rho, H.M., 2002. Transcriptional regulation and environmental induction of gene encoding copper- and zinc-containing superoxide dismutase. Methods Enzymol. 349, 293–305.

Fridovich, I., 1995. Superoxide radical and superoxide dismutases. Annu. Rev. Biochem. 64, 97–112.

Gutteridge, B.H.A.J., 2007. Free Radicals in Biology and Medicine. Oxford University Press, Great Britain.

Heinrich, P., Georg, L., Petro, E.P., 2006. Biochemie und Pathobiochemie. Springer, Berlin.

Henkle-Duhrsen, K., Kampkoetter, A., 2001. Antioxidant enzyme families in parasitic nematodes. Mol. Biochem. Parasitol. 114, 129–142.

Khalife, J., Godin, C., Capron, A., 1995. Transcriptional regulation of *Schistosoma mansoni* calreticulin: possible role of AP-1. Parasitology 111 (Pt. 4), 469–475.

Laemmli, U.K., 1970. Cleavage of structural proteins during the assembly of the head of bacteriophage T4. Nature 227, 680–685.

Levanon, D., Bernan-Wurtzel, J., Dafni, N., Wigderson, M., Sherman, L., Bernstein, Y., Laver-Rudich, Z., Danziger, E., Stein, O., Groner, Y., 1985. Architecture and anatomy of the chromosomal locus in human chromosome 21 encoding the Cu/Zn superoxide dismutase. EMBO J. 4, 77–84.

Li, Y., Huang, T.T., Carlson, E.J., Melov, S., Ursell, P.C., Olson, J.L., Noble, L.J., Yoshimura, M.P., Berger, C., Chan, P.H., Wallace, D.C., Epstein, C.J., 1995. Dilated cardiomyopathy and neonatal lethality in mutant mice lacking manganese superoxide dismutase. Nat. Genet. 11, 376–381.

McCord, J.M., Fridovich, I., 1969. Superoxide dismutase. An enzymic function for erythrocuprein (hemocuprein). J. Biol. Chem. 244, 6049–6055.

Mei, H., Hirai, H., Tanaka, M., Hong, Z., Rekosh, D., LoVerde, P.T., 1995. *Schistosoma mansoni*: cloning and characterization of a gene encoding cytosolic Cu/Zn superoxide dismutase. Exp. Parasitol. 80, 250–259.

Miao, L., St Clair, D.K., 2009. Regulation of superoxide dismutase genes: implications in disease. Free Radic. Biol. Med. 47, 344–356.

Mkoji, G.M., Smith, J.M., Prichard, R.K., 1988. Antioxidant systems in *Schistosoma mansoni*: evidence for their role in protection of the adult worms against oxidant killing. Int. J. Parasitol. 18, 667–673.

Molina-Lopez, J., Jimenez, L., Ochoa-Sanchez, A., Landa, A., 2006. Molecular cloning and characterization of a 2-Cys peroxiredoxin from Taenia solium. J. Parasitol. 92, 796–802.

Nguyen, H.A., Bae, Y.A., Lee, E.G., Kim, S.H., Diaz-Camacho, S.P., Nawa, Y., Kang, I., Kong, Y., 2010. A novel sigma-like glutathione transferase of Taenia solium metacestode. Int. J. Parasitol. 40, 1097–1106.

Orr, W.C., Sohal, R.S., 1994. Extension of life-span by overexpression of superoxide dismutase and catalase in *Drosophila melanogaster*. Science 263, 1128–1130.

Phillips, J.P., Campbell, S.D., Michaud, D., Charbonneau, M., Hilliker, A.J., 1989. Null mutation of copper/zinc superoxide dismutase in Drosophila confers hypersensitivity to paraquat and reduced longevity. Proc. Natl. Acad. Sci. USA 86, 2761–2765.

Piedrafita, D., Spithill, T.W., Dalton, J.P., Brindley, P.J., Sandeman, M.R., Wood, P.R., Parsons, J.C., 2000. Juvenile Fasciola hepatica are resistant to killing in vitro by free radicals compared with larvae of *Schistosoma mansoni*. Parasite Immunol. 22, 287–295.

Reveillaud, I., Phillips, J., Duyf, B., Hilliker, A., Kongpachith, A., Fleming, J.E., 1994. Phenotypic rescue by a bovine transgene in a Cu,Zn superoxide dismutase-null mutant of *Drosophila melanogaster*. Mol. Cell. Biol. 14, 1302–1307.

Root, R.K., Metcalf, J., Oshino, N., Chance, B., 1975. H_2O_2 release from human granulocytes during phagocytosis. I. Documentation, quantitation, and some regulating factors. J. Clin. Invest. 55, 945–955.

Sambrook, J., Fritsch, E.F., Maniatis, A.N.D.T., 1989. *Molecular Cloning: A Laboratory Manual*. Cold Spring Harbor, New York.

Satoh, S., Noaki, T., Ishiguro, T., Osada, S., Imagawa, M., Miura, N., Yamada, K., Noguchi, T., 2005. Nuclear factor 1 family members interact with hepatocyte nuclear factor 1alpha to synergistically activate L-type pyruvate kinase gene transcription. J. Biol. Chem. 280, 39827–39834.

Serra, E., Zamzoumi, K., Trolet, J., Capron, A., Dissous, C., 1996. Functional analysis of the *Schistosoma mansoni* 28 kDa glutathione S-transferase gene promoter: involvement of SMNF-Y transcription factor in multimeric complexes. Mol. Biochem. Parasitol. 83, 69–80.

Seto, N.O., Hayashi, S., Tener, G.M., 1987. The sequence of the Cu-Zn superoxide dismutase gene of Drosophila. Nucleic Acids Res. 15, 10001.

Tainer, J.A., Getzoff, E.D., Beem, K.M., Richardson, J.S., Richardson, D.C., 1982. Determination and analysis of the 2 A-structure of copper, zinc superoxide dismutase. J. Mol. Biol. 160, 181–217.

Tawe, W.N., Eschbach, M.L., Walter, R.D., Henkle-Duhrsen, K., 1998. Identification of stress-responsive genes in Caenorhabditis elegans using RT-PCR differential display. Nucleic Acids Res. 26, 1621–1627.

Tawe, W., Walter, R.D., Henkle-Duhrsen, K., 2000. Onchocerca volvulus superoxide dismutase genes: identification of functional promoters for pre-mRNA transcripts which undergo trans-splicing. Exp. Parasitol. 94, 172–179.

Towbin, H., Staehelin, T., Gordon, J., 1979. Electrophoretic transfer of proteins from polyacrylamide gels to nitrocellulose sheets: procedure and some applications. Proc. Natl. Acad. Sci. USA 76, 4350–4354.

Vaca-Paniagua, F., Parra-Unda, R., Landa, A., 2009. Characterization of one typical 2-Cys peroxiredoxin gene of Taenia solium and Taenia crassiceps. Parasitol. Res. 105, 781–787.

Please cite this article in press as: Parra-Unda, R., et al. Cu,Zn superoxide dismutase: Cloning and analysis of the Taenia solium gene and Taenia crassiceps cDNA. Exp. Parasitol. (2011), doi:10.1016/j.exppara.2011.10.002

Vibanco-Perez, N., Jimenez, L., Mendoza-Hernandez, G., Landa, A., 2002. Characterization of a recombinant mu-class glutathione S-transferase from Taenia solium. Parasitol. Res. 88, 398–404.
Winterbourn, C.C., 1993. Superoxide as an intracellular radical sink. Free Radic. Biol. Med. 14, 85–90.
Zelck, U.E., Von Janowsky, B., 2004. Antioxidant enzymes in intramolluscan Schistosoma mansoni and ROS-induced changes in expression. Parasitology 128, 493–501.
Zelko, I.N., Mariani, T.J., Folz, R.J., 2002. Superoxide dismutase multigene family: a comparison of the Cu/Zn-SOD (SOD1), Mn-SOD (SOD2), and EC-SOD (SOD3) gene structures, evolution, and expression. Free Radic. Biol. Med. 33, 337–349.

Please cite this article in press as: Parra-Unda, R., et al. Cu,Zn superoxide dismutase: Cloning and analysis of the Taenia solium gene and Taenia crassiceps cDNA. Exp. Parasitol. (2011), doi:10.1016/j.exppara.2011.10.002

Current Topics in Medicinal Chemistry, 2008, *8*, 393-399 393

Taenia solium: Antioxidant Metabolism Enzymes as Targets for Cestocidal Drugs and Vaccines

F. Vaca-Paniagua, A. Torres-Rivera, R. Parra-Unda and A. Landa*

Departamento de Microbiología y Parasitología, Facultad de Medicina, Universidad Nacional Autónoma de México, Edificio A, 2° Piso, Ciudad Universitaria, 04510 México D. F., México

Abstract: This review focuses in the role that antioxidant enzymes play in protection and other important physiological functions such as signal transduction, cell differentiation, growth and apoptosis. Parasites use these enzymes to evade ROS produced by the host immune response and for development inside the host. In the cestode *Taenia solium*, three antioxidant enzymes have been studied: a cytosolic Cu_2Zn superoxide dismutase that is a target of cestocidal drugs (benzimidazoles), a 2-Cys peroxiredoxin that is a regulatory enzyme of H_2O_2 molecule essential for several physiological functions; and two isoforms of glutathione transferases that are immunological targets, since they protect immunized mice against cysticercosis. Moreover, all three enzymes are present in all stages of the parasite. These findings suggest that antioxidant enzymes have an important role in *T. solium* physiology and infection, therefore they might represent the Achilles' heel of the parasite.

Keywords: *Taenia solium*, antioxidant metabolism, superoxide dismutase, 2-Cys peroxiredoxin, glutathione transferase.

ENZYMES OF ANTIOXIDANT METABOLISM

Taenia solium, in human and pig infection, must confront host immune response [1]. Oxidative damage produced by reactive oxygen species (ROS) such as superoxide anion ($O_2^{\cdot-}$), hydrogen peroxide (H_2O_2) and hydroxyl radical is one of the major challenges that the parasite must confront. Besides, ROS attack all cellular components and produce new and more aggressive ROS such as lipid hydroperoxidasi and reactive carbonyls [2]. It is well known that these molecules can damage or kill parasites [3]. Nevertheless, ROS are necessary for the physiology of organisms, in processes such as signal regulation, cell differentiation, growth and apoptosis [4, 5]. *Taenia solium* is armed with enzymatic ROS scavengers such as superoxide dismutase (SOD), 2-Cys peroxiredoxin (2-Cys Prx), and two glutathione transferases (GSTs). Antioxidant enzymes are also responsible for maintaining a fine balance between external and internal ROS in cells. To date, only these three enzymes from the antioxidant metabolism have been studied in *T. solium*.

1) Superoxide dismutases are a family (SOD, E.C. 1.15.1.1) of metalloenzymes which catalyze the $O_2^{\cdot-}$ dismutation into H_2O_2 and oxygen (O_2). They are classified in four types, according to the metal present in the catalytic site of the enzyme: manganese (Mn-SOD); copper-zinc (Cu_2Zn-SOD); iron (Fe-SOD); and nickel (Ni-SOD) [6, 7, 8]. Each SOD is encoded by a different gene and they have different structures and subcellular localizations. To date, two types of SODs have been reported in helminths: a Mn-SOD that is localized into the mitochondrial matrix with a homotetrameric structure of ~96 kDa, constituted by monomers of ~22 kDa. Every monomer contains a Mn^{2+} atom coordinated with the H^{69}, H^{73}, H^{157}, D^{161}, Q^{165} amino acids [9]. It is an essential gene, since knock out mice (Mn-SOD$^{-/-}$) are severely affected and die only a few days after birth [10]. Helminths also possess two enzymes of Cu_2Zn-SOD, an extracellular Cu_2Zn-SOD (ECCu_2Zn-SOD), which is secreted, due it has a hydrophobic signal peptide, and a cytoplasmic Cu_2Zn-SOD (Cu_2Zn-SOD), widely distributed in the cytosol and in the cell nucleus. ECCu_2Zn-SOD is a tetrameric glycoprotein composed by four identical 30kDa subunits and prevents cell damage initiated by extracellular superoxide [11]. In contrast, Cu_2Zn-SOD has a homodimeric structure with ~32 kDa. Recent reports showed that Cu_2Zn-SOD-null *Drosophila melanogaster* and knock-out mice (Cu_2Zn-SOD$^{-/-}$) exhibit a decreased growth rate and shortened lifespan [12, 13]. In addition, Cu_2Zn-SOD expression is upregulated by phosphatidylinositol 3 kinase and nuclear factor-κB in rat cells [14]. Also, SOD is implicated in regulation and cell growth through the control of $O_2^{\cdot-}$ levels in the activation of signaling pathways (e.g. ras/rac-Raf1-MAPK and Raf/MEK-ERK) [15, 16].

Both Cu_2Zn-SOD enzymes contain one atom of Cu^{2+} and one of Zn^{2+} at the active site. Copper is coordinated with histidines (H^{46}, H^{48}, H^{63}, H^{120}), one of which makes a bridge between Cu and Zn. Zinc is bound to amino acids H^{63}, H^{71}, H^{80} and D^{83}, forming a structure that resembles a Zn finger domain [17]. Each monomer folds as a flattened Greek-key β-barrel, made of eight antiparallel β-strands connected by seven loops. This barrel forms a channel by which $O_2^{\cdot-}$ is directed to the active site by a positive electrostatic field constituted by charged residues. The channel and metal-binding amino acid residues are conserved in virtually all known Cu_2Zn-SODs [13]. The mechanism of catalysis involves two general steps. 1) Cu^{2+} reduction by one molecule of $O_2^{\cdot-}$ to produce molecular oxygen, and 2) Cu^{+} oxidation by another $O_2^{\cdot-}$ molecule to generate H_2O_2. First step involves coordination of $O_2^{\cdot-}$ to the oxidized copper center stabilized by a conserved R^{141}, where one electron is transferred from $O_2^{\cdot-}$ to SOD-Cu^{2+}, yielding O_2 and the reduced SOD-Cu^{+}(H^{+}) complex. In this process imidazole ring of H^{80} is protonated. In the second step another $O_2^{\cdot-}$ is driven electrostatically through the channel to the active site and coordinated with SOD-Cu^{+} and R^{141}. The proton gained by H^{80} is transferred to the $O_2^{\cdot-}$, while another proton is taken from one water

*Address correspondence to this author at the Departamento de Microbiología y Parasitología, Facultad de Medicina, Universidad Nacional Autónoma de México, Edificio A, 2° Piso, Ciudad Universitaria, 04510México D. F., México; Tel: (52 55) 5623-2357; Fax: (52 55) 5623-2382; E-mail: landa@servidor.unam.mx

1568-0266/08 $55.00+.00

molecule. This reaction produces H_2O_2 and the regeneration of active-site copper ($SOD\text{-}Cu^{2+}$) and H^+, completing the catalytic cycle.

$$SOD\text{-}Cu^{2+} + O_2^{\cdot-} + H^+ \rightarrow SOD\text{-}Cu^{+}(H^+) + O_2 \quad (1)$$

$$SOD\text{-}Cu^{+}(H^+) + O_2^{\cdot-} + H^+ \rightarrow SOD\text{-}Cu^{2+} + H_2O_2 \quad (2)$$

In platyhelminthes such as *Schistosoma mansoni* (Trematoda), two Cu,Zn-SOD enzymes have been identified: a cytosolic and other extracellular that contains a signal peptide. Both are coded by different genes. They are localized in the subtegumental tissue and one is secreted to the host-parasite interface [18, 19]. The Cu,Zn-SOD cDNAs of *S. mansoni* and *Fasciola hepatica* have been cloned and characterized [20, 21]. Recently, a crystal structure of *S. mansoni* cytosolic Cu,Zn-SOD (SmCtSOD) was solved [22]. This study showed that SmCtSOD and human Cu,ZnSOD have differences in two amino acids (I^{102} and V^{103}) that are in the entrance of the channel near the active site. These amino acids play an important role in conformation and charge distribution for substrate attraction; therefore they could be used to develop inhibitors against the parasite enzyme. On the other hand, SOD has been used as target for drugs and in vaccination studies. For example, immunization experiments using *S. mansoni* Cu,Zn-SOD enzyme and DNA constructs of the gene showed significant levels of protection in mice [23]. Moreover, *in vitro* inhibition assays with benzimidazoles and pirimidine derivatives on crude extracts from trematodes (*F. hepatica* and *Dicrocoelium dendriticum*) and cestodes (*Moniezia expansa*, *M. benedeni*, *Avitellina centripunctata*, *Dipylidium caninum* and *T. hydatigena*) showed a decrease in SOD activity [24, 25]. In other study, mice infected with *Echinococcus granulosus* cysts, treated with mebendazole showed an increase in the parasite SOD activity. In contrast, albendazole and praziquantel had no effect on the activity of this enzyme [26]. On the other hand, there are several reports in nematodes of the existence of Mn-SOD [27], and only one report in trematodes [28], but there are not reports for cestodes.

Cu,Zn-SOD has been purified of cysticerci extracts from *T. taeniaeformis* and *T. solium* (Cestoda). These enzymes have tetrameric and dimeric structures, with ~64 and ~30 kDa, respectively [29, 30]. In *T. solium* a clone encoding a Cu,Zn-SOD was isolated from a cDNA library of the larval stage. The deduced amino acid clone indicates that the enzyme has a predictive monomeric Mr of ~15.6 kDa, the classical metals and amino acids involved in the function of cytosolic Cu,Zn enzymes. Amino acid sequence analysis revealed 71% identity with *S. mansoni*, 60% with mammalian and less than ~34% with other helminth Cu,Zn-SODs, and the conserved β-barrel structure of the enzyme consisting of eight antiparallel β-strands joined by loops (Fig. 1). This barrel constitutes the channel through $O_2^{\cdot-}$ is conduced to the catalytic site, where H_2O_2 and O_2 are produced. A functional recombinant *T. solium* Cu,Zn-SOD of 30 kDa was produced and western blot analysis with antibodies against this enzyme showed that this enzyme is expressed in all stages of the parasite. Antibodies did not affect the enzymatic activity; nevertheless, they cross-reacted with several *Taenia* species but not with trematodes, nematodes, pig, human or bovine Cu,Zn-SOD enzymes. *In*

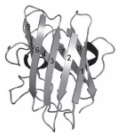

Fig. (1). Structural model of *Taenia solium* Cu,Zn-SOD monomer. It shows the β-barrel structure formed of eight antiparallel β-strands (arrows) joined by loops (lines). Model was constructed by MODELLER program [32].

vitro studies with thiabendazole and albendazole inhibited the activity of *T. solium* Cu,Zn-SOD, but not the bovine Cu,Zn-SOD [31]. Interestingly, these data show structural differences between the SOD of this parasite and its hosts.

2) Peroxiredoxins (Prxs; E.C. 1.11.1.15) are conserved enzymes reported from archaebacteria to humans, covering plants, mammals, protozoa and helminths [33]. These peroxidases catalyze the reduction of 1) hydrogen peroxide (H_2O_2) to water, 2) hydroperoxides (ROOH) to the corresponding alcohol and water, and 3) peroxynitrite ($OONO^-$) to nitrite and water, using thioredoxin as electron donor [34-36].

$$H_2O_2 + e^- \rightarrow 2H_2O \quad (1)$$

$$ROOH + e^- \rightarrow ROH + H_2O \quad (2)$$

$$OONO^- + e^- \rightarrow NO_2 + H_2O \quad (3)$$

Prxs do not need prosthetic groups, metals or coenzymes for their catalysis. Their structural classification is based on whether they use one or two cysteines for catalysis. According to this, there are 1-Cys and 2-Cys Prxs. The 1-Cys Prxs have only one cysteine inside the amino terminal motif PVCT (N-Cys), while the 2-Cys have the conserved N-Cys in the motif FVCP and a carboxy terminal cysteine (C-Cys) in the motif VCPA [37]. Additionally, 2-Cys Prxs can be further divided into 2-Cys typical and 2-Cys atypical. In the first classes the first step of catalysis, thiolate and sulfenic acid formation, is the same. Typical 2-Cys Prxs are homodimers joined head to tail, where the N-Cys is facing the C-Cys of the adjacent monomer. Their catalytic mechanism involves the formation of the thiolate form of the N-Cys (*N*-Cys-S$^-$), stabilized by guanidino group of R^{127}. This highly reactive thiolate reduces the peroxide in a nucleophilic attack yielding the cysteine sulfenic acid (*N*-Cys-SOH) and water. The reaction causes a local rearrangement of the active site exposing the N-Cys-SOH to the solvent. This structural modification brings the otherwise far (~10 Å) C-Cys of the other monomer close enough for the formation of an intermolecular disulphide bond in a condes-

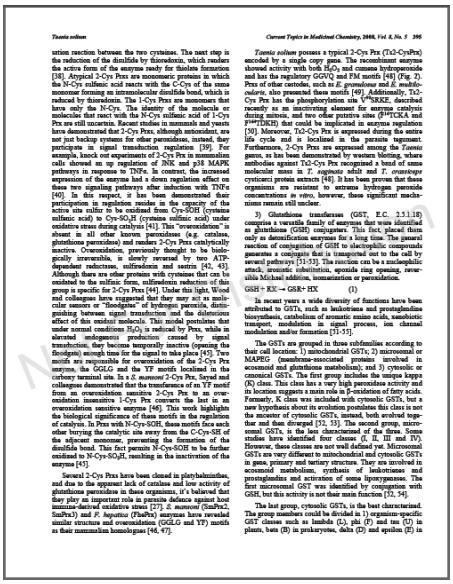

ution reaction between the two cysteines. The next step is the reduction of the disulfide by thioredoxin, which renders the active form of the enzyme ready for thiolate formation [38]. Atypical 2-Cys Prxs are monomeric proteins in which the N-Cys sulfenic acid reacts with the C-Cys of the same monomer forming an intramolecular disulfide bond, which is reduced by thioredoxin. The 1-Cys Prxs are monomers that have only the N-Cys. The identity of the molecule or molecules that react with the N-Cys sulfenic acid of 1-Cys Prx are still uncertain. Recent studies in mammals and yeasts have demonstrated that 2-Cys Prxs, although antioxidant, are not just backup systems for other peroxidases, instead, they participate in signal transduction regulation [39]. For example, knock out experiments of 2-Cys Prx in mammalian cells showed an up regulation of JNK and p38 MAPK pathways in response to TNFα. In contrast, the increased expression of the enzyme had a down regulation effect on these two signaling pathways after induction with TNFα [40]. In this respect, it has been demonstrated their participation in regulation resides in the capacity of the active site sulfur to be oxidized from Cys-SOH (cysteine sulfenic acid) to Cys-SO$_2$H (cysteine sulfinic acid) under oxidative stress during catalysis [41]. This "overoxidation" is absent in all other known peroxidases (e.g. catalase, glutathione peroxidase) and renders 2-Cys Prxs catalytically inactive. Overoxidation, previously thought to be biologically irreversible, is slowly reversed by two ATP-dependent reductase, sulfiredoxin and sestrin [42, 43]. Although there are other proteins with cysteines that can be oxidated to the sulfinic form, sulfiredoxin reduction of this group is specific for 2-Cys Prxs [44]. Under this light, Wood and colleagues have suggested that they may act as molecular sensors or "floodgates" of hydrogen peroxide, distinguishing between signal transduction and the deleterious effect of this oxidant molecule. This model postulates that under normal conditions H_2O_2 is radical by Prxs, while in elevated endogenous production caused by signal transduction, they become temporally inactive (opening the floodgate) enough time for the signal to take place [42]. Two motifs are responsible for overoxidation of the 2-Cys Prx enzyme, the GGLG and the YF motifs localized in the carboxy terminal site. In *S. mansoni* 2-Cys Prx, Sayed and colleagues demonstrated that the transference of an YF motif from an overoxidation sensitive 2-Cys Prx to an overoxidation insensitive 1-Cys Prx converts the last in an overoxidation sensitive enzyme [46]. This work highlights the biological significance of these motifs in the regulation of catalysis. In Prxs with N-Cys-SOH, these motifs face each other burying the catalytic site away from the C-Cys-SH of the adjacent monomer, preventing the formation of the disulfide bond. This fact permits N-Cys-SOH to be further oxidized to N-Cys-SO$_2$H, resulting in the inactivation of the enzyme [45].

Several 2-Cys Prxs have been cloned in platyhelminthes, and due to the apparent lack of catalase and low activity of glutathione peroxidase in these organisms, it's believed that they play an important role in parasite defance against host immune-derived oxidative stress [27]. *S. mansoni* (SmPrx2, SmPrx3) and *F. hepatica* (FhePrx) enzymes have revealed similar structure and oxeoxidation (GGLG and YF) motifs as their mammalian homologues [46, 47].

Taenia solium possess a typical 2-Cys Prx (Tx2-CysPrx) encoded by a single copy gene. The recombinant enzyme showed activity with both H_2O_2 and cumene hydroperoxide and has the regulatory GGVG and FM motifs [48] (Fig. 2). Prxs of other cestodes, such as *E. granulosus* and *E. multilocularis*, also presented these motifs [49]. Additionally, Tx2-Cys Prx has the phosphorylation site V^{99}SRKE, described recently as an inactivating element for enzyme catalysis during mitosis, and two other putative sites (S^{105}TCKA and F^{107}DKH) that could be implicated in enzyme regulation [50]. Moreover, Tx2-Cys Prx is expressed during the entire life cycle and is localized in the parasite tegument. Furthermore, 2-Cys Prxs are expressed among the *Taenia* genus, as has been demonstrated by western blotting, where antibodies against Tx2-Cys Prx recognized a band of same molecular mass in *T. asiatica* adult and *T. crassiceps* cysticerci protein extracts [48]. It has been proven that these organisms are resistant to extreme hydrogen peroxide concentrations *in vitro*, however, these significant mechanisms remain still unclear.

3) Glutathione transferases (GST, E.C. 2.5.1.18) comprise a versatile family of enzymes that were identified as glutathione (GSH) conjugaters. This fact, placed them only as detoxification enzymes for a long time. The general reaction of conjugation of GSH to electrophilic compounds generates a conjugate that is transported out to the cell by several pathways [51-53]. The reaction can be a nucleophilic attack, aromatic substitution, epoxide ring opening, reversible Michael addition, isomerization or peroxidation.

$$GSH + RX \rightarrow GSR + HX \quad (1)$$

In recent years a wide diversity of functions have been attributed to GSTs, such as leukotriens and prostaglandins biosynthesis, catabolism of aromatic amino acids, xenobiotic transport, modulation in signal process, ion channal modulation and/or formation [51-53].

The GSTs are grouped in three subfamilies according to their cell location: 1) mitochondrial GSTs; 2) microsomal or MAPEG (membrane-associated proteins involved in eicosanoid and glutathione metabolism); and 3) cytosolic or canonical GSTs. The first group includes the unique kappa (K) class. This class has a very high peroxidase activity and its location suggests a main role in β-oxidation of fatty acids. Formerly, K class was included with cytosolic GSTs, but a new hypothesis about its evolution postulates this class is not the ancestor of cytosolic GSTs, instead, both evolved together and then diverged [52, 53]. The second group, microsomal GSTs, is the less characterized of the three. Some studies have identified four classes (I, II, III and IV). However, these classes are not well defined yet. Microsomal GSTs are very different to mitochondrial and cytosolic GSTs in gene, primary and tertiary structure. They are involved in eicosanoid metabolism, synthesis of leukotrienes and prostaglandins and activation of some lipoxygenases. The first microsomal GST was identified by conjugation with GSH, but this activity is not their main function [52, 54].

The last group, cytosolic GSTs, is the best characterized. The group members could be divided in 1) organism-specific GST classes such as lambda (L), phi (F) and tau (U) in plants, beta (B) in prokaryotes, delta (D) and epsilon (E) in

```
HsPrx2       --------------MASGN-------ARIGKPAPDFKATAVVDGAFKEVKLSDYKGKYVV  39
SmPrx2       -------------------------MLLPNQPAPDFEGTAVIGTELRPISLSQFQGKYVL  35
SmPrx3       MLLQGFIKGALRYNRSSVSNLCRHYAAHVQRPAPDFCGTAVVDGQFKEIKLRDFAGKYLV  60
Ts-2CysPrx   --------------------MHEAAAVIGRPAPGFTCKALVDGELKDVSLSDYKGKYVI  39
EgPrx        -----------------------MAAVVGKLAPSFTCKALVDGELKDVSLSDYRGKYVI  36
EmPrx        -----------------------MVALVGKLAPSFTCKALVDGELKDVSLSDYRGKYVI  36

HsPrx2       LFFYPLDFTFVCPTEIIAFSNRAEDFRKLGCEVLGVSVDSQFNHLAWINTPRKEGGLGPL  99
SmPrx2       LVFYPLDFTFVCPTELIAFSERAAEFQSRGCQVIACSTDSVYAHLAWTKLDRKAGGLGQM  95
SmPrx3       LFFYPLDFTFVCPTELTAFSDRIDEFKNRGVEVVGVSTDSHFSHLAWINTPRKEGGLGGL 120
Ts-2CysPrx   LFFYPMDFTFVCPTEIIAFNDRAGEFHQRGCQLLACSTDSAYSHLAWNNVSRKEGGVQGM  99
EgPrx        LFFYPMDFTFVCPTEIIAFNDRADEFHQRGCQLLACSTDSGYCHLAWNNVSRKEGGVQGM  96
EmPrx        LFFYPMDFTFVCPTEIIAFNDRADEFRQRGCQLLACSTDSGYCHLAWNNVSRKEGGVQGM  96
                     ****

HsPrx2       NIPLLGDVTRRLSEDYGVLKTDEGIAYRGLFIIDGKGVLRQITVNDLPVGRSVDEALRLV 159
SmPrx2       NIPLLSDKNLRISRAYEVLDEQEGHAFRGMFLIDRKGILRQITVNDRPVGRSVDEAIRLL 155
SmPrx3       RYPLLADYQKQVTRDYGVLHEELGVALRGLFIISADGIIRQITINDLPAGRSVDEVLRLV 180
Ts-2CysPrx   KIPMLADTNHRISRDYGVLIEEQGVALRGLFIIDDKGILRQITIDDLPVGRCVDEALRLL 159
EgPrx        RIPMLADTNHKISRDYGVLIEDQGIALRGLFIIDDKGVLRQITINDLPVGRSVDEALRLL 156
EmPrx        RIPMLADTNHKISRDYGVLIEDQGIALRGLFIIDDKGVLRQITINDLPVGRSVDEALRLL 156

HsPrx2       QAFQYTDEHGEVCPAGWKPGSDTIKPNVDDSKEYFSKHN 198
SmPrx2       DAFIFFEKHGEVCPANWKPNSATIKPDPVASLSYFSSVH 194
SmPrx3       RAFQYTDKYGEVCPADWQPKGPTIKPDLKKYKEYFHKVN 219
Ts-2CysPrx   DAFQFTDKHGEVCPANWRPGSKAPKPNAGDLKSFMSSR- 197
EgPrx        DAFQFTDKHGEVCPANWQPGSKTFKPSAGDLKSFMSS-- 193
EmPrx        DAFQFTDKHGEVCPANWHPGSKTFKPSAGDLKSFMSS-- 193
                       ****
```

Fig. (2). Alignment of 2-Cys Prxs of human and platyhelminthes. HsPrx2, *Homo sapiens* (P32119); SmPrx2, *Schistosoma mansoni* (AAG15598); SmPrx3, *Schistosoma mansoni* (AAG15509); Ts-2CysPrx, *Taenia solium* (AAV91322); EgPrx, *Echinococcus granulosus* (AAD02002); EmPrx, *Echinococcus multilocularis* (BAC11863). Catalytic domains are marked with asterisks, overoxidation regulatory motifs are in bold and Cestoda putative phosphorylation sites are underlined. Alignment was done with ClustalW (http://www.ebi.ac.uk/clustalw/).

insects; and 2) ubiquitous classes such as mu (M), alpha (A), pi (P), theta (T), sigma (S), zeta (Z) and omega (O) classes. This classification was established according to biochemical, genetic, immunological and structural properties. All these enzymes have subunits of 24 to 27 kDa, with an average of 250 amino acids in their primary structure and all share the same tertiary and quaternary structure: dimers with subunits composed of two domains. The first domain, the G site, is located at the N-terminal portion and is responsible for GSH binding. This domain is conserved in all classes and has a tiorredoxin like fold constructed by three helices and four sheets (βαβαββα). In the G site, according to the class, the amino acids Y^7 (M, P and A classes) or S^{17} (T, Z, F, U and D classes) or C^{30} (O and B classes) are responsible for GSH activation. Activation allows the nucleophilic attack to the electrophilic compound. Second domain, named H site, embraces C-terminal region. This region binds the substrate and it is constituted exclusively by α-helices. The number of the helices can change from four to seven among classes. This variation has been used as an argument to explain the wide range of substrates for detoxification and also specificity among classes [51-53, 55]. Each monomer contains the G and H domains. The dimer can be formed by identical (homodimers) or different (heterodimers) subunits of the same class. Until now, the reason for activity of GST as dimers is not clear, however, the stabilization of dimeric structure has been related to the cooperativity between subunits. This process has been shown in some GSTs, although alosteric changes have not been demonstrated [56].

In Platyhelminthes, first GSTs identified came from the Trematoda *S. japonicum*, *S. mansoni* and *F. hepatica* [58, 59]. In Cestoda two native GSTs of *T. solium* with a molecular mass of 25.5 (SGSTM1) and 26.5 kDa (SGSTM2) were copurified from a soluble extract of cysticerci [60]. Amino terminal sequences and preliminary activity determinations with 1-Chloro-2, 4-nitrobenzene (CNDB, the universal substrate for GSTs) and other substrates showed that both GSTs have resemblance to the M class [60, 61]. Primary structure of a recombinant SGSTM1 revealed the presence of the mu-loop, the typical motif of that class. In addition, the activity ranges with substrates such as ethacrynic acid, bromosulfophtalein, some alkenals, cumene hydroperoxide, and its sensitivities to inhibitors such as cibacron blue, bromosulfophtalein and chlorotriphenyltin, confirmed its mu nature. Furthermore, vaccination assays carried out in a *T. crassiceps* murine cysticercosis model with both GSTs as antigens, showed a 90% decrease in parasite load, where 25% of that protection was given by SGSTM1 and the resting other 65% by SGSTM2. This finding suggests that both GSTs have great significance for the parasite survival [61]. Recently, a SGSTM2 was purified from a soluble extract of cysticerci, and characterized. In that study, properties such as activities with different substrates and sensitivities to class-specific inhibitors suggested that the

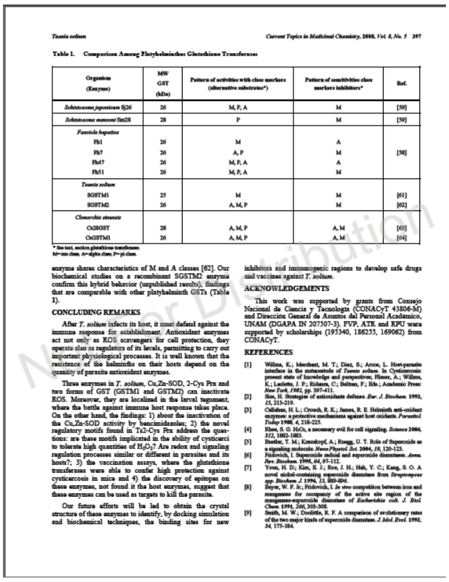

Table 1. Comparison Among Platyhelminthes Glutathione Transferases

Organism (Enzyme)	MW GST (kDa)	Pattern of activities with class markers (alternative substrates*)	Pattern of sensitivities class markers inhibitors*	Ref.
Schistosoma japonicum Sj26	26	M, P, A	M	[59]
Schistosoma mansoni Sm28	28	P	M	[59]
Fasciola hepatica				
Fh1	26	M	A	[58]
Fh7	26	A, P	M	
Fh47	26	M, P, A	A	
Fh51	26	M, P, A	M	
Taenia solium				
SGSTM1	25	M	M	[61]
SGSTM2	26	A, M, P	M	[62]
Clonorchis sinensis				
Cs28GST	28	A, M, P	A, M	[63]
CsGSTM1	26	A, M, P	A, M	[64]

* See text, section glutathione transferases.
M= mu class, A= alpha class, P= pi class.

enzyme shares characteristics of M and A classes [62]. Our biochemical studies on a recombinant SGSTM2 enzyme confirm this hybrid behavior (unpublished results), findings that are comparable with other platyhelminth GSTs (Table 1).

CONCLUDING REMARKS

After *T. solium* infects its host, it must defend against the immune response for establishment. Antioxidant enzymes act not only as ROS scavengers for cell protection, they operate also as regulators of its levels, permitting to carry out important physiological processes. It is well known that the resistance of the helminths on their hosts depend on the quantity of parasite antioxidant enzymes.

Three enzymes in *T. solium*, Cu,Zn-SOD, 2-Cys Prx and two forms of GST (GSTM1 and GSTM2) can inactivate ROS. Moreover, they are localized in the larval tegument, where the battle against immune host response takes place. On the other hand, the findings: 1) about the inactivation of the Cu,Zn-SOD activity by bencimidazoles; 2) the novel regulatory motifs found in Ts2-Cys Prx address the questions: are these motifs implicated in the ability of cysticerci to tolerate high quantities of H_2O_2? Are redox and signaling regulation processes similar or different in parasites and its hosts?; 3) the vaccination assays, where the glutathione transferases were able to confer high protection against cysticercosis in mice and 4) the discovery of epitopes on these enzymes, not found it the host enzymes, suggest that these enzymes can be used as targets to kill the parasite.

Our future efforts will be led to obtain the crystal structure of these enzymes to identify, by docking simulation and biochemical techniques, the binding sites for new inhibitors and immunogenic regions to develop safe drugs and vaccines against *T. solium*.

ACKNOWLEDGEMENTS

This work was supported by grants from Consejo Nacional de Ciencia y Tecnología (CONACyT 43806-M) and Dirección General de Asuntos del Personal Académico, UNAM (DGAPA IN 207507-3). FVP, ATR and RPU were supported by scholarships (195340, 186255, 169062) from CONACyT.

REFERENCES

[1] Willms, K.; Merchant, M. T.; Diaz, S.; Arcos, L. Host-parasite interface in the metacestode of *Taenia solium*. In Cysticercosis: present state of knowledge and perspectives; Flisser, A.; Willms, K.; Laclette, J. P.; Ridaura, C.; Beltran, F.; Eds.; Academic Press: *New York, 1982*, pp. 397-411.
[2] Sies, H. Strategies of antioxidants defense. *Eur. J. Biochem.* 1993, *15*, 213-219.
[3] Callahan, H. L.; Crouch, R. K.; James, R. E. Helminth anti-oxidant enzymes: a protective mechanisms against host oxidants. *Parasitol. Today* 1988, *4*, 218-225.
[4] Rhee, S. G. H_2O_2, a necessary evil for cell signaling. *Science* 2006, *312*, 1882-1883.
[5] Buetler, T. M.; Krauskopf, A.; Ruegg, U. T. Role of Superoxide as a signaling molecule. *News Physiol. Sci.* 2004, *19*, 120-123.
[6] Fridovich, I. Superoxide radical and superoxide dismutases. *Annu. Rev. Biochem.* 1995, *64*, 97-112.
[7] Youn, H. D.; Kim, E. J.; Roe, J. H.; Hah, Y. C.; Kang, S. O. A novel nickel-containing superoxide dismutase from *Streptomyces spp. Biochem. J.* 1996, *15*, 889-896.
[8] Beyer, W. F. Jr.; Fridovich, I. *In vivo* competition between iron and manganese for occupancy of the active site region of the manganese-superoxide dismutase of *Escherichia coli*. *J. Biol. Chem.* 1991, *266*, 303-308.
[9] Smith, M. W.; Doolittle, R. F. A comparison of evolutionary rates of the two major kinds of superoxide dismutase. *J. Mol. Evol.* 1992, *34*, 175-184.

[10] Li, Y.; Huang, T. T.; Carlson, E. J.; Melov, S.; Ursell, P. C.; Olson, J. L.; Noble, L. J.; Yoshimura, M. P.; Berger, C.; Chan, P. H.; Wallace, D. C.; Epstein, C. J. Dilated cardiomyopathy and neonatal lethality in mutant mice lacking manganese superoxide dismutase. *Nat. Genet.* 1995, *11*, 376-381.

[11] Fattman, C. L.; Schaefer, L. M.; Oury, T. D. Extracellular superoxide dismutase in biology and medicine. *Free Radic. Biol. Med.* 2003, *35*, 236-256.

[12] Reveillaud, I.; Phillips, J.; Duyf, B.; Hilliker, A.; Kongpachith, A.; Fleming, J. E. Phenotypic rescue by a bovine transgene in a Cu/Zn superoxide dismutase-null mutant of *Drosophila melanogaster*. *Mol. Cell. Biol.* 1994, *14*, 1302-1307.

[13] Reaume, A. G.; Elliott, J. L.; Hoffman, E. K.; Kowall, N. W.; Ferrante, R. J.; Siwek, D. F.; Wilcox, H. M.; Flood, D. G.; Beal, M. F.; Brown, R. H. Jr.; Scott, R. W.; Snider, W. D. Motor neurons in Cu/Zn superoxide dismutase-deficient mice develop normally but exhibit enhanced cell death after axonal injury. *Nat. Genet.* 1996, *13*, 43-47.

[14] Rojo, A.I.; Salinas, M.; Martin, D.; Perona, R.; Cuadrado, A. Regulation of Cu/Zn-superoxide dismutase expression via the phosphatidylinositol 3 kinase/Akt pathway and nuclear factor-kappaB. *J. Neurosci.* 2004, *24*, 7324-7334.

[15] Zimmerman, M. C.; Lazartigues, E.; Lang, J. A.; Sinnayah, P.; Ahmad, I. M.; Spitz, D. R.; Davisson, R. L. Superoxide mediates the actions of angiotensin II in the central nervous system. *Circ. Res.* 2002, *91*, 1038-1045.

[16] Huang, W. C.; Chio, C. C.; Chi, K. H.; Wu, H. M.; Lin, W. W. Superoxide anion-dependent Raf/MEK/ERK activation by peroxisome proliferator activated receptor gamma agonists 15-deoxy-delta12,14-prostaglandin J2, ciglitazone, and GW1929. *Exp. Cell. Res.* 2002, *277*, 192-200.

[17] Banci, L.; Benedetto, M.; Bertini, I.; Del Conte, R.; Piccioli, M.; Viezzoli, M. S. Solution structure of reduced monomeric Q133M2 copper, zinc superoxide dismutase (SOD). Why is SOD a dimeric enzyme?. *Biochemistry* 1998, *37*, 11780-11791.

[18] Hong, Z.; LoVerde, P.T.; Thakur, A.; Hammarskjold, M.L.; Rekosh, D. *Schistosoma mansoni*: a Cu/Zn superoxide dismutase is glycosylated when expressed in mammalian cells and localizes to a subtegumental region in adult schistosomes. *Exp. Parasitol.* 1993, *76*, 101-114.

[19] Mei, H.; LoVerde, P. T. *Schistosoma mansoni*: the developmental regulation and immunolocalization of antioxidant enzymes. *Exp. Parasitol.* 1997, *86*, 69-78.

[20] Mei, H.; Hirai, H.; Tanaka, M.; Hong, Z.; Rekosh, D.; LoVerde, P. T. *Schistosoma mansoni*: cloning and characterization of a gene encoding cytosolic Cu/Zn superoxide dismutase. *Exp. Parasitol.* 1995, *80*, 250-259.

[21] Kim, T. S.; Jung, Y.; Na, B. K.; Kim, K. S.; Chung, P. R. Molecular cloning and expression of Cu/Zn-containing superoxide dismutase from *Fasciola hepatica*. *Infect. Immun.* 2000, *68*, 3941-3948.

[22] Cardoso, R. M.; Silva, C. H.; Ulian de Araujo, A. P.; Tanaka, T.; Tanaka, M.; Garratt, R. C. Structure of the cytosolic Cu,Zn superoxide dismutase from *Schistosoma mansoni*. *Acta Crystallogr. D. Biol. Crystallogr.* 2004, *60*, 569-578.

[23] Shalaby, K. A.; Yin, L.; Thakur, A.; Christen, L.; Niles, E. G.; LoVerde, P.T. Protection against *Schistosoma mansoni* utilizing DNA vaccination with genes encoding Cu/Zn cytosolic superoxide dismutase, signal peptide-containing superoxide dismutase and glutathione peroxidase enzymes. *Vaccine* 2003, *22*, 130-136.

[24] Sanchez-Moreno, M.; Garcia-Ruiz, M. A.; Garcia-Rejon, L.; Valero, A.; Leon, P. Superoxide dismutase in cestodes. Isoenzymatic characterization and studies of inhibition by a series of benzimidazoles and by pyrimidine derivatives of recent synthesis. *Arzneimittelforschung* 1989, *39*, 759-761.

[25] Sanchez-Moreno, M.; Leon, P.; Salas-Peregrin, J. M.; Garcia-Ruiz, M. A.; Monteoliva, M. Superoxide dismutase in trematodes. Isoenzymatic characterization and studies of inhibition by a series of benzimidazoles and by pyrimidines of recent syntheses. *Arzneimittelforschung* 1987, *37*, 903-905.

[26] Feng, J. J.; Guo, H. F.; Yao, M. Y.; Xiao, S. H. Effects of mebendazole, albendazole, and praziquantel on glutathione S-transferase and superoxide dismutase of *Echinococcus granulosus* cyst wall harbored in mice. *Zhongguo Yao Li Xue Bao.* 1995, *16*, 297-300.

[27] Henkle-Duhrsen, K.; Kampkotter, A. Antioxidant enzyme families in parasitic nematodes. *Mol. Biochem. Parasitol.* 2001, *114*, 129-142.

[28] Li, A. H.; Kong, Y.; Cho, S. H.; Lee, H. W.; Na, B. K.; Pak, J. K.; Kim, T. S. Molecular cloning and characterization of the copper/zinc and manganese superoxide dismutase genes from the human parasite *Clonorchis sinensis*. *Parasitology* 2005, *130*, 687-697.

[29] Leid, R. W.; Suquet, C. M. A superoxide dismutase of metacestodes of *Taenia taeniaeformis*. *Mol. Biochem. Parasitol.* 1986, *18*, 301-311.

[30] Gonzalez, R.; Mendoza-Hernandez, G.; Plancarte, A. Purification of *Taenia solium* cysticerci superoxide dismutase and myoglobin copurification. *Parasitol.* 2002, *88*, 881-887.

[31] Castellanos-Gonzalez, A; Jiménez, L.; Landa, A. Cloning, production and characterisation of a recombinant Cu/Zn superoxide dismutase from *Taenia solium*. *Int. J. Parasitol.* 2002, *32*, 1175-1182.

[32] Sali, S.; Blundell, T. L. Comparative protein modeling by satisfaction of spatial restraints. *J. Mol. Biol.* 1993, *234*, 779-815.

[33] Rhee, S. G.; Kang, S.W.; Chang, T. S.; Jeong, W.; Kim, K. Peroxiredoxin, a novel family of peroxidases. *IUBMB Life* 2001, *52*, 35-41.

[34] Jacobson, F. S.; Morgan, R. W.; Christman, M. F.; Ames, B. N. An alkyl hydroperoxide reductase from *Salmonella typhimurium* involved in the defense of DNA against oxidative damage. Purification and properties. *J. Biol. Chem.* 1989, *264*, 1488-1496.

[35] Dubuisson, M.; Vander-Stricht, D.; Clippe, A.; Etienne, F.; Nauser, T.; Kissner, R.; Koppenol W. H.; Rees, J. F.; Knoops, B. Human peroxiredoxin 5 is a peroxynitrite reductase. *FEBS. Lett.* 2004, *571*, 161-165.

[36] Fujii, J.; Ikeda, Y. Advances in our understanding of peroxiredoxin, a multifunctional, mammalian redox protein. *Redox Rep.* 2002, *7*, 123-130.

[37] Rhee, S. G.; Chae, H. Z.; Kim, K. Peroxiredoxins: a historical overview and speculative preview of novel mechanisms and emerging concepts in cell signaling. *Free Radic. Biol. Med.* 2005, *38*, 1543-1552.

[38] Wood, Z. A.; Schroder, E.; Robin-Harris, J.; Poole, L. B. Structure, mechanism and regulation of peroxiredoxins. *Trends Biochem. Sci.* 2003, *28*, 32-40.

[39] Kang, S. W.; Rhee, S. G.; Chang, T. S.; Jeong, W.; Choi, M. H. 2-Cys peroxiredoxin function in intracellular signal transduction: therapeutic implications. *Trends Mol. Med.* 2005, *11*, 571-578.

[40] Kang, S. W.; Chang, T. S.; Lee, T. H.; Kim, E. S.; Yu, D. Y.; Rhee, S. G. Cytosolic peroxiredoxin attenuates the activation of Jnk and p38 but potentiates that of Erk in Hela cells stimulated with tumor necrosis factor-alpha. *J. Biol. Chem.* 2004, *279*, 2535-2543.

[41] Woo, H. A.; Kang, S. W.; Kim, H. K.; Yang, K. S.; Chae, H. Z.; Rhee, S. G. Reversible oxidation of the active site cysteine of peroxiredoxins to cysteine sulfinic acid. Immunoblot detection with antibodies specific for the hyperoxidized cysteine-containing sequence. *J. Biol. Chem.* 2003, *278*, 47361-47364.

[42] Biteau, B.; Labarre, J.; Toledano, M. B. ATP-dependent reduction of cysteine-sulphinic acid by S. cerevisiae sulphiredoxin. *Nature* 2003, *425*, 980-984.

[43] Budanov, A. V.; Sablina, A. A.; Feinstein, E.; Koonin, E. V.; Chumakov, P. M. and Regeneration of peroxiredoxins by p53-regulated sestrins, homologs of bacterial AhpD. *Science* 2004, *304*, 596-600.

[44] Woo, H. A.; Jeong, W.; Chang, T. S.; Park, K. J.; Park, S. J.; Yang, J. S.; Rhee, S. G. Reduction of cysteine sulfinic acid by sulfiredoxin is specific to 2-cys peroxiredoxins. *J. Biol. Chem.* 2005, *280*, 3125-3128.

[45] Wood, Z. A.; Poole, L. B.; Karplus, P. A. Peroxiredoxin evolution and the regulation of hydrogen peroxide signaling. *Science* 2003, *300*, 650-653.

[46] Sayed, A. A.; Williams, D. L. Biochemical characterization of 2-Cys peroxiredoxins from *Schistosoma mansoni*. *J. Biol. Chem.* 2004, *279*, 26159-26166.

[47] Salazar-Calderon, M.; Martin-Alonso, J. M.; Ruiz de Eguino, A. D.; Casais, R.; Marin, M. S.; Parra, F. *Fasciola hepatica*: heterologous expression and functional characterization of a thioredoxin peroxidase. *Exp. Parasitol.* 2000, *95*, 63-70.

Parasitol Res (2009) 105:781–787
DOI 10.1007/s00436-009-1461-6

ORIGINAL PAPER

Characterization of one typical 2-Cys Peroxiredoxin gene of *Taenia solium* and *Taenia crassiceps*

Felipe Vaca-Paniagua · Ricardo Parra-Unda · Abraham Landa

Received: 26 March 2009 / Accepted: 24 April 2009 / Published online: 8 May 2009

Abstract The *Taenia* genus is capable of living for long periods within its hosts. Reports have shown that this successful establishment is related to its efficient defense mechanisms against host immune response and its high tolerance to oxidative stress. In this work, we describe the genomic sequences of one *Taenia solium* and *Taenia crassiceps* typical 2-Cys peroxiredoxins (*Ts2-CysPrx*, *Tc2-CysPrx*) genes, which are 94% identical in primary sequence with the typical 2-Cys Prxs catalytic motifs. Both genes have the same genomic architecture, showing a TATA box and Initiator (Inr) sequence in their proximal promoter, two exons split by a 67-bp type III intron and one unique transcription start site located inside the Inr. We show that *T. crassiceps* cysticerci are highly tolerant to H_2O_2 presenting a lethal concentration 50 of 3.0 mM and demonstrate that the typical *Tc2-CysPrx* gene is not induced by H_2O_2, showing a behavior of an antioxidant housekeeping gene. This study describes for first time the gene structure of a typical 2-Cys Prx in the *Taenia* genus.

Introduction

The cestode *Taenia solium* is the causal agent of cysticercosis in humans and pigs. This parasite is present in most non-developed countries and massive human migration has spread it to developed countries as well. The most severe form of the disease, neurocysticercosis, is of worldwide importance due to its impact in human health and economy and although many efforts have been oriented to parasite control or eradication, it is still a public health problem; therefore, more studies are needed to fully accomplish this goal (Cambin et al. 2006).

Several reports have shown that the successful establishment of this taeniid and other helminths in the host is related to its evasion of the immune response and its antioxidant defense (Alvarez et al. 2008; Vaca-Paniagua et al. 2008; Batra et al. 1993) It is known that in the Taeniidae family of parasitic worms the enzymatic antioxidant system is composed by a Cu/Zn superoxide dismutase, two glutathione transferases, a thioredoxin glutathione reductase, and one typical 2-Cys Peroxiredoxin (Vaca-Paniagua et al. 2008; Torres-Rivera and Landa 2008; Rendón et al. 2004; Leid and Suquet 1986; Salinas et al. 1998; Salinas and Cardozo 2000; Li et al. 2004; Bonilla et al. 2008; Chalar et al. 1999). Peroxiredoxins (Prx) are antioxidant enzymes that reduce hydrogen peroxide (H_2O_2) to water and a wide range of hydroperoxides to the corresponding alcohol (Rhee et al. 2005). They are classified in 1-Cys Prxs and 2-Cys Prxs depending on if they use one or two cysteines for catalysis. The 2-Cys Prxs are further divided in typical and atypical regarding if they are dimeric or monomeric, respectively. In human helminth parasites, only typical 2-Cys Prxs have been found and they have been characterized principally in trematodes and nematodes, but in cestodes their studies are limited. They are involved in redox state balance (Sayed et al. 2006), signal and transcriptional regulation (Wood et al. 2003), and antioxidant and parasite defense (Li et al. 2004). For example, in the trematode parasites *Schistosoma mansoni* and *Schisto-*

This work was supported by the Consejo Nacional de Ciencia y Tecnología (CONACyT 80134) and Dirección General de Asuntos del Personal Académico, UNAM (DGAPA IN 207507-3). FVP was supported by CONACyT (195340) and is a student of PDCB.

F. Vaca-Paniagua · R. Parra-Unda · A. Landa (✉)
Departamento de Microbiología y Parasitología, Facultad de Medicina, Universidad Nacional Autónoma de México, Edificio A 2do piso, Ciudad Universitaria, México City 04510, México
e-mail: landap@servidor.unam.mx

soma japonicum, three typical 2-Cys Prxs have been characterized, of which Prx1 is induced under oxidant conditions, while Prx2 and Prx3 are housekeeping genes (Kumagai et al. 2006; Sayed and Williams 2004; Sayed et al. 2006). The silencing of typical 2-Cys Prxs genes with dsRNAi drastically increased parasite sensibility against H_2O_2 (Sayed et al. 2006). The lack of catalase and the fact that no high H_2O_2-reducing activity glutathione peroxidase has been found in the Platyhelminthes phylum (Callahan et al. 1988; Mei and LoVerde 1997) highlight the biological role of typical 2-Cys Prx as a major source of H_2O_2 detoxification in these parasites (Pérez-Torres et al. 2002; Lu et al. 1998). Moreover, the localization of *T. solium* 2-Cys Prxs on the parasite tegument suggests that they are in direct contact with the host immune response (Molina-López et al. 2006).

Here, we describe the genomic structure of a *T. solium* and a *Taenia crassiceps* typical 2-Cys Prx gene (*Ts2-CysPrx*, *Tc2-CysPrx*) and show that *Tc2-CysPrx* is not induced under oxidant conditions. Additionally, we show that *T. crassiceps* is highly resistant to H_2O_2.

Materials and methods

Biological materials

T. solium cysticerci were dissected from naturally infected pork, washed three times with sterile phosphate-buffered saline (PBS), and stored at −70°C until use. *T. crassiceps* WFU strain was extracted from the peritoneum of infected BALB/cAnN female mice killed with CO_2 and washed three times with sterile PBS (Everhart et al. 2004).

Cloning of *Ts2-CysPrx* and *Tc2-CysPrx* genes

T. solium and *T. crassiceps* genomic DNA was extracted as described previously (Campos et al. 1990). Briefly 1.5 g cysticerci was digested with Proteinase K for 2–3 h at 55°C in TRIS 50 mM, EDTA 1 mM, and sarcosyl 0.5%, followed by centrifugation at 1,000× g for 15 min, phenol/chloroform extractions, and isopropanol precipitation. *Eco*RI-digested *T. solium* genomic DNA was used for the construction of a λ-ZAP library using the Uni-ZAP®XR vector System (Stratagene, La Jolla, CA, USA). One hundred and twenty thousand clones were screened overnight at 60°C with a [α-^{32}P]dCTP-labeled *Ts2-CysPrx* probe comprising the complete complementary DNA (cDNA) sequence of the gene labeled by nick-translation with random primers (Amersham Biosciences). After secondary and tertiary screenings, phage-positive clones were converted to Bluescript plasmids using ExAssist helper phage (Stratagene). Bacterial colonies containing the plasmid Bluescript were grown overnight in LB ampicillin (100 μg/mL) medium. Plasmid DNA was prepared with alkaline lysis standard method and sequenced on an automated fluorescent dye DNA sequencer AB1 Prism model 373 (Perkin-Elmer, Applied Biosystems). *T. crassiceps 2-Cys Prx* gene cloning was done by polymerase chain reaction (PCR) amplification using 100 ng of parasite DNA and primers designed from 5′ and 3′ non-coding sequences of *Ts2-CysPrx* (forward: 5′-$^{-88}$GCCAATGTGTT TAAGGCTAGG^{-68}-3′ and reverse: 5′-^{705}CAACCAGTT CAAAGAGTGGC^{685}-3′) with the following program: 1 cycle of 94°C, 30 cycles of 94°C for 30 s, 55°C for 1 min, 72°C for 1 min; and one final extension of 72°C 5 min. The PCR product was cloned into pCRII dual promoter (Invitrogen) and the plasmid preparation was sequenced as mentioned before. Putative transcription factor binding sites were determined with the sequence analysis program PROMO: http://alggen.lsi.upc.es/cgi-bin/promo_v3/promo/promoinit.cgi?dirDB=TF_8.3).

Transcription start site determination

T. solium and *T. crassiceps* total RNA was prepared with TRIzol (Invitrogen) and used as template for transcription start site (TSS) determination using the Smart RACE cDNA Amplification Kit and Advantage 2 Polymerase Mix (Clontech). Both 5′ parasite Prx RACE fragments were amplified by PCR using reverse primer Prx6R (5′-AACA TCTTTGAGTTCACCATCGACAA-3′) and forward primer SMARTII (5′-AAGCAGTGGTATCAACGCAGAGTAC GCGGG-3′), following the manufacturer's directions. The 5′ fragment of *T. solium* actin *pAT6* gene was done using the reverse primer PAT6R (5′-AGGGAGGGGAAGACAG CACGAGG-3′) designed from the pAT6 gene (Campos et al. 1990) and SMARTII. The resulting band of each PCR reaction was cloned into pCRII and sequenced.

Determination of *T. crassiceps* viability under oxidative conditions

After a preincubation of 4 h in RPMI 1640 (Sigma) with 5% CO_2 at 37°C, parasites were immediately incubated in medium with 1–7.5 mM of H_2O_2 for 1 h at the same conditions. Afterwards, parasites were washed and incubated in 0.2 mL of pig bile diluted 1:3 in RPMI 1640 for 30–60 min to evaluate scolex evagination, which was observed in an inverted microscope (Nikon Eclipse TS100).

Tc2-CysPrx messenger RNA expression

Three different groups of *T. crassiceps* cysticerci were used for the expression studies: (1) in RPMI 1640 medium for 0, 1, 4, and 24 h; (2) in medium with H_2O_2 (0.25, 0.5, 1, and 2 mM) for 30 min; and (3) in medium with H_2O_2 1 mM for

0, 0.5, 1, 2, 3, and 24 h. Groups 2 and 3 were preincubated 4 h as mentioned before the addition of the medium with H_2O_2. Messenger RNA expression was determined by reverse transcriptase (RT)-PCR with One Step RT-PCR kit (Invitrogen) using 1 µg of *T. crassiceps* total RNA template and primers PRX-3 (5′-CTCCGTGGTCTCTTTATCA-3′) and PRX-9R (5′-CTATCTTGAGCTCATGAACG-3′) to amplify 2-Cys Prx. Likewise, β-actin amplification was done with primers PAT6-5′ (5′-TCCGGTATGTGCAAAGCC-3′) and PAT6-3′ (5′-GTGATGCCAGATCTTCTCC-3′). Empirically, we determined that in 30 cycles of PCR amplification all the amplicons were within the linear range of product formation and did not plateau as a saturated product. The program used in all reactions was 50°C for 30 min for reverse transcriptase reaction and 30 cycles of 94°C for 30 s, 50°C for 1 min, of 72°C for 1 min; and final extension of 72°C 5 min for PCR reaction. Amplicons were visualized by electrophoresis in 2% agarose gels stained with ethidium bromide.

Tt2-CysPrx protein expression by Western blot

Preincubated *T. crassiceps* cysts were incubated in RPMI medium with H_2O_2 (0, 1, and 2 mM for 30 min) and used to prepare crude protein extracts. Approximately 60 mg of tissue was sonicated four times at 40 W for 1 min leaving 1 min on ice between each pulse in 500 µL of lysis buffer (urea 8 M, CHAPS 0.5 M, pepstatin 1 µM, leupeptin 0.6 µM, phenylmethanesulfonyl fluoride 0.2 mM, DTT 0.5 mM). One hundred microliters of the parasite suspension was purified with 2-D Clean-Up Kit (Amersham) following the manufacturer's instructions. The resulting pellets containing the total crude proteins were resuspended in 100 µL and centrifuged at 12,000×*g* for 5 min at 4°C. The supernatant was quantified by the Bradford method, aliquoted, and stored until use at −20°C. Protein extract (15 µg/lane) integrity was determined in 12% sodium dodecyl sulfate polyacrylamide gel electrophoresis (SDS-PAGE) with 2-mercaptoethanol and stained with Coomassie blue. For Western blot, 12% SDS-PAGE gels with 2 µg of protein extracts per millimeter of lane were transferred to PVDF membranes (Towbin et al. 1979). Membranes were incubated with rabbit serum anti-*Tt2-CysPrx* (1:1,000) or rabbit anti-β-actin (Abcam, 1:2,000), washed, and incubated with peroxidase-conjugated anti-rabbit IgG. Bound antibodies were revealed with 3,3′-diaminobenzidine and 1% H_2O_2.

Results

Analysis of 2-Cys Prx gene structure

The *Tt2-CysPrx* and *Tc2-CysPrx* genes were cloned from a genomic λ-ZAP library and by PCR using genomic DNA, respectively. The genomic sequences of both genes were deposited in GenBank under accession numbers FJ621569 and FJ621570, respectively. Both Prxs have the typical 2-Cys Prxs catalytic motifs (^{47}FVCP^{50}, ^{168}EVCP^{171} for *Tt2-CysPrx*; and ^{46}FVCP^{49}, ^{167}EVCP^{170} for *Tc2-CysPrx*), where amino-terminal catalytic and resolving carboxy-terminal cysteines are located. They also have residues and motifs similar to that reported for phosphorylation in S^{88} and overoxidation in ^{92}GGVQ^{95} and ^{198}FM^{192} in *Tt2-CysPrx* and in *Tc2-CysPrx* in S^{87}, ^{91}GGVQ^{94}, and ^{190}FM^{191} (Wood et al. 2008). As seen in Fig. 1, sequence analysis showed that both proximal promoters have a TATA box and an Initiator (Inr) sequence, as well as putative binding sites for NF-1 (at −62 and −65 pb for *Tt2-CysPrx* and *Tc2-CysPrx*, respectively), Nrf-2 (at −46 and −153 for *Tt2-CysPrx* and at −49 for *Tc2-CysPrx*), and Sp1 (at −275 for *Tt2-CysPrx*). It is interesting to note that both genes contain the −3 and +4 guanines (in respect to the translation start codon; GNNATGG) described by Kozak to be translation enhancers (Kozak 1987). Both genes had two exons separated by one small type III intron of 67 bp that has NGT-AGN donor-acceptor sites placed in codon 102 for *Tt2-CysPrx* and 101 for *Tc2-CysPrx*. Sequence analysis of both introns showed a putative U1 recognition sequence (*Tt2-CysPrx*: ^{155}GTGAGT^{160}; *Tc2-CysPrx*: ^{160}GTGACT^{165}; numbering from the first transcribed nucleotide, see below) spanning the donor site (underlined), and a pyrimidine-rich tract for U2 Associated Factor (U2AF) binding (*Tt2-CysPrx*: ^{206}TTACGTTGCTCTTCCTAG^{221}; *Tc2-CysPrx*: ^{206}TAG CGTTGCTCTTCTTAG^{225}) positioned in the acceptor site (underlined). For *Tc2-CysPrx*, exon 1 is 134 pb and exon 2 is 454 pb, while exon 1 and 2 of *Tt2-CysPrx* are 131 and 454 nt.

Transcription start site

Analysis of the sequences located upstream of the ATG in *Tt2-CysPrx* and *Tc2-CysPrx* indicated the presence of an Inr sequence and a TATA box. To localize the TSS in both genes, we performed 5′ RACE experiments and sequenced of the amplified products of *Tt2-CysPrx* and *Tc2-CysPrx*. The TSS in *Tt2-CysPrx* was mapped 20 nt upstream of the translation start codon (ATG), whereas in *Tc2-CysPrx* it was located 27 nt upstream of the ATG. In both cases, the TSS corresponds to an A located within Inr sequence (TGAATTCC, for *Tt2-CysPrx* and TGAATCC for *Tc2-CysPrx*; where the A is the first transcribed nucleotide; Fig. 1). Further sequence analysis showed that the Inr and TATA sequences of *Tt2-CysPrx* and *Tc2-CysPrx* are conserved in the Cestoda genes, such as *T. solium* actin genes *pAT5* and *pAT6*, as well as to the *Echinococcus granulosus* actin genes *Egact1* and *Egact11* (Campos et al. 1990; da Silva et al. 1993); moreover, the nucleotide distance between both elements is conserved in all the

Fig. 1 Gene structure of *T. solium* (*Ts*) and *T. crassiceps* (*Tc*) 2-Cys Prxs. The transcription start point is marked with an *arrow*. Initiator (Inr) sequence, TATA box, start (ATG) and stop (TAG) codons, donor and acceptor intron sequences, and protein regulatory and catalytic motifs are in *bold*. Nucleotide and amino acid identity is denoted with *asterisks and dots*, respectively. The *Tc2-CysPrx* polyadenylation site is denoted with a *triangle*. Putative splicing factor sites for U1 and U2AF are *underlined*. Putative transcription factor binding sites are written above their corresponding motifs

sequences analyzed (Fig. 2). In order to know if the TSS located in the Inr sequence of the Prxs genes studied is conserved in *T. solium pAT6*, we conducted more 5′ RACE experiments, which mapped actin gene TSS also inside the Inr sequence (Fig. 2). This result demonstrates sequence conservation between different taeniids gene proximal promoters. The *T. solium* splice leader sequence reported for a group of parasite genes was absent in all transcripts analyzed (Brehm et al. 2002).

Viability of *T. crassiceps* and *Tc2-CysPrx* expression under oxidant conditions

In order to know if *T. crassiceps 2-Cys Prx* gene is induced under oxidant conditions, expression experiments were conducted using *T. crassiceps* cysticerci in controlled conditions. First, we established a concentration curve to determine viability in cysticerci incubated in medium with H_2O_2 for 1 h. Viability of the parasites was assumed as the

Fig. 2 Multiple alignment of Cestoda promoter nucleotide sequences. Non-coding 5′ upstream sequences of *E. granulosus* actin I and actin II (*EgactI*, *EgactII*) (da Silva et al. 1993), *T. solium* actins *pAT5* and *pAT6* (M28996, M28997), *Tc2-CysPrx* (*TcPrx*, FJ621569), and *Tc2-CysPrx* (*TcPrx*, FJ621570) were manually aligned. TATA box and Inr sequence, and ATG start codon are in *bold*. The TSS is *underlined*. The symbol // denotes the lacking nucleotides 5′-AGAA GA-CAAAT CCTTTGGTGAGCC-3′

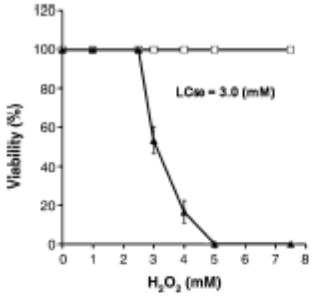

Fig. 3 Determination of the lethal concentration (LC_{50}) of *T. crassiceps* to H_2O_2. Cysticerci were exposed to different H_2O_2 concentrations for 1 h (*triangles*) prior viability determination (see "Materials and methods"). Parasites incubated in medium without H_2O_2 were used as a control (*open bones*). Data are mean ± SD (n=8)

capacity of cysticerci scolex evagination, to follow its life cycle to adult worm. We found that parasite viability is reduced when H_2O_2 concentration is increased. Parasite viability remains unaffected up to 2 mM of H_2O_2, and after this concentration, it begins to decrease until it reaches zero at 5 mM. This viability kinetics showed that lethal concentration 50 (LC_{50}) of H_2O_2 is 3.0 mM (Fig. 3). These data were used to determine conditions for *Tc2-CysPrx* messenger RNA (mRNA) and protein expression assays. We evaluated the expression profile of the gene in parasites incubated in medium without oxidative insult. These experiments showed that *Tc2-CysPrx* mRNA expression levels remained unchanged in cysticerci incubated in medium for up to 24 h (Fig. 4a). Therefore, we used 4 h of preincubation prior to the incubation of parasites with H_2O_2. As seen in Fig. 4b, *Tc2-CysPrx* mRNA expression level did not change in parasites incubated for 30 min with H_2O_2 concentrations ranging from 0 to 2 mM. Also gene mRNA expression level was not changed in parasites incubated with 1 mM of H_2O_2 for 0.5, 1, 2, 3, and 24 h (Fig. 4c). In these experiments, the expression level of *Tc2-CysPrx* mRNA was constant and the intensity of the bands was similar throughout time and concentrations of H_2O_2 used. On the other hand, *Tc2-CysPrx* protein expression level remained the same in parasites incubated with 0, 1, and 2 mM of H_2O_2 for 30 min (Fig. 4d).

Discussion

We have cloned one gene of a typical 2-Cys Prx in *T. solium* and *T. crassiceps*. Their genomic architecture and high identity at the level of primary and nucleotide sequence suggest that both genes are homologous. Computational analyses showed two putative sites for Nrf2 in their promoter sequence, a factor involved in the regulation of antioxidant genes (Lee and Johnson 2004). Besides we found putative sites for the transcription factors NF1 and Sp1, it is known that these transcription factors can interact with members of the basal transcription factor machinery, such as TBP and TFIIB (Xiao et al. 1994; Kim and Roeder 1994; Emili et al. 1994). However, functional studies should be done to corroborate these findings.

The proximal promoters of both genes have a TATA box, an Inr sequence, and a single TSS that corresponds to an A

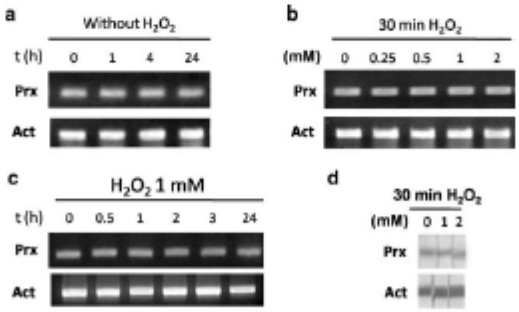

Fig. 4 Gene expression profile of *Tc2-CysPrx* from cysticerci exposed to H_2O_2 determined by RT-PCR and WB. Determination of expression of *Tc2-CysPrx* mRNA in cysticerci: a incubated in RPMI medium without H_2O_2 at 0 to 24 h; b exposed to different H_2O_2 concentrations for 30 min and c exposed to H_2O_2 1 mM for different times. d Determination of Tc2-CysPrx protein expression in parasites incubated 30 min in RPMI with H_2O_2 1 and 2 mM. Expression experiments were done by triplicate and β-actin was used as a control. A representative gel and blot of each experiment is shown

located within the Inr sequence. This result is consistent with the data reported for a subset of mammalian genes where TSS is located in the Inr consensus sequence (YYANWYY) comprising −2 to +5 and which has a TATA box located at −28 to −34 from the TSS (Smale and Kadonaga 2003; Sandelin et al. 2007). Additional sequence analysis of other Cestoda genes showed that *pAT5*, *pAT6*, *Egact1*, and *Egact11* proximal promoters present strong similarities to the ones reported in this work, since all have a TATA and an Inr sequence with a conserved A placed in the mapped TSS on *Tt2-CysPrx* and *Tc2-CysPrx*. Therefore, we mapped the TSS of *pAT6* and found it matches to the TSS of *Tt2-CysPrx* and *Tc2-CysPrx*, which suggests that the Inr present in the genes analyzed could be functional and the TSS of *pAT5*, *Egact1*, and *Egact11* is conserved. The structural region of *Tt2-CysPrx* and *Tc2-CysPrx* has two exons split by one intron with known splicing sequences (Padgett et al. 1986; Schellenberg et al. 2008). These analyses showed that proximal promoter sequences, such as Inr and TATA boxes, characterized in mammalian genes are also present in Cestoda genes and that splicing signals in *Taenia* genus are not different from other eukaryotic organisms.

Besides, we showed in vitro that *T. crassiceps* cysticerci have a LC_{50} to H_2O_2 of 3 mM. This extreme concentration of H_2O_2 is never reached in the host. Therefore, the lack of catalase and probably the presence of a low GPx activity toward H_2O_2 in these parasites suggests that resistance to high H_2O_2 concentration in the medium could be conferred mainly by the typical 2-Cys Prxs. In this context, reports on *S. mansoni* and *S. japonicum* show that there are three typical 2-Cys Prxs isoforms in schistosomatids: a cytosolic overoxidation insensitive Prx1, which is overexpressed under oxidant conditions and which could participate in responsive antioxidant defense against exogenous H_2O_2; and a cytosolic Prx2 and a peptide-targeted mitochondrial Prx3, which are both housekeeping genes. The latter two are prone to overoxidation by the presence of a C-terminal overoxidation FM motif, which is similar to the YF motif of the *Taenia* genes studied (Sayed and Williams 2004; Molina-López et al. 2006). The absence of a mitochondrial signal peptide and the presence of the C-terminal YF motif suggest that *Tt2-CysPrx* and *Tc2-CysPrx* are cytosolic overoxidation susceptible Prxs, such as schistosomal Prx2. We found that at the RNA and protein levels *Tt2-CysPrx* is not overexpressed under oxidant conditions. This expression pattern has been observed in other typical 2-Cys Prxs, such as human Prx2 (Diet et al. 2007), the nematode *Haemonchus contortus* 2-Cys Prx (Bagnall and Kotze 2004), the *S. mansoni* Prx2 (Sayed et al. 2006) and *Plasmodium falciparum* PfTPX-1 (Yano et al. 2005). Lack of induction of *Tc2-CysPrx* suggests that this protein could be an antioxidant housekeeping gene for endogenous H_2O_2 that possibly participates as a redox regulator, rather than a responsive gene against exogenous oxidative stress. This is in accordance with our previous observations made in *Tt2-CysPrx*, where gene expression persists through all the life cycle of *T. solium*, even in the adult stage which is not subject to oxidative stress (Molina-López et al. 2006). It is likely that other non-enzymatic antioxidant systems could act to protect the parasite, as seen in *S. mansoni*, where oxidant conditions induce albumin silent gene expression as a sacrificial protein prone to oxidation (Sayed et al. 2006).

The shared proximal promoter architecture found in the Cestoda genes presented here suggests that the transcription machinery in these parasites is similar to their mammalian counterpart, and that Cestoda genes possess TATA and Inr sequences that serve for TSS positioning. This is the first report which describes a proximal promoter sequence of a gene in cestodes. Our findings provide new insights for further investigations of genes in taeniids of medical interest, which could contribute for their eradication.

Acknowledgments We thank MD. Alicia Ochoa Sánchez for technical help. The authors declare that the experiments comply with the current laws for animal use and care (NOM-062-ZOO-1999) of the country in which they were performed.

References

Alvarez JI, Rivera J, Teale JM (2008) Differential release and phagocytosis of tegument glycoconjugates in neurocysticercosis: implications for immune evasion strategies. PLoS Negl Trop Dis 2:e218

Batra S, Srivastava JK, Gupta S, Katiyar JC, Srivastava VM (1993) Role of reactive oxygen species in expulsion of *Nippostrongylus brasiliensis* from rats. Parasitology 106:185–192

Bonilla M, Denicola A, Novoselov SV, Turanov AA, Protasio A, Izmendi D, Gladyshev VN, Salinas G (2008) Platyhelminth mitochondrial and cytosolic redox homeostasis is controlled by a single thioredoxin glutathione reductase and dependent on selenium and glutathione. J Biol Chem 283:17898–17907

Brehm K, Hubert K, Sciutto E, Garate T, Frosch M (2002) Characterization of a spliced leader gene and of trans-spliced mRNAs from *Taenia solium*. Mol Biochem Parasitol 122:105–110

Callahan HL, Crouch RK, James ER (1988) Helminth anti-oxidant enzymes: a protective mechanism against host oxidants? Parasitol Today 4:218–225

Campos A, Bernard P, Fauconnier A, Landa A, Gómez E, Hernández R, Willms K, Laclette JP (1990) Cloning and sequencing of two actin genes from *Taenia solium* (Cestoda). Mol Biochem Parasitol 40:87–93

Cleaban H, Krecek RC, Cowan LD, Michael L, Foyaca-Sibat H, Nash T, Willingham AL (2006) Estimation of the cost of *Taenia solium* cysticercosis in Eastern Cape Province, South Africa. Trop Med Int Health 11:906–916

Chalar C, Martínez C, Agorio A, Salinas G, Soto J, Ehrlich R (1999) Molecular cloning and characterization of a thioredoxin gene from *Echinococcus granulosus*. Biochem Biophys Res Commun 262:302–307

da Silva CM, Henrique FR, Picón M, Gorfinkiel N, Ehrlich R, Zaha A (1993) Molecular cloning and characterization of actin genes from *Echinococcus granulosus*. Mol Biochem Parasitol 60:209–219

Dixt A, Abbas K, Bouton C, Guillon B, Tomasello F, Fourquet S, Toledano MB, Drapier JC (2007) Regulation of peroxiredoxins by nitric oxide in immunostimulated macrophages. J Biol Chem 282:36199–36205

Emili A, Greenblatt J, Ingles CJ (1994) Species-specific interaction of the glutamine-rich activation domains of Sp1 with the TATA box-binding protein. Mol Cell Biol 14:1582–1593

Everhart ME, Kuhn RE, Zelmer DA (2004) Infrapopulation dynamics of a wild strain of *Taenia crassiceps* (WFU) (Cestoda: Taeniidae) in BALB/cJ mice. J Parasitol 90:79–84

Kim TK, Roeder RG (1994) Proline-rich activator CTF1 targets the TFIIB assembly step during transcriptional activation. Proc Natl Acad Sci U S A 91:4170–4174

Kozak M (1987) An analysis of 5'-noncoding sequences from 699 vertebrate messenger RNAs. Nucleic Acids Res 20:8125–8148

Kumagai T, Osada Y, Kanazawa T (2006) 2-Cys peroxiredoxins from *Schistosoma japonicum*: the expression profile and localization in the life cycle. Mol Biochem Parasitol 149:135–143

Lee JM, Johnson JA (2004) An important role of Nrf2-ARE pathway in the cellular defense mechanism. J Biochem Mol Biol 37:139–143

Leid RW, Suquet CM (1986) A superoxide dismutase of metacestodes of *Taenia taeniaeformis*. Mol Biochem Parasitol 18:301–311

Li J, Zhang WB, Loukas A, Lin RY, Ito A, Zhang LH, Jones M, McManus DP (2004) Functional expression and characterization of *Echinococcus granulosus* thioredoxin peroxidase suggests a role in protection against oxidative damage. Gene 326:157–165

Lu W, Egerton GL, Bianco AE, Williams SA (1998) Thioredoxin peroxidase from *Onchocerca volvulus*: a major hydrogen peroxide detoxifying enzyme in filarial parasites. Mol Biochem Parasitol 91:221–235

Mei H, LoVerde PT (1997) *Schistosoma mansoni*: the developmental regulation and immunolocalization of antioxidant enzymes. Exp Parasitol 86:69–78

Molina-López J, Jiménez L, Ochoa-Sánchez A, Landa A (2006) Molecular cloning and characterization of a 2-Cys peroxiredoxin from *Taenia solium*. J Parasitol 92:796–802

Padgett RA, Grabowski PJ, Konarska MM, Seiler S, Sharp PA (1986) Splicing of messenger RNA precursors. Annu Rev Biochem 55:1119–1150

Pérez-Torres A, Ustarroz M, Constantino F, Villalobos N, de Aluja AA (2002) *Taenia solium* cysticercosis: lymphocytes in the inflammatory reaction in naturally infected pigs. Parasitol Res 88:150–152

Rendón JL, del Arenal IP, Guevara-Flores A, Uribe A, Plancarte A, Mendoza-Hernández G (2004) Purification, characterization and kinetic properties of the multifunctional thioredoxin-glutathione reductase from *Taenia crassiceps* metacestode (cysticerci). Mol Biochem Parasitol 133:61–69

Rhee SG, Chae HZ, Kim K (2005) Peroxiredoxins: a historical overview and speculative preview of novel mechanisms and emerging concepts in cell signaling. Free Radic Biol Med 38:1543–1552

Salinas G, Cardozo S (2000) *Echinococcus granulosus*: heterogeneity and differential expression of superoxide dismutases. Exp Parasitol (94):56–59

Salinas G, Fernández V, Fernández C, Selkirk ME (1998) *Echinococcus granulosus*: cloning of a thioredoxin peroxidase. Exp Parasitol 90:298–301

Sandelin A, Carninci P, Lenhard B, Ponjavic J, Hayashizaki Y, Hume DA (2007) Mammalian RNA polymerase II core promoters: insights from genome-wide studies. Nat Rev Genet 8:424–436

Sayed AA, Williams DL (2004) Biochemical characterization of 2-Cys peroxiredoxins from *Schistosoma mansoni*. J Biol Chem 279:26159–26166

Sayed AA, Cook SK, Williams DL (2006) Redox balance mechanisms in *Schistosoma mansoni* rely on peroxiredoxins and albumin and implicate peroxiredoxins as novel drug targets. J Biol Chem 281:17001–17010

Schellenberg MJ, Ritchie DB, MacMillan AM (2008) Pre-mRNA splicing: a complex picture in higher definition. Trends Biochem Sci 33:243–246

Smale ST, Kadonaga JT (2003) The RNA polymerase II core promoter. Annu Rev Biochem 72:449–479

Torres-Rivera A, Landa A (2008) Cooperative kinetics of the recombinant glutathione transferase of *Taenia solium* and characterization of the enzyme. Arch Biochem Biophys 477:372–378

Towbin H, Staehelin T, Gordon J (1979) Electrophoretic transfer of proteins from polyacrylamide gels to nitrocellulose sheets: procedure and some applications. Proc Natl Acad Sci U S A 76:4350–4354

Vaca-Paniagua F, Torres-Rivera A, Parra-Unda R, Landa A (2008) *Taenia solium*: antioxidant metabolism enzymes as targets for cestocidal drugs and vaccines. Curr Top Med Chem 8:393–399

Wood ZA, Poole LB, Karplus PA (2003) Peroxiredoxin evolution and the regulation of hydrogen peroxide signaling. Science 300:650–653

Xiao H, Lis JT, Xiao H, Greenblatt J, Friesen JD (1994) The upstream activator CTF/NF1 and RNA polymerase II share a common element involved in transcriptional activation. Nucleic Acids Res 22:1966–1973

Yano K, Komaki-Yasuda K, Kobayashi T, Takemae H, Kita K, Kano S, Kawazu S (2005) Expression of mRNAs and proteins for peroxiredoxins in *Plasmodium falciparum* erythrocytic stage. Parasitol Int 54:35–41

the FEBS Journal

Crystal structure of Cu/Zn superoxide dismutase from *Taenia solium* reveals metal-mediated self-assembly

Alejandra Hernández-Santoyo[1], Abraham Landa[2], Edith González-Mondragón[2], Martha Pedraza-Escalona[1], Ricardo Parra-Unda[2] and Adela Rodríguez-Romero[1]

1 Instituto de Química, Universidad Nacional Autónoma de México, Mexico
2 Departamento de Microbiología y Parasitología, Facultad de Medicina, Universidad Nacional Autónoma de México, Mexico

Keywords
crystal structure; metal-mediated self-assembly; superoxide dismutase; *Taenia solium*

Correspondence
A. Hernández-Santoyo, A. Rodríguez-Romero, Instituto de Química, Universidad Nacional Autónoma de México, México 04510, DF, Mexico
Fax: +52 55 56162217
Tel: +52 55 56224668
E-mail: hersan@servidor.unam.mx, adela@servidor.unam.mx

(Received 20 July 2010, revised 14 June 2011, accepted 13 July 2011)

doi:10.1111/j.1742-4658.2011.08247.x

Taenia solium is the cestode responsible for porcine and human cysticercosis. The ability of this parasite to establish itself in the host is related to its evasion of the immune response and its antioxidant defence system. The latter includes enzymes such as cytosolic Cu/Zn superoxide dismutase. In this article, we describe the crystal structure of a recombinant *T. solium* Cu/Zn superoxide dismutase, representing the first structure of a protein from this organism. This enzyme shows a different charge distribution at the entrance of the active channel when compared with human Cu/Zn superoxide dismutase, giving it interesting properties that may allow the design of specific inhibitors against this cestode. The overall topology is similar to other superoxide dismutase structures; however, there are several His and Glu residues on the surface of the protein that coordinate metal ions both intra- and intermolecularly. Interestingly, one of these ions, located on the β2 strand, establishes a metal-mediated intermolecular β–β interaction, including a symmetry-related molecule. The factors responsible for the abnormal protein–protein interactions that lead to oligomerization are still unknown; however, high metal levels have been implicated in these phenomena, but exactly how they are involved remains unclear. The present results suggest that this structure could be useful as a model to explain an alternative mechanism of protein aggregation commonly observed in insoluble fibrillar deposits.

Database
The atomic coordinates and structure factors have been deposited in the Protein Data Bank under the accession number 3MND.

Structured digital abstract
- Cu/Zn SOD binds to Cu/Zn SOD by dynamic light scattering (View Interaction 1, 2)
- Cu/Zn SOD binds to Cu/Zn SOD by mass spectrometry studies of complexes (View interaction)
- Cu/Zn SOD binds to Cu/Zn SOD by molecular sieving (View Interaction 1, 2)
- Cu/Zn SOD binds to Cu/Zn SOD by x-ray crystallography (View interaction)

Introduction

Superoxide dismutases (SODs, 1.15.1.1) are metalloenzymes that use Cu/Zn, Mn, Fe or Ni in their active sites to transform superoxide radicals ($O_2^{\bullet-}$) into hydrogen peroxide and molecular oxygen ($2O_2^{\bullet-} + 2H^+ \rightarrow H_2O_2 + O_2$). The metal ions function as cofactors that play important roles in the defence against oxygen-derived

Abbreviations
Aβ, amyloid-β; ALS, amyotrophic lateral sclerosis; PDB, Protein Data Bank; ROS, reactive oxygen species; SOD, superoxide dismutase; Ts, *Taenia solium*.

free radicals; therefore, these enzymes are important from a pharmaceutical point of view [1,2]. There are two forms of Cu/Zn-SOD enzymes: one extracellular (ECCu/Zn-SOD) tetramer composed of 30-kDa subunits, and a cytosolic (Cu/Zn-SOD) dimer with an M_r value of 16 kDa per subunit. Sequence alignment between the two enzymes shows 50% identity, and both contain a binuclear Cu^{2+}, Zn^{2+} centre per subunit [3,4]. Cu is involved in the catalytic reaction in two steps: first, Cu^{2+} reduction by one molecule of $O_2^{\bullet-}$ produces molecular oxygen, and Cu^{+} oxidation by another $O_2^{\bullet-}$ molecule generates H_2O_2. In contrast, Zn^{2+} plays a structural role. The structures of Cu/Zn-SODs from different eukaryotes have been investigated extensively, and each monomer is a flattened Greek-key β-barrel, characterized by eight antiparallel β strands (β1–β8) connected by seven loops (L1–L7) [5,6]. Two of these, the electrostatic (L7) and Zn-binding (L4) loops, with some residues of the β-barrel, form the walls of the active site cavity that steer $O_2^{\bullet-}$ from the enzyme surface to the active site. Several positively charged residues within the electrostatic loop create a charge gradient, which drives the substrate to the metal site at which catalysis occurs [7].

An important characteristic of human Cu/Zn-SOD enzymes is that they are involved in inflammation, tumour proliferation, aging, cell growth and neurodegenerative diseases, such as amyotrophic lateral sclerosis (ALS) [1,2,8,9].

In helminths, such as *Schistosoma mansoni* and *Taenia solium*, both Cu/Zn-SOD enzymes have been considered as targets for drug and vaccine development because they are important for the detoxification of reactive oxygen species (ROS) [10]. Recently, the crystal structure of *S. mansoni* Cu/Zn-SOD at 1.5 Å resolution has been reported. This enzyme is different from human Cu/Zn-SOD with regard to two amino acids (Leu132 and Val135) which are localized at the entrance of the channel that leads $O_2^{\bullet-}$ to the active site [11]. We produced a recombinant *T. solium* Cu/Zn-SOD (TsCu/Zn-SOD) that possesses the classical motifs and biochemical properties of cytosolic enzymes. *In vitro* studies showed that the enzyme is completely inhibited by 500 mM thiabendazole and 300 mM albendazole; in contrast, neither anthelminthic affected bovine Cu/Zn-SOD [12]. It is worth mentioning that *T. solium* is the causal agent of taeniosis in humans and cysticercosis in humans and pigs worldwide; moreover, neurocysticercosis in humans is a debilitating and sometimes mortal disease which requires expensive treatment [13].

In this article, we report the crystal structure of a recombinant TsCu/Zn-SOD and some of its relevant features. The presence of His and Glu residues on the surface of the protein favours protein–protein interactions through metal coordination. The β sheet formed by the β1, β2, β3 and β6 strands is a key motif that establishes β–β interactions with symmetry molecules. The β2 strand, in particular, promotes protein oligomerization through the metal-mediated self-assembly of dimers of TsCu/Zn-SOD. We confirmed these aggregation phenomena in the presence of different concentrations of metal ions using gel filtration, mass spectrometry analyses and dynamic light-scattering experiments.

Results and Discussion

Enzyme preparation, thermal stability and oligomerization analysis

After expression in *Escherichia coli* in the presence of Zn^{2+} and Cu^{2+} ions, sequential purification using a DEAE column at pH 7.4 and pH 8.9, respectively, yielded the dimeric holoenzyme (TsCu/Zn-SOD) with a molecular mass of 32 kDa and a specific activity of 2940 U·mg^{-1}. This value is comparable with those of other eukaryotic SODs, such as the human and bovine enzymes [14], and is obtained when the protein is completely metallated.

The purified holoenzyme presents greater temperature stability in the presence of additional Cu^{2+} or Zn^{2+} ions. Figure 1A shows how the activity of TsCu/Zn-SOD decreases with increasing temperature, but is unaffected in the range 10–37 °C. The activity abruptly decreases by 80% at 80 °C and this level is then maintained for 30 min. Incubation at 100 °C for more than 5 min completely deactivates the enzyme. When 1.0 mM Cu^{2+} or Zn^{2+} ions are added to the reaction cell, an increase in the thermostability of the enzyme is observed. At 80 °C in the presence of additional metal ions, the enzyme activity is not affected for 30 min (Fig. 1B), whereas incubation of the enzyme at 100 °C results in 30% of its original activity, as shown in Fig. 1C. These results show that metal ions diminish the thermal inactivation of the holoenzyme, as has been reported for the porcine and *E. coli* Cu/Zn-SOD enzymes [15,16].

Another interesting characteristic of this protein is that its molecular mass distribution changes in the presence of different concentrations of $ZnSO_4$, as determined by gel filtration (Fig. S1). For example, the pure holoprotein (0.05 mg·mL^{-1}) is dimeric in 0.1 M Tris, pH 8.5, 0.2 M NaCl in the absence of $ZnSO_4$. On addition of 0.5–1.0 mM $ZnSO_4$ to the protein solution, a new broad peak centred at approximately 64 kDa

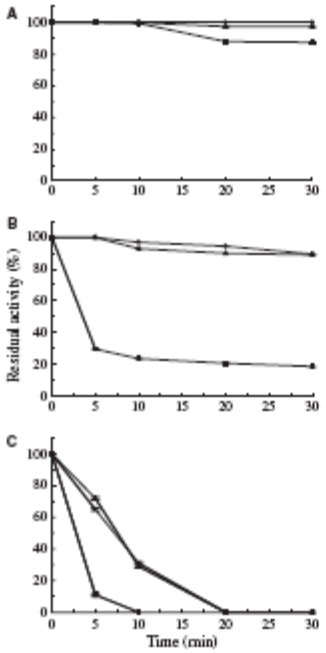

Fig. 1. *Taenia solium* Cu/Zn superoxide dismutase (TsCu/Zn-SOD) thermostability. Enzyme activity of the holoenzyme (squares), after the addition of 1.0 mM $ZnSO_4$ (triangles) and of $CuSO_4$ (circles) at 37 °C (A), 80 °C (B) and 100 °C (C). All measurements were performed as triplicates and error bars are presented.

appears at the expense of the dimeric species (32 kDa). These results were confirmed by mass spectrometry, which showed several species from monomer to tetramer or even higher molecular weight species, indicating that the protein oligomerizes in the presence of metal ions (Fig. 2). The molecular mass of one monomer of native TsCu/Zn-SOD is 15 905.34 Da; notably, if we compare this value with the theoretical value obtained from the amino acid sequence (15 588.48 Da), the difference can be explained by the presence of one Zn^{2+} and one Cu^{2+} ion, in the active site, and approximately two to three extra Zn^{2+} ions per monomer. In accordance with these results, the crystal structure

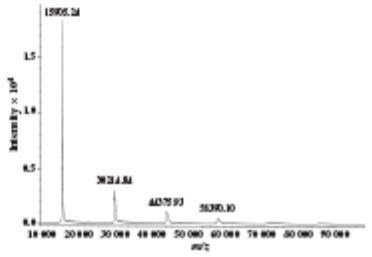

Fig. 2. Matrix-assisted laser desorption ionization time-of-flight mass spectrum of *Taenia solium* Cu/Zn superoxide dismutase (TsCu/Zn-SOD). Several oligomerization species were observed when 1.0 mM $ZnSO_4$ was added to the protein solution.

reported in this work showed three metal ions in regions exposed to the solvent (see below).

Dynamic light-scattering measurements allow us to analyse the aggregation processes in the presence of Zn^{2+}, Cu^{2+} and Ni^{2+} ions. As the scattering intensity is proportional to the second power of the particle mass, the contribution to scattering from larger particles dominates the scattering signal [17], as shown in Fig. S2. It is interesting to note that, in Tris buffer, pH 8.0, the protein at a concentration of 1.0 mg·mL^{-1} is a tetramer. This result differs from that obtained in gel filtration, where the protein behaves as a dimer, as a consequence of the lower protein concentration in the latter experiment. After addition of the ions, distinct species appeared in the size distribution extrapolated from the dynamic light-scattering data using MALVERN DTS software (Malvern Instruments, Malvern, Worcestershire, UK). Figure S2 shows the holoenzyme behaviour in the presence of different ions. When 1 mM $ZnSO_4$ was added to the dynamic light-scattering cell, we observed oligomerization with a peak centred at approximately 300 kDa (Fig. S2A). When $CuSO_4$ was used, oligomerization was also observed; however, twice the concentration of Cu^{2+} ions was needed to observe a peak centred at 200 kDa (Fig. S2B). Conversely, 1 mM $NiCl_2$ produced the opposite effect and the dimeric state was obtained (Fig. S2C), suggesting that this ion could favour a monodisperse state in crystallization conditions.

There exist in the literature conflicting statements about the role of Cu^{2+} and Zn^{2+} ions as promoters of oligomerization; nonetheless, several reports have demonstrated that Zn^{2+} efficiently induces the aggregation

of synthetic amyloid-β (Aβ) peptide under conditions similar to physiological conditions in the normal brain [18,19]. Moreover, Stellato *et al.* [20] have demonstrated, using X-ray absorption spectroscopy, that Zn^{2+} favours Aβ peptide aggregation, supporting our results. In the case of ALS, where *Homo sapiens* SOD is involved, it has been reported that the immature nascent enzyme is prone to aggregation as a result of the absence of metal ions or mis-metallation [21]. Nonetheless, for TsCu/Zn-SOD, oligomerization occurs through a different mechanism.

Crystal structure overview

TsCu/Zn-SOD crystals grew in about 1 week with a rod-shaped morphology and diffracted at 2.2 Å resolution. The analysis of the diffraction pattern showed that the crystals belonged to the space group $P2_12_12_1$ with unit cell parameters of a = 42.17 Å, b = 53.80 Å and c = 117.26 Å. The calculated Matthews' coefficient [22] for two monomers per asymmetric unit is 2.13 $Å^3 \cdot Da^{-1}$ and gives an estimated solvent content of 42.2%. The refined structure contains two monomers, each consisting of 152 amino acid residues and 109 ordered water molecules, with a final R_{work} of 0.192 and R_{free} of 0.249. Details of the refinement statistics are listed in Table 1.

The TsCu/Zn-SOD structure shows the canonical features conserved throughout the phyla, including the Greek-key β-barrel motif (Fig. 3A). The active site includes a catalytically active Cu^{2+} ion and a structural Zn^{2+} ion. Figure 3B shows secondary structure elements with their canonical nomenclature indicated [23]. The Cu^{2+} ion in both monomers is coordinated by four His residues in a distorted tetrahedral geometry. Solvent molecules are observed at 2.48 and 2.91 Å from the Cu^{2+} ion in the active site of monomers A and B, respectively (Fig. 4A, C). In general, when compared with *Homo sapiens* SOD [Protein Data Bank (PDB) entry **2V0A**], water molecules around the Cu^{2+} ion occupy similar positions and are similar in number (four); only monomer A in TsCu/Zn-SOD lacks one of these molecules. It is worth mentioning at this point that the catalytic activity of Cu/Zn SOD seems to be unrelated to the presence of water and that the electron transfer is not water mediated [24]. The Cu–His60–Zn imidazolate bridge that is intact in both monomers is consistent with Cu^{2+}. In the reduced form, the imidazolate bridge is ruptured and the catalytic metal is three coordinated [25], whereas, if Cu is oxidized, it is coordinated to four His residues and is also connected to Zn through a bridging His residue [26]. In the *Taenia* enzyme, His60 makes a bridge between Cu^{2+} and Zn^{2+} ions, spanning 6.12 and 6.33 Å for monomers A and B, respectively. In oxidized SODs, a typical Cu–Zn separation should be around 6.0 Å, whereas, for the reduced enzyme, this distance should be > 6.5 Å [26]; therefore, in this work, both TsCu/Zn-SOD monomers have been captured in the oxidized form. The Zn^{2+} ion is four coordinated with three His and one Asp (Fig. 4B, D) in a tetrahedral geometry. Interestingly, electron density maps show that TsCu/Zn-SOD contains three additional ions, one in monomer A and two in monomer B, coordinated to residues exposed to the solvent (Figs 3A and 5). We included Zn^{2+} ions in the latter

Table 1. Data collection and structure refinement statistics.

Data collection	
X-Ray source	Beamline X12B, NSLS
Wavelength (Å)	0.9795
Space group	$P2_12_12_1$
Unit cell (Å, deg)	a = 42.17, b = 53.80, c = 117.26, $\alpha = \beta = \gamma = 90°$
Resolution range (Å)[a]	53.8–2.2 (2.32–2.2)
V_M ($Å^3 \cdot Da^{-1}$)	2.08
R_{merge} (%)[a,b]	11.6 (35.6)
Completeness (%)[a]	98.8 (97.7)
Total reflections	44634
Unique reflections	13934
Redundancy[a]	3.2 (3.0)
$I/\sigma(I)$[a]	7.0 (2.8)
B-factors of data from Wilson plot ($Å^2$)	20.9
Refinement	
Resolution range (Å)[a]	39.6–2.2 (2.28–2.2)
Number of reflections[a]	13820 (1064)
R_{work} (%)/R_{free} (%)[a,c]	19.2/24.5
R.m.s.d bond length (Å)	0.007
R.m.s.d bond angle (deg)	1.082
Protein atoms	2200
Metal ions Cu/Zn	2/5
Glycerol molecules	2
Water molecules	109
Average B-factor ($Å^2$)	
Protein/solvent/metal ions/glycerol	20.9/21.8/28.7/26.4
Ramachandran plot (%)[d]	
Preferred	95.2
Allowed regions	4.8

[a] Values in parentheses correspond to the last resolution shell. [b] $R_{merge} = \Sigma_h\Sigma_i|I_{ih} - \langle I_h\rangle|/\Sigma_h\Sigma_i\langle I_h\rangle$, where subscript h is the unique reflection index, I_{ih} is the intensity of the symmetry-related reflection and $\langle I_h\rangle$ is the mean intensity. [c] $R = \sum_h||F_o|_h - |F_c|_h|/\sum_h|F_o|_h$ for all reflections, where F_o and F_c are the observed and calculated structure factors, respectively, and h defines unique reflections. [c] R_{free} is calculated analogously for the test reflections, randomly selected and excluded from the refinement. [d] Ramachandran plots were prepared for all residues other than Gly and Pro.

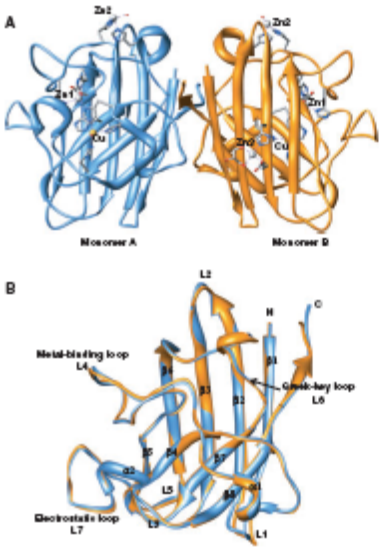

Fig. 3. Structure of *Taenia solium* Cu/Zn superoxide dismutase (TsCu/Zn-SOD). (A) Ribbon representation of the dimeric TsCu/Zn-SOD where the metals are shown as spheres in yellow (copper) and grey (zinc). (B) Superposition of TsCu/Zn-SOD monomers. Each one contains an eight-strand β sandwich (β1–β8) with seven loops (L1–L7) (canonical nomenclature is included).

positions on the basis of metal coordination, results from dynamic light-scattering experiments with different ions and appropriate behaviour during refinement. Space group symmetry expansion shows that, in monomers A and B, additional metal ions (Zn2) are coordinated intramolecularly by two His residues (64 and 107) and a solvent molecule. These ions stabilize two very flexible regions: the metal binding (L4) and the Greek-key (L6) loops, as shown in Figs 3A and 5C. This could explain the higher temperature stability observed when metal ions are added to the protein solutions. The third ion, which is located in monomer B (Zn3), is pentacoordinated intermolecularly by residues His29, Glu31 and His29 of a symmetry-related molecule, and O1 and O3 of a glycerol molecule which is present as the fourth ligand. These results are in line with the proposal that physiological Zn binding by metal-sequestering proteins is necessary to ensure cell homeostatic control [27].

Another interesting feature of the protein is the entrance of the channel connecting the active site, which shows that *T. solium* and *S. mansoni* Cu/Zn-SODs differ from the human enzyme. This area, known as the electrostatic loop, contains several highly conserved charged residues and has been proposed to be responsible for the long-range routing of superoxide towards the catalytic site [23]. In human Cu/Zn-SOD, this area is positively charged, whereas, in TsCu/Zn-SOD, nonpolar residues predominate. These amino acids play an important role in the conformation and charge distribution for substrate attraction. Indeed, *in vitro* studies have shown that the TsCu/Zn-SOD enzyme is completely inhibited by 300 mM albendazole, whereas this compound does not affect the bovine enzyme [12]. This could be explained by the hydrophobic nature of albendazole, which interacts more favourably with the hydrophobic amino acid residues at the entrance of the electrostatic loop. These studies suggest that TsCu/Zn-SOD could be used as a target protein to design agents for the treatment of cysticercosis.

Interface analysis

Eukaryotic Cu/Zn-SODs are dimeric structures with conserved subunit interfaces. The interaction of the two monomers is based on a contact region defined by four clusters. The first consists of the β1 and β2 strands of each monomer, the second is located in the loop formed between the β4 strand and helix 1, the third is formed by residues located in the L6 (Greek-key) loop and the fourth is formed by residues in the β8 strand (C-terminal). The *Taenia* (this work), *Schistosoma* (PDB entry 1TO4) and human (PDB entry 2V0A) Cu/Zn-SOD interfaces are very similar and consist of the same clusters; however, they vary slightly in their amino acid composition.

The Cα atoms of the three structures were superimposed, showing rmsd values ranging from 0.37 to 0.49 Å in monomers A and B, respectively. The most important difference is observed when the dimers of these three SODs (Fig. 6) are compared. They superimpose with rmsd values of 0.64 and 1.02 Å for human [28] and *Schistosoma* [11] Cu/Zn-SODs, respectively. Interestingly, although the sequence identities of TsCu/Zn-SOD with the *Schistosoma* and human Cu/Zn-SODs are 71% and 57.9%, respectively, structurally the *Taenia* enzyme is similar to the human enzyme.

The three enzymes present four conserved hydrogen bonds among residues Ile148, Gly48 and Gly111

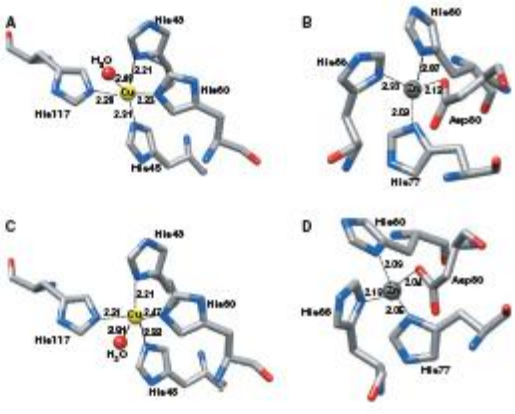

Fig. 4. Close-up view of the active site in the *Taenia solium* Cu/Zn superoxide dismutase (TsCu/Zn-SOD). (A, C) Coordination environment of Cu^{2+} ions in monomers A and B. (B, D) Zinc-binding residues in monomers A and B. The interatomic distances between coordination residues are shown.

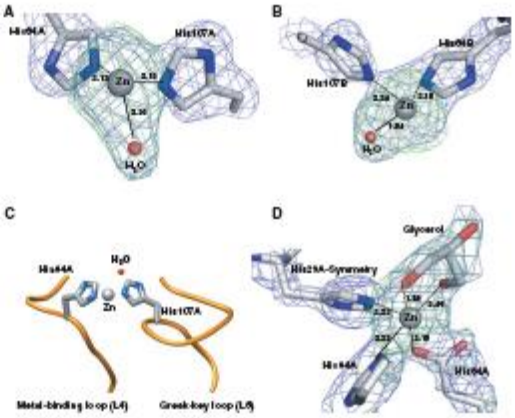

Fig. 5. Details of the additional metal-binding sites. $2F_o - F_c$ (blue) and $F_o - F_c$ (green) electron density maps of these sites. (A, B) Zinc ion is coordinated by His107, His64 and a water molecule in monomers A and B. (C) Stabilization of L4 and L6 loops by metal ion coordination. (D) Zn^{2+} ion coordinated with His26, Glu31 of monomer B, His26 of a symmetry-related molecule A and a glycerol molecule. The interatomic distances between coordinating residues and solvent water molecules are indicated.

(numbering of TsCu/Zn-SOD) at their interfaces. In all cases, monomer A has a greater contact area relative to monomer B, which is more mobile. These differences are highlighted in Fig. 6, in which it is clear that the orientation between the two monomers in the TsCu/Zn-SOD and *Schistosoma* Cu/Zn-SOD dimers differs by about 17°, whereas this difference for human Cu/Zn-SOD is only about 6°. Hough *et al.* [29] have reported this dimer interface alteration in the crystal structures of two mutants (Ala4Val and Ile113Thr) of *Homo sapiens* Cu/Zn-SOD, confirming that they are significantly destabilized in comparison with wild-type

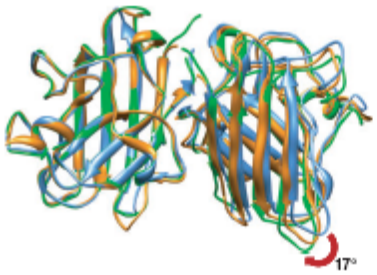

Fig. 6. Structural alignment of Cu/Zn superoxide dismutases from *Taenia solium* (blue), *Schistosoma* (red) and *Homo sapiens* (green). Crystal structures were superimposed onto one monomer (left).

SOD. The Ala4Val mutant accounts for approximately 50% of the SOD-linked ALS cases [30]. Similar results have been observed for other amyloidogenic proteins, such as light chains, which, after alteration of their interfaces, show an increased tendency to form amyloid fibre [31,32].

Intermolecular packing interactions

Analysis of the intermolecular packing contacts reveals interesting interactions (Fig. 7). The most relevant contact is observed with monomer B, in which a parallel β interaction with a symmetry-related molecule is established involving Zn^{2+} ion coordination (top inset). The strands implicated in this interaction generate a periodic stack with strands that are perpendicular to the direction of the longitudinal array (Fig. 7). Notably, when we superimpose this region on the human enzyme, the latter presents a β-bulge-like structure in strand β2 (Fig. 7, bottom inset), and a difference of about 2.8 Å is observed between the Cα atoms of these strands in both proteins. Several reports have indicated that proteins can acquire structural adaptations that enable them to avoid undesired protein aggregation and fibril formation, and β bulges are considered to be anti-aggregation motifs [33]. It is worth mentioning that the native human SOD has less tendency to aggregate than ALS mutants [28], whereas the TsCu/Zn-SOD oligomerizes, probably because the latter does not present the β bulge (Fig. 7, bottom inset) and therefore establishes the parallel β interactions mediated by metal ions coordinated to several residues (His and Glu) exposed to the solvent. This type of interaction has not been described previously

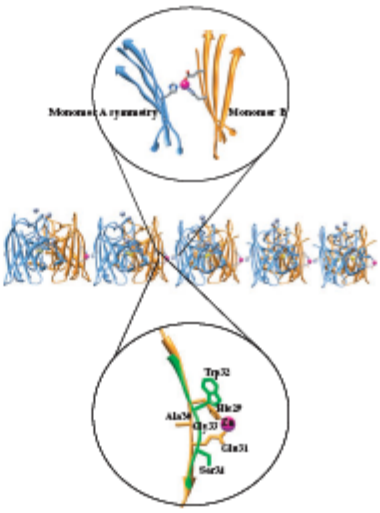

Fig. 7. Crystal packing interactions of *Taenia solium* Cu/Zn superoxide dismutase (TsCu/Zn-SOD). β–β interactions through ion metal coordination are established with symmetry-related molecules. The Zn^{2+} ion involved is shown as a purple sphere and the residues implicated in the metal ion coordination are shown as sticks. The top inset shows a close-up view of the β–β arrangement. The bottom inset shows the β-bulge-like structure for the human enzyme (green), but not for TsCu/Zn-SOD (orange).

for other SODs. Nonetheless, the metal-mediated self-assembly of natural [34] and engineered [35] proteins has already been reported in several examples in which blocks with noninteracting surfaces were assembled into aggregates by metal coordination. Therefore, mutants of human SOD containing His, Glu or Asp residues exposed to the solvent could present this behaviour, and such chemical control of protein–protein interactions might be physiologically relevant or be involved in neurodegenerative diseases.

Protein oligomerization, aggregation and the formation of insoluble amyloid deposits are commonly observed in neurodegenerative diseases, but the factors initiating and modulating the abnormal interactions that lead to oligomerization remain unknown. Metal ions have been implicated in these phenomena, but the

structural basis for their involvement remains unclear [36]. Huang *et al.* [37] have shown evidence that metals are the initiators of the oligomerization and amyloid fibril formation of Aβ in Alzheimer's disease. Interestingly, Cherny *et al.* [38] have demonstrated that homogenization of Alzheimer's disease brains in buffer containing chelators liberates more Aβ than buffer alone, indicating that metal ions are key components in maintaining the structural integrity of amyloid deposits. Later, Dong *et al.* [39], using Raman spectroscopy, demonstrated that Cu^{2+} and Zn^{2+} bind Aβ subunits in brain plaque amyloid through His residues. In addition, it has been observed that tissues affected by ALS are rich in metal ions, including Zn^{2+} ions [40].

In humans, ALS is a progressive neurodegenerative disorder selectively affecting motor neurones, in which 2% of the total cases are associated with mutations in the gene coding for the enzyme Cu/Zn-SOD. The causes of motor neurone death in ALS are poorly understood in general, but, for Cu/Zn-SOD-linked familial ALS, aberrant oligomerization of SOD mutant proteins has been strongly implicated. Several authors have suggested that metal-free human SOD is prone to aggregation as a result of conformational changes that can even form abnormal disulfide bridges [21,36]. Based on our findings, we suggest that TsCu/Zn-SOD could be useful as an alternative model for the interpretation of the mechanisms involved in protein aggregation and the formation of insoluble fibrillar deposits that are commonly observed in neurodegenerative diseases.

Materials and methods

Protein expression, purification and crystallization

Recombinant TsCu/Zn-SOD protein was expressed and purified as described previously [12]. Briefly, transformed bacteria containing the pRSET vector with the coding region for TsCu/Zn-SOD were induced using 1.0 mM isopropyl thio-β-D-galactoside (IPTG), 0.2 mM $CuSO_4$ and 0.17 mM $ZnSO_4$. Cells were harvested by centrifugation, and the bacterial pellet was sonicated in 10 mM Tris/acetate, pH 7.5, with 0.1 mM phenylmethanesulfonyl fluoride and 0.75 M sucrose. The suspension obtained was centrifuged at 11 000 *g* to give a clear supernatant that was applied to a HiPrep 16/10 DEAE FF column. Bound proteins were eluted using a linear saline gradient. Fractions with Cu/Zn-SOD activity were pooled, dialysed in 50 mM Tris/HCl, pH 8.9, and applied to the same column. Final fractions were dialysed against Tris buffer and concentrated.

Crystallization experiments were carried out at room temperature by the hanging-drop vapour diffusion technique. Drops contained a 1 : 1 volume ratio of the recombinant TsCu/Zn-SOD (4 mg·mL^{-1}) and precipitant solution 45 from Crystal Screen 2 (Hampton Research, Aliso Viejo, CA, USA), which includes 20% w/v polyethylene glycol monomethyl ether 2000 in hexahydrate 0.1 M Tris buffer, pH 8.5, and 0.01 M nickel(II) chloride.

Determination of Cu/Zn-SOD activity

Cu/Zn-SOD activity was determined indirectly by the inhibition of cytochrome c reduction at 25 °C. This method uses the xanthine–xanthine oxidase system to generate superoxide radical. The total volume of the reaction was 1 mL in 50 mM phosphate buffer, pH 7.8, containing 1.0 mM EDTA and 57 mU of xanthine oxidase, 10 μM cytochrome c and 50 μM xanthine. The concentrations of Cu/Zn-SOD used for the assay were from 0 to 5 μg·mL^{-1}. One unit of SOD activity is defined as the amount causing 50% inhibition of the reduction of cytochrome c [41].

Effects of temperature and metal ions (Cu^{2+} or Zn^{2+}) on the thermal stability of TsCu/Zn-SOD

The effect of temperature on enzyme stability was determined in 50 mM Tris/HCl, pH 7.8, incubating TsCu/Zn-SOD (100 U·mL^{-1}) in a water bath at temperatures of 10, 25, 37, 80 and 100 °C. We added 1.0 mM $CuSO_4$ or $ZnSO_4$ to the protein solution to determine their effect on protein thermal stability. Aliquots of 200 μL at different times (0, 5, 10, 20 and 30 min) were transfered to a 4 °C bath and assayed by the xanthine–xanthine oxidase method. Residual activity was determined after 30 min. As controls for the assay, TsCu/Zn-SOD with buffer and without metals was used.

Monitoring of TsCu/Zn-SOD aggregation by gel filtration

TsCu/Zn-SOD (0.5 mg·mL^{-1}) aliquots were incubated with different $ZnSO_4$ concentrations from 0.5 to 1.0 mM. One-hundred-microlitre aliquots of the enzyme samples were applied to a size exclusion Superdex 75 HL 16/60 column (GE Healthcare, Sweden) in a fast protein liquid chromatography system. The column was equilibrated with 0.1 M Tris, 200 mM NaCl buffer, pH 8.5, and the flow rate was set to 1.0 mL·min^{-1}. Elution of the species formed during incubation was detected by monitoring the absorbance at 280 nm. The column was calibrated with standards of known molecular mass (ubiquitin, 8.5 kDa; cytochrome C, 12 kDa; hen white lysozyme, 14.3 kDa; thaumatine, 24 kDa; bovine serum albumin, 66.4 kDa).

Characterization of TsCu/Zn-SOD using matrix-assisted laser desorption ionization time-of-flight mass spectrometry

The enzyme alone or in the presence of $ZnSO_4$ at different concentrations was mixed with sinapinic acid in 30% acetonitrile, 70% water and 0.1% trifluoroacetic acid, and analysed in a MICROFLEX matrix-assisted laser desorption ionization time-of-flight instrument (Bruker Daltonik GmbH, Leipzig, Germany) equipped with a 20-Hz nitrogen laser. Spectra were recorded in the positive linear mode for the mass range 2000–70 000 Da.

Dynamic light-scattering measurements

These data were obtained using a Zetasizer Nano S dynamic light-scattering device from MALVERN Instruments at 20 °C and fitted using DTS software from Malvern Instruments. The TsCu/Zn-SOD filtered samples (pore size, 0.22 μm) were placed in a quartz cuvette (50 μL) and used to test the effect of metal ion ($CuSO_4$, $ZnSO_4$ and $NiCl_2$) addition on the oligomerization behaviour. The buffer was filtered (pore size, 0.22 μm) immediately before use and care was taken to reduce contamination of the samples by dust. At least 25 measurements were collected for each sample. Size distributions in percentage volume were calculated using MALVERN Instruments software by approximating the protein as a spherical object.

Data collection and processing

Diffraction data were collected using synchrotron radiation at the National Synchrotron Light Source (NSLS), Brookhaven National Laboratory (Upton, NY, USA) on beamline X12B, with an ADSC Quantum-4 CCD detector at 100 K. The crystal was cryoprotected with 15% glycerol in the mother liquor. The dataset was indexed and integrated with XDS [42] and scaled with SCALA [43], contained in the CCP4 crystallographic package [44]. A summary of data collection and processing is given in Table 1.

Structure determination and refinement

Analysis of the unit cell content suggested the presence of two protein molecules in the asymmetric unit, consistent with a solvent content of 42.78% [22]. The structure was solved by molecular replacement using the program Phaser [45] as implemented in PHENIX [46], and, as a template, the crystal structure of *S. mansoni* Cu/Zn-SOD at 1.55 Å resolution (PDB entry code 1TO4 [11]) was used, which shares 71% identity with TsCu/Zn-SOD. The solution of the molecular replacement gave a final *Z* score of 36.5 and a log likelihood gain of 1405. Refinement was carried out with PHENIX [46] using a random test set of 10% of the reflections for cross-validation. Briefly, we used a rigid body refinement, followed by simulated annealing and successive rounds of Cartesian and temperature factor minimization with manual model building in Coot [47]. All of the active-site metals, as well as three additional metal sites, were visible in the electron density maps from the first stages of refinement. Noncrystallographic symmetry constraints were not imposed to ensure that potential structural differences between the monomers were not doubtful. Water molecules were added to the model near the end of the refinement by a search procedure based on peaks observed in the difference maps and bond distance criteria. PROCHECK [48] was used for the analysis of the stereochemistry of the model and validation. Molecular comparisons with other SODs were performed with the ALIGN program [49] and figures prepared with Pymol [50] and Chimera [51]. Statistics on data collection and refinement are reported in Table 1.

PDB accession number

The atomic coordinates and structure factors have been deposited in the Protein Data Bank with accession number 3MND.

Acknowledgements

This work was supported in part by grants from Consejo Nacional de Ciencia y Tecnología (contracts 82947 to A.R.-R. and 80134 to A.L.) and Dirección General de Asuntos del Personal Académico, Universidad Nacional Autónoma de México (IN207507-3 to A.L.). The characterization of crystals was performed at Laboratorio Nacional de Estructura de Macromoléculas, Instituto de Química, Universidad Nacional Autónoma de México. X-Ray data were measured at beamline X12B of the National Synchrotron Light Source. We thank Alexei Soares for his help during data collection. The National Synchrotron Light Source is supported by the US Department of Energy through contract no. DEAC02-98CH10886. We also thank M. C. Georgina Espinosa for technical assistance.

References

1 Fridovich I (1998) Oxygen toxicity: a radical explanation. *J Exp Biol* **201**, 1203–1209.
2 Fattman CL, Schaefer LM & Oury TD (2003) Extracellular superoxide dismutase in biology and medicine. *Free Radic Biol Med* **35**, 236–256.
3 Tainer JA, Getzoff ED, Beem KM, Richardson JS & Richardson DC (1982) Determination and analysis of the 2 A-structure of copper, zinc superoxide dismutase. *J Mol Biol* **15**, 181–217.

4 Henkle-Dührsen K & Kampkötter A (2001) Antioxidant enzyme families in parasitic nematodes. *Mol Biochem Parasitol* **114**, 129–142.

5 Antonyuk SV, Strange RW, Marklund SL & Hasnain SS (2009) The structure of human extracellular copper–zinc superoxide dismutase at 1.7 Å resolution: insights into heparin and collagen binding. *J Mol Biol* **388**, 310–326.

6 Richardson JS, Thomas KA, Rubin BH & Richardson DC (1975) Crystal structure of bovine Cu,Zn superoxide dismutase at 3Å resolution: chain tracing and metal ligands. *Proc Natl Acad Sci USA* **72**, 1349–1353.

7 Tainer JA, Getzoff ED, Richardson JS & Richardson DC (1983) Structure and mechanism of copper, zinc superoxide dismutase. *Nature* **306**, 284–287.

8 Shaw BF & Valentine JS (2007) How do ALS-associated mutations in superoxide dismutase 1 promote aggregation of the protein? *Trends Biochem Sci* **32**, 78–85.

9 Valdivia A, Pérez-Alvarez S, Aroca-Aguilar JD, Ikuta I & Jordán J (2009) Superoxide dismutases: a physiopharmacological update. *J Physiol Biochem* **65**, 195–208.

10 Vaca-Paniagua F, Torres-Rivera A, Parra-Unda R & Landa A (2008) *Taenia solium*: antioxidant metabolism enzymes as targets for cestocidal drugs and vaccines. *Curr Top Med Chem* **8**, 393–399.

11 Cardoso RM, Silva CH, Ulian de Araújo AP, Tanaka T, Tanaka M & Garratt RC (2004) Structure of the cytosolic Cu,Zn superoxide dismutase from *Schistosoma mansoni*. *Acta Crystallogr D Biol Crystallogr* **60**, 1569–1578.

12 Castellanos-González A, Jiménez L & Landa A (2002) Cloning, production and characterisation of a recombinant Cu/Zn superoxide dismutase from *Taenia solium*. *Int J Parasitol* **32**, 1175–1182.

13 Montresor A & Palmer K (2006) Taeniasis/cysticercosis trend worldwide and rationale for control. *Parasitol Int* **55**, Suppl–S301.

14 Marklund SL (1982) Human copper-containing superoxide dismutase of high molecular weight. *Proc Natl Acad Sci USA* **79**, 7634–7638.

15 Lin CW, Yang JH & Su LC (1997) The extraction and properties of superoxide dismutase from porcine blood. *Meat Sci* **46**, 303–312.

16 Benov L, Sage H & Fridovich I (1997) The copper- and zinc-containing superoxide dismutase from *Escherichia coli*: molecular weight and stability. *Arch Biochem Biophys* **340**, 305–310.

17 Lomakin A, Benedek GB & Teplow DB (1999) Monitoring protein assembly using quasielastic light scattering spectroscopy. *Methods Enzymol* **309**, 429–459.

18 Bush AI, Pettingell WH, Multhaup G, Parads MD, Vonsattel JP, Gusella JF, Beyreuther K, Masters CL & Tanzi RE (1994) Rapid induction of Alzheimer Ab amyloid formation by zinc. *Science* **265**, 1464–1467.

19 Esler WP, Stimson ER, Jennings JM, Ghilardi JR, Mantyh PW & Maggio JE (1996) Zinc-induced aggregation of human and rat b-amyloid peptides in vitro. *J Neurochem* **66**, 723–732.

20 Stellato F, Menestrina G, Dalla-Serra M, Potrich C, Tomazzolli R, Meyer-Klaucke W & Morante S (2006) Metal binding in amyloid β-peptides shows intra- and inter-peptide coordination modes. *Eur Biophys J* **35**, 340–351.

21 Seetharaman SV, Prudencio M, Karch C, Holloway SP, Borchelt DR & Hart PJ (2009) Immature copper–zinc superoxide dismutase and familial amyotrophic lateral sclerosis. *Exp Biol Med* **234**, 1140–1154.

22 Matthews BW (1968) Solvent content of protein crystals. *J Mol Biol* **33**, 491–497.

23 Getzoff ED, Tainer JA, Weiner PK, Kollman PA, Richardson JS & Richardson DC (1983) Electrostatic recognition between superoxide and copper, zinc superoxide dismutase. *Nature* **306**, 284–287.

24 Banci L, Bertini I, Hallewell RA, Luchinat C & Viezzoli MS (1989) Water in the active cavity of copper/zinc superoxide dismutase. A water 1H-nuclear-magnetic-relaxation-dispersion study. *Eur J Biochem* **184**, 125–129.

25 Ascone I, Castaller R, Tarricone C, Bolognesi M, Stoppolo ME & Desideri A (1997) Evidence of His61 imidazolate bridge rupture in reduced crystalline Cu,Zn superoxide dismutase. *Biochem Biophys Res Commun* **241**, 119–121.

26 Hough MA & Hasnain SS (2003) Structure of fully reduced bovine copper zinc superoxide dismutase at 1.15 Å. *Structure* **11**, 937–946.

27 Palmiter RD & Findley SD (1995) Cloning and functional characterization of a mammalian zinc transporter that confers resistance to zinc. *EMBO J* **14**, 639–649.

28 Strange RW, Yong CW, Smith W & Hasnain SS (2007) Molecular dynamics using atomic-resolution structure reveal structural fluctuations that may lead to polymerization of human Cu–Zn superoxide dismutase. *Proc Natl Acad Sci* **104**, 10040–10044.

29 Hough MA, Grossman JG, Antonyuk SV, Strange RW, Doucette PA, Rodriguez JA, Whitson LJ, Hart PJ, Hayward LJ, Valentine JS *et al.* (2004) Dimer destabilization in superoxide dismutase may result in disease-causing properties: structures of motor neuron disease mutants. *Proc Natl Acad Sci* **101**, 5976–5981.

30 Cudkowicz ME, McKenna-Yasek D, Sapp PE, Chin W, Geller B, Hayden DL, Schoenfeld DA, Hosler BA, Horvitz H & Brown RH (1997) Epidemiology of mutations in superoxide dismutase in amyotrophic lateral sclerosis. *Ann Neurol* **41**, 210–221.

31 Baden EM, Owen BA, Peterson FC, Volkman BF, Ramirez-Alvarado M & Thompson JR (2008) Altered dimer interface decreases stability in an amyloidogenic protein. *J Biol Chem* **283**, 15853–15860.

32 Hernández-Santoyo A, del Pozo-Yauner L, Fuentes-Silva D, Ortiz E, Rudiño-Piñera E, Horjales E, Becerril B & Rodríguez-Romero A (2010) A single mutation at the sheet switch region results in conformational changes favoring λ6-light-chain fibrillogenesis. *J Mol Biol* **396**, 280–292.

33 Richardson JS & Richardson DC (2002) Natural beta-sheet proteins use negative design to avoid edge-to-edge aggregation. *Proc Natl Acad Sci* **99**, 2754–2759.

34 Jabeen T, Sharma S, Singh N, Bhushan A & Singh TP (2005) Structure of the zinc-saturated C-terminal lobe of bovine lactoferrin at 2.0 Å resolution. *Acta Crystallogr D Biol Crystallogr* **61**, 1107–1115.

35 Salgado EN, Lewis RA, Faraone-Mennella J & Tezcan FA (2008) Metal-mediated self-assembly of protein superstructures: influence of secondary interactions on protein oligomerization and aggregation. *J Am Chem Soc* **130**, 6082–6084.

36 Banci L, Bertini I, Durazo A, Girotto S, Gralla EB, Martinelli M, Valentine JS, Vieru M & Whitelegge JP (2007) Metal-free superoxide dismutase forms soluble oligomers under physiological conditions: a possible general mechanism for familial ALS. *Proc Natl Acad Sci* **104**, 11263–11267.

37 Huang X, Atwood CS, Moir RD, Hartshorn MA, Tanzi RE & Bush AI (2004) Trace metal contamination initiates the apparent auto-aggregation, amyloidosis, and oligomerization of Alzheimer's Abeta peptides. *J Biol Inorg Chem* **9**, 954–960.

38 Cherny RA, Legg JT, McLean CA, Fairlie DP, Huang X, Atwood CS, Beyreuther K, Tanzi RE, Masters CL & Bush AI (1999) Aqueous dissolution of Alzheimer's disease Abeta amyloid deposits by biometal depletion. *J Biol Chem* **274**, 23223–23228.

39 Dong J, Atwood CS, Anderson VE, Siedlak SL, Smith MA, Perry G & Casey PR (2003) Metal binding and oxidation of amyloid-beta within isolated senile plaque cores: Raman microscopic evidence. *Biochemistry* **42**, 2768–2773.

40 Szczerbowska-Boruchowska M, Lankosz M, Ostachowicz J, Adamek D, Krygowska-Wajs A, Tomik B, Szczudlik A, Simionovici A & Bohic S (2004) Topographic and quantitative microanalysis of human central nervous system tissue using synchrotron radiation. *X-ray Spectrom* **33**, 3–11.

41 McCord JM & Fridovich I (1969) Superoxide dismutase. An enzymic function for erythrocuprein (hemocuprein). *J Biol Chem* **244**, 6049–6055.

42 Kabsch W (1993) Automatic processing of rotation diffraction data from crystals of initially unknown symmetry and cell constants. *J Appl Crystallogr* **26**, 795–800.

43 Evans P (2006) Scaling and assessment of data quality. *Acta Crystallogr D Biol Crystallogr* **62**, 72–82.

44 Collaborative Computational Project, Number 4 (1994) The CCP4 Suite: programs for protein crystallography. *Acta Crystallogr D Biol Crystallogr* **50**, 760–763.

45 McCoy AJ, Grosse-Kunstleve RW, Adams PD, Winn MD, Storoni LC & Read RJ (2007) Phaser crystallographic software. *J Appl Crystallogr* **40**, 658–674.

46 Adams PD, Afonine PV, Bunkóczi G, Chen VB, Davis IW, Echols N, Headd JJ, Hung LW, Kapral GJ, Grosse-Kunstleve RW *et al.* (2010) PHENIX: a comprehensive Python-based system for macromolecular structure solution. *Acta Crystallogr D Biol Crystallogr* **66**, 213–221.

47 Emsley P & Cowtan K (2004) Coot: model-building tools for molecular graphics. *Acta Crystallogr D Biol Crystallogr* **60**, 2126–2132.

48 Laskowski RA, MacArthur MW, Moss DS & Thornton JM (1993) PROCHECK: a program to check the stereochemical quality of protein structures. *J Appl Crystallogr* **26**, 283–291.

49 Cohen GH (1997) ALIGN: a program to superimpose protein coordinates, accounting for insertions and deletions. *J Appl Crystallogr* **30**, 1160–1161.

50 DeLano WL (2002) *The PyMOL Molecular Graphics System*. DeLano Scientific, San Carlos, CA. http://www.pymol.org.

51 Pettersen EF, Goddard TD, Huang CC, Couch GS, Greenblatt DM, Meng EC & Ferrin TE (2004) UCSF Chimera – a visualization system for exploratory research and analysis. *J Comput Chem* **25**, 1605–1612.

Supporting information

The following supplementary material is available:

Fig. S1. Elution profile of size exclusion chromatography.

Fig. S2. Dynamic light-scattering analysis of *Taenia solium* Cu/Zn superoxide dismutase (TsCu/Zn-SOD).

This supplementary material can be found in the online version of this article.

Please note: As a service to our authors and readers, this journal provides supporting information supplied by the authors. Such materials are peer-reviewed and may be reorganized for online delivery, but are not copy-edited or typeset. Technical support issues arising from supporting information (other than missing files) should be addressed to the authors.

J Comput Aided Mol Des (2011) 25:1135–1145
DOI 10.1007/s10822-011-9498-x

Novel inhibitors to *Taenia solium* Cu/Zn superoxide dismutase identified by virtual screening

P. García-Gutiérrez · A. Landa-Piedra · A. Rodríguez-Romero · R. Parra-Unda · A. Rojo-Domínguez

Received: 21 April 2011 / Accepted: 21 November 2011 / Published online: 4 December 2011

Abstract We describe in this work a successful virtual screening and experimental testing aimed to the identification of novel inhibitors of superoxide dismutase of the worm *Taenia solium* (*Ts*Cu/Zn–SOD), a human parasite. Conformers from LeadQuest® database of drug-like compounds were selected and then docked on the surface of *Ts*Cu/Zn–SOD. Results were screened looking for ligand contacts with receptor side-chains not conserved in the human homologue, with a subsequent development of a score optimization by a set of energy minimization steps, aimed to identify lead compounds for in vitro experiments. Six out of fifty experimentally tested compounds showed μM inhibitory activity toward *Ts*Cu/Zn–SOD. Two of them showed species selectivity since did not inhibit the homologous human enzyme when assayed in vitro.

Keywords Taenia solium · Superoxide dismutase · Cu/Zn–SOD · Neurocysticercosis · Inhibition · Docking · Molecular operating environment, MOE

Introduction

Cysticercosis is a parasitic disease caused by infection with the larval stage of *Taenia solium* which occurs when humans become the intermediate host in the life cycle of the helminth [1]. The parasite infects the central nervous system thus producing neurocysticercosis (NCC), considered the most common parasitic disease of the CNS and affects millions of people in developing countries of Latin America, Africa and Asia, as well as in developed countries with a high migration ratio of subjects from endemic areas [2–4]. This condition is associated with severe neurological manifestations including epilepsy, headaches, seizures and other neurological disorders [5]. Conservative estimates describe 50,000 deaths worldwide every year due to neurocysticercosis [6]. The treatment for NCC in humans is based on two drugs: albendazole and praziquantel. Both drugs can cause adverse symptoms in the host, but in general are well tolerated. These drugs are often administered with dexamethasone to decrease the inflammatory reaction produced by the host in response to the death of the parasite, a reaction that some times can also kill the host [7]. To date, there is only one report on drug-resistance to praziquantel and albendazole in Cestode infections found in a patient with neurocysticercosis [8], but resistance to these and other drugs has been reported

Electronic supplementary material The online version of this article (doi:10.1007/s10822-011-9498-x) contains supplementary material, which is available to authorized users.

P. García-Gutiérrez · A. Rojo-Domínguez
Área de Biofisicoquímica, Departamento de Química, Universidad Autónoma Metropolitana–Iztapalapa, 09340 México, D.F., México
e-mail: pgarcia@ciencias.unam.mx

A. Landa-Piedra · R. Parra-Unda
Departamento de Microbiología y Parasitología, Facultad de Medicina, Universidad Nacional Autónoma de México, 04510 México, D.F., México

A. Rodríguez-Romero
Departamento de Biomacromoléculas, Instituto de Química, Universidad Nacional Autónoma de México, 04510 México, D.F., México

A. Rojo-Domínguez (✉)
Departamento de Ciencias Naturales, Universidad Autónoma Metropolitana–Cuajimalpa, Pedro A. de los Santos 84, Col. San Miguel Chapultepec, 01120 México, D.F., México
e-mail: arojo@correo.cua.uam.mx

for other helminths such as schistosomes and some nematodes [9, 10]. Therefore, there is an urgent need to develop new drugs with different mechanisms of action.

Superoxide dismutases (SODs) are a group of metalloenzymes essential for defending organisms against oxidation by the superoxide anion (O_2^-) [11, 12]. SODs catalyze in two steps the dismutation of the O_2^- to molecular oxygen and hydrogen peroxide. Although O_2^- is a mild reductant, it can cause direct or indirect damage to cell membranes and DNA [13]. Three major classes of SODs have been described on the basis of their prosthetic groups: Fe, Mn, or Cu/Zn. So far, three types of SOD enzymes have been identified in helminths: the mitochondrial Mn–SOD, the cytosolic and an extracellular Cu/Zn–SOD [14, 15]. Organisms lacking these enzymes exhibit a decreased growth rate, shorter life span, hypersensitivity towards redox cycling compounds such as paraquat and quinones, and an increment in spontaneous mutagenesis and death rates [11, 12]. As a other parasitic organisms, *T. solium* must remove endogenous and exogenous O_2^- produced by its own metabolic processes and, because its larval and adult stages live in tissues, the one produced by host inflammatory response [16].

As reported by some authors [9], albendazole inhibits microtubule formation in parasite by binding to β-tubulin, however, as shown by Sánchez-Moreno et al. [17–19], this drug also inhibits SOD enzymes in helmints, but at high concentrations in the case of *T. solium*, as reported by us [20]. Gómez-Contreras et al. [21] reported recently the synthesis of benzo[*g*]phthalazine derivatives which selectively inhibit Fe-SOD activity and growth of *Trypanosoma cruzi*. Benznidasole, a drug currently used against trypanosomiasis act trough inducing formation of toxic oxygen metabolites such as superoxide anion and hydrogen peroxide [22].

These and other reports suggest that SOD enzymes are involved in parasite defense [15]. Our hypothesis is that inactivation of this enzyme may contribute to weaken the defense mechanisms of the parasite and aid destroying it, thus SOD can be considered a good target for drug design.

Recently, we resolved the crystal structure of recombinant *Ts*Cu/Zn–SOD at 2.7 Å resolution, an homodimer with 152 residues and one Cu and one Zn atom per active site by monomer (PDB entry 3MND) [23]. It possesses the classical motifs of Cu/Zn–SOD enzymes. All residues directly or indirectly involved in metal binding are completely conserved. Nevertheless an analysis comparing the amino acid sequence of *Ts*Cu/Zn–SOD with other SODs reported in databases, showed low global identity of 57.2, 57.9 and 59.6% with mammals such as *Sus scrofa* (pig), *Homo sapiens* (human) and *Bos taurus* (bovine), respectively, suggesting that differences in *Ts*Cu/Zn–SOD can be used to design specific inhibitors.

Materials and methods

Molecular modeling, electric partial-charge assignation, ligand conformer, searching of potential binding sites, energy minimizations, visualization and docking were performed with molecular operating environment (MOE) [24] package with default parameters, unless otherwise stated. Energy minimizations were carried out until an RMSD (root mean square deviation) force lower than 0.001 was obtained using CHARMM27, an all-atom force field parameterized for proteins, or MMFF94x, parameterized for small organic molecules in medicinal chemistry.

Generation of 3D conformers from LeadQuest® database

Exelgen LeadQuest® database [25] was used as the initial chemical space for this study. Each of the 51,068 compounds was prefiltered using Lipinski-like rules as follows: molecular weight <600, LogP <7, donors + acceptors <12, rotatable bonds <7, and transformed into 3D molecular structures using *Import_Database–MOE*. Then, we generated a chemically diverse 3D conformational database of drug-like molecules with *Conformer_Import–MOE*, using a cut-off conformational energy of 3 kcal/mol from the minimum energy structure of each compound, as calculated with the MMFF94x force field. The adopted procedure allowed the generation of a chemically diverse 3D conformational database of multiple conformers for each molecule, which was then used for docking. The X-ray structure of *Ts*Cu/Zn–SOD and human Cu/Zn–SOD (*Hs*Cu/Zn–SOD, PDB entry 2V0A) were used as protein targets for docking procedures.

Potential binding sites were identified with the *Site_Finder–MOE* and with CASTp server [26]. All crystallographic water molecules were removed from the protein structures before docking. Hydrogen atoms and partial charges were added to the enzyme using the CHARMM27 force field. Charge for Cu and Zn was set to 2^+. *Dock–MOE* studies used the alpha-site-triangle method [27] to bias the orientation search of the ligand to meaningful trials, and the docking score function named *Affinity dG* was used as implemented in MOE [28]. GW572016 (Lapatinib) is a tyrosine kinase inhibitor that is a potent dual inhibitor of epidermal growth factor receptor (EGFR, ErbB-1) and ErbB-2. X-ray structure of EGFR bound to GW572016 was well resolved and published [29]. That complex (PDB entry 1XKK) was used as a docking validation. Docking score found with MOE was −11.3, with a root mean square deviation of the pose from the original ligand of 1.93 Å.

Docking on *Tr*Cu/Zn–SOD X-ray structure

In a first screening, 15,000 orientations or poses on potential binding sites were proved and evaluated for each conformer from each compound in the 3D conformational database; the top ten scoring poses for each conformer were written out to a new database [30]. In a second step, conformers of compounds with good scores (docking scores <−7.5 units) were resubmitted for evaluation, but allowing in this case the search of 100,000 poses. Only those compounds for which the top scoring energies achieve values lower than −8.6 were selected for further analysis. Energy minimization of the best and/or the most frequently found docked poses for each compound was carried out to refine the orientation of the ligand in the receptor site, and to find the local energy minimum of the ligand–enzyme interactions. Three protocols were designed for optimizing the ligand–enzyme complexes. In method 1, the receptor was treated as a rigid structure and the ligand was allowed to relax into the active site. For method 2, residues of the active site (≤4.5 Å) and the inhibitor were allowed to relax while the rest of the receptor were fixed; 3. Finally, in method 3 all residues at 4.5 Å from the ligand were subjected to an energy minimization with the coordinates of the ligand fixed, then only the ligand was relaxed with the fixed new positions of the nearby residues; and finally new energy minimization of contact residues was carried out, again with the ligand fixed. This latter method was the most efficient in further lowering the ligand–enzyme energy interaction.

After visual inspection of the minimized protein–compound complex, a set of compounds were selected for in vitro testing of their inhibitory potency against pure recombinant *Tr*Cu/Zn–SOD and commercial *Ht*Cu/Zn–SOD (Sigma) on basis of several criteria: we searched for ligand binding contacts to non-conserved side chains of the enzyme, shape complementarily, docking score before minimizing energy of complex, predicted LogP less than 5.5, number of hydrogen bonds formed, among others (see Results and discussion for more details).

Compounds 1–6 were docked on *Ht*Cu/Zn–SOD X-ray structure with an extensive search of 100,000 poses of each conformer in order to determine their docking score and compare it with *Tr*Cu/Zn–SOD.

In order to compare docking scores from *Dock-MOE* for compounds 1–6, we carried out an extensive docking procedure using alternative software. The *AutoDock–Vina* (*Vina*) software [31] was used for flexible docking simulations. The compounds 1–6 were docked into binding site 1 on *Tr*Cu/Zn–SOD surface. Before docking, water molecules were removed from the X-ray structure. Polar hydrogens and Gasteiger charges were assigned using the *AutoDock–Tools* interface [32]. Then, the size of search spaces in each dimension (x, y and z) for site 1 was 26 × 26 × 30 Å^3 with center in −10.784, 0.686 and −31.058; for site 2, dimensions are 24 × 24 × 24 Å^3 with center in −13.799, −1.323 and −1.359. The other *Vina* default optimization parameters were maintained for docking simulation. Docking scores for the best poses for compounds 1–6 according to *Vina* shown in Table 5 in Supplementary Material.

*Tr*Cu/Zn–SOD enzyme inhibition assays

Recombinant *Tr*Cu/Zn–SOD enzyme was expressed and purified as described previously [20]. Enzyme inactivation was determined indirectly by measuring inhibition of cytochrome *c* reduction caused by $O_2^{\cdot-}$, which is produced by the xanthine–xanthine-oxidase system [33]. The reaction was carried out in a final volume of 1.0 mL in the presence of 10 units of recombinant enzyme (specific activity 2,940 units/mg, 3.5 μg enzymes) incubated for 30 min at 37 °C with 100 μM of the selected LeadQuest® compounds [20]. One unit of SOD is defined as the amount of enzyme that causes 50% inhibition of the reduction of cytochrome *c* with incubation times of 2 min [33]. Only compounds with inhibitory activity (more than 30%) against *Tr*Cu/Zn–SOD were incubated against *Ht*Cu/Zn–SOD (Sigma, specific activity 4,000 units/mg). For those compounds with a percentage of inhibition of *Tr*Cu/Zn–SOD greater than the threshold of 60%, a complete set of measurements was performed to determine the IC_{50} values.

The tested compounds were purchased from Exelgen Inc. (formerly LeadQuest®). Purity reported by the manufacturer was greater than 95% checked by LC/MS. Stock solutions (10 mM) of each compound were made in DMSO, with similar aliquots of the pure solvent in blank experiments.

Results and discussion

Conformer search

MOE is a drug discovery package [24] used to perform several tasks in this work. In order to simulate ligand flexibility in our docking studies, we generated a set of low-energy conformers for each of the about fifty thousand compounds of the LeadQuest® database as described in the Materials and methods section. A high-throughput fragment-based conformational search [24] allowed the transformation of the original 51,068 compounds library into a new database of about 2 million conformers with energies ≤3.0 kcal/mol respects to the lowest minimum conformation of each compound. In this sense, Perola and Charifson [34] found that a 3.0 kcal/mol energy cut-off would retain

about 80% (50%) of bioactive ligands with 1–3 (4–6) rotatable bonds. For computational convenience we used this same threshold and accordingly we expect our conformational ensembles to contain a significant number of biologically relevant conformations. This new *in*-house database was then used for docking studies against the X-ray structure of *Tc*Cu/Zn–SOD.

Molecular docking

Before starting our docking calculations we determined potential sites for ligand binding from the 3D atomic coordinates of the *Tc*Cu/Zn–SOD. Active sites are usually hydrophobic pockets that involve side chain atoms tightly packed [35]; thus we searched for these sites on the

Table 1 Structure and biological activity of LeadQuest® compounds identified by virtual screening procedure that showed in vitro inhibition activity for *Tc*Cu/Zn–SOD

Compound	Structure	Best score against *Tc*Cu/Zn–SOD (and against the human homologue)	Preferred binding site according to best scores	*Tc*Cu/Zn–SOD IC_{50} (μM)
1	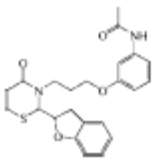	−8.6 (−5.5)	1	_*
2	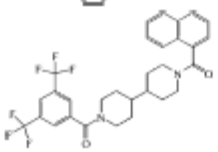	−8.7 (−6.0)	1, 2	23.9
3	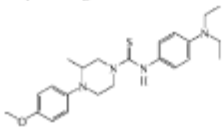	−8.8 (−6.1)	1	9.8
4	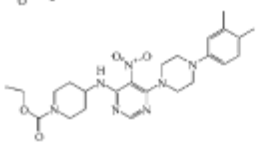	−9.0 (−6.0)	1	25.9
5	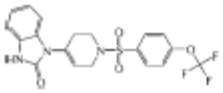	−9.0 (−6.3)	1, 2	_*
6	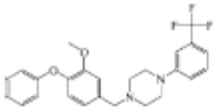	−8.7 (−5.9)	1, 2	_*

* IC_{50} values were only measured when the % inhibition was >60% at 100 μM of compound (see Materials and methods for more details)

molecule surface by filtering out sites with significant convex surfaces too exposed to solvent. The residues directly or indirectly involved in metal binding are conserved among the Cu/Zn–SODs from all species so far examined, from bacteria to mammals; therefore in order to attain species selectivity, the cavities from these sites were also discarded. On this basis, more than twenty potential sites were detected and distributed over the entire surface of the dimer, which were labeled as site 1, site 2, site 3, and so on (see Table 1 in Supplementary Material for the whole list and description). Sites 1 and 2 are the more prominent in size; they are located near the interface region and formed by atoms from 32 to 20 different residues, respectively, a reflection of their large site dimension. Site 1 and 2 are located in opposed parts of the dimer interface, so that potential binding sites are facing away from each other. Site 1 has an extended shape while site 2 is more compact one; both sites are rich in hydrophobic residues. Moreover, sites 1 and 2 are not strictly conserved between *Tr*Cu/Zn–SOD and *Hs*Cu/Zn–SOD sequences, which transform these sites in attractive targets for designing species-specific inhibitors. In contrast, the rest of the potential sites (3–22) are much smaller, exposed to solvent, and in many cases, well conserved respect to the human enzyme.

In a first stage, the previously generated conformers for each ligand were scanned against all sites on the *Tr*Cu/Zn–SOD surface, using 15,000 poses of probe for each conformer. We noticed that sites 1 and 2 always presented the highest docking scores while other sites always showed lower scores; therefore in the subsequent step, ligands with docking scores better than −7.5 (*c.a.* 500 different compounds) were re-scanned only on sites 1 and 2, but now with 100,000 poses of each conformer in order to include virtually all orientations for binding each of those compounds. This procedure yielded complexes with much better docking scores, those whose docking scores were better than −8.6 were then submitted to an energy minimization process in order to improve the interactions at the binding sites. This optimization process was carefully designed testing and evaluating different schemes of partial minimizations of the structure of the complexes (see Materials and methods for more details). We found a procedure aimed to find a better positioning of the ligands into the binding site, as judged from lowering the previously obtained ligand–enzyme energy interaction. This procedure consist in (1) first all residues at 4.5 Å from the ligand were subjected to an energy minimization with the coordinates of the ligand fixed, (2) then only the ligand was relaxed with the fixed new positions of the nearby residues, and finally (3) a new energy minimization of contact residues was carried out, again with the ligand fixed. This 3-step methodology optimized the protein–ligand contacts by allowing a better rearrangement of the side chains of the binding site and the position of the ligand as is reflected in the potential energy of the protein–ligand contacts (see Table 4 in Supplementary Material for more information).

Overall, the search for conformers and binding energy in three steps used in this work intended to include part of the conformational response of the enzyme due to the presence of the ligand in its binding site. From our results, a set of fifty compounds were selected to be tested in vitro against recombinant pure *Tr*Cu/Zn–SOD enzyme. The final compound selection which yielded the set of 50 compounds, included a final screening from the highest scored ligands identified by docking, it also included considerations of docking score, ligand–enzyme energy interaction, hydrophilicity, selectivity, molecular weight and robustness of prediction. Since it is our experience that hydrophobic compounds aggregate when dissolved from DMSO stock solution into aqueous inhibition tests, we privileged hydrophilicity in the final selection process. With respect to selectivity we gave preference to compounds forming contacts (e.g. hydrogen bonds) to non-conserved side chains of the receptor, to gain selective inhibition to

Fig. 1 *Tr*Cu/Zn–SOD and *Hs*Cu/Zn-SOD sequence alignment. Several (identity: 57.9%) residues are not conserved between sequences. Residues in contact (≤4.5 Å) with ligands 1–6 at site 1 on the *Tr*Cu/Zn–SOD surface are indicated by *circles*. *Black color* indicates that the ligand interacts with the residues in the chains A and B; *gray color* indicates that the ligand interacts with the residue only in one chain. Intrachain disulphide cysteine residues, conserved residues in the active site, and involved in Cu and Zn binding are in *bold letters*. *Lines* bellow the *circles* indicate the number of hydrogen bonds between ligand and residues, see Figure 1 in Supplementary Material for more details

parasitic SOD with respect to the human enzyme. In this respect, Fig. 1 shows *Ts*Cu/Zn–SOD and *Hs*Cu/Zn–SOD sequence alignment (identity: 57.9%). Residues in contact with ligands 1–6 at site 1 on the *Ts*Cu/Zn–SOD surface, according to our docking results, are indicated by circles: several residues present only in *Ts*Cu/Zn–SOD interact with 1–6 through hydrogen bonds. Finally, with robustness we mean the frequent finding of slightly different poses of the same compound with high scores, which means that small changes in orientation still yield a good predicted docking score. In addition, we also included ten compounds with medium and low docking score to use them as negative controls (structures, identifications and scores for all compounds used are depicted in Tables 2 and 3 in Supplementary Material). This includes compounds with low affinity for sites 1 and 2 and some of the best ligands for other binding sites. All candidate compounds were first evaluated for their ability to inhibit the activity of *Ts*Cu/Zn–SOD at 100 μM: six of the fifty tested compounds demonstrated >30% inhibition of the enzyme at μM concentrations. Table 1 and Fig. 2 show the structures of active compounds (1–6), and the residual activity of recombinant *Ts*Cu/Zn–SOD obtained after incubation with 100 μM of these compounds, respectively. Examination of these active compounds revealed a diversity of chemical structures, they have molecular weights between 430 and 560 Da, estimated LogP [36] lower than 5.5, no more than 10 H-bond acceptors and a low flexibility. A common structural feature present in compounds 3, 4 and 5 is a piperazine group. Three other chemical classes are constituted by sulfonamide, bipiperidinyl and acetanisidide derivatives. Clearly, their inhibitory capacity comes from their tight fitting to the binding site more than being variations or derivatives from a common structure. Six real in vitro hits out of fifty putative inhibitors represent an experimental-hit ratio of 12% [(6/50) × 100], which demonstrates the success of the virtual screening procedure. The rest of the tested compounds, including the negative controls, yielded very low or no inhibition and were considered as inactive. The aim of this work was to find agents that selectively inactivate *Ts*Cu/Zn–SOD. Therefore, in order to determine the docking scores of compounds 1–6 to *Hs*Cu/Zn–SOD we carried out an extensive docking procedure on the surface of this human enzyme. We found that the docking scores were always lower for the human enzyme than for the *T. solium* SOD, in good agreement with our experimental results: the best score occurs when compound 5 binds to site 2 with a docking score equal to −5.5.

Finally, we found that the *Vina* docking scores and poses for compounds 1–6 over site 1 on *Ts*Cu/Zn–SOD were in good agreement with *Dock–MOE* results (see Table 5 in Supplementary Material).

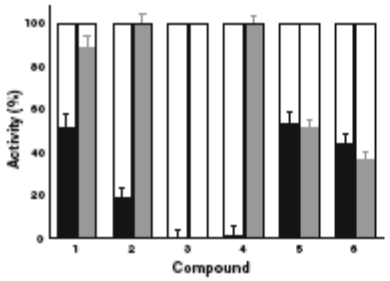

Fig. 2 Inhibition of *T. solium* and human Cu/Zn–SOD activity by incubation with active LeadQuest® compounds, determined by xantine–xantine-oxidase method. *T. solium* (*black bars*; 10 Units, 3.5 μg enzymes) and human Cu/Zn–SOD (*grey bars*; 10 Units) were incubated in presence of 100 μM for 30 min at 35 °C of compounds 1, 2, 3, 5 and 6, and 50 μM of compound 4. Effects of compound 3 on human enzyme could not be assayed because unexpected and systematic precipitation in the reaction medium was observed

Enzyme inhibition assay

Concentration of 100 μM of compound 2 diminished the *Ts*Cu/Zn–SOD activity in 73%; in contrast, the same concentration of this compound did not show any effect on *Hs*Cu/Zn–SOD activity. Compound 3 had an important impact on the *Ts*Cu/Zn–SOD activity, showing 100% inhibition. Unfortunately, effects on human enzyme could not be assayed because unexpected and systematic precipitation in the reaction medium was observed, hence the lacking bar for this assay in Fig. 2. However, the residual activity of *Hs*Cu/Zn–SOD and *Ts*Cu/Zn–SOD at 10 μM of the same compound are 92% and 52%, respectively. The most remarkable results were obtained with compound 4, which affected *Ts*Cu/Zn–SOD activity in 96% at 50 μM, whereas it had no detectable effect on human Cu/Zn–SOD at the same concentration. With respect to compounds 1, 5 and 6, they considerably affected the enzymatic activity of *Ts*Cu/Zn–SOD (49, 48 and 48% of inhibition, respectively) after incubation at 100 μM, but affecting the activity of human enzyme at similar levels; therefore, they can be considered as nonspecific inhibitors. The IC_{50} for compounds 2, 3 and 4, (23.9, 10.9 and 25.9 μM, respectively, Fig. 3) confirm that these compounds are good inhibitors, and the last two are also specific for the taenia enzyme. The inactivating effect of 2, 3 and 4 was concentration dependent. It is noted that the inactivating curves were sigmoidal.

The procedure and results presented here are outstanding due to the identification of novel lead compounds to

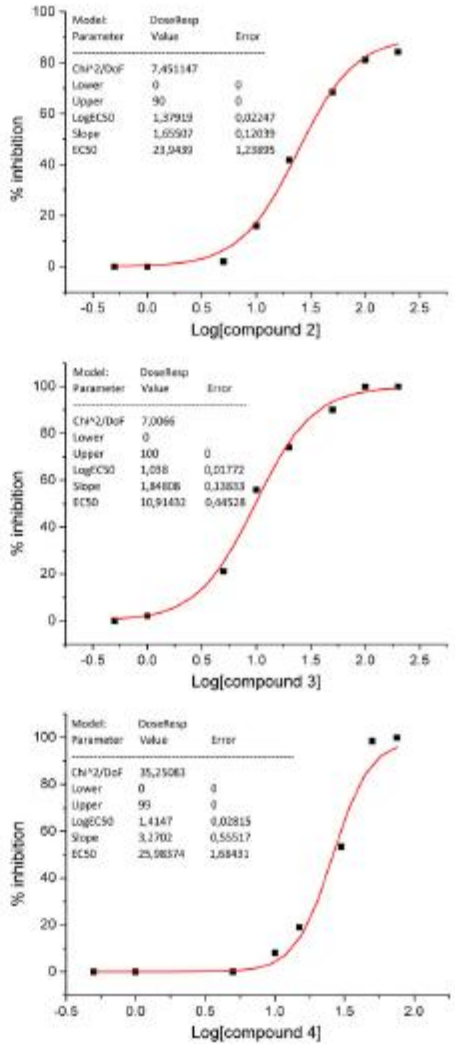

Fig. 3 Curves of inhibition versus inhibitor concentration for compounds 2, 3 and 4. See Materials and methods for more details

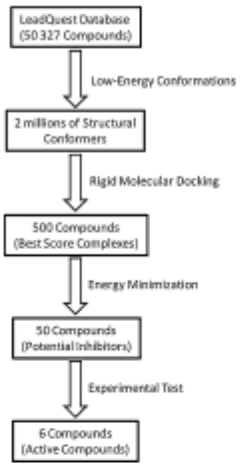

Fig. 4 Flow chart showing the search for lead compounds as inhibitors of *Ts*Cu/Zn–SOD activity by virtual screening followed by experimental assays. *Numbers* represent the amount of molecules selected after each stage

develop more powerful compounds in a future aimed to the design of specific drugs against parasites (Fig. 4).

According to our docking results, compounds 1–6 bind near the dimer interface (i.e. sites 1 and/or 2) where the interaction with various conserved and non-conserved residues is strong. For example, compound **4** presented the best inhibitory activity toward *Ts*Cu/Zn–SOD and did not inhibited *Hs*Cu/Zn–SOD at all. Interestingly, we found that all the docked complexes of this compound with docking scores below −7.5 could only be indentified at site 1 (Fig. 5). Compound **4**, docked in its most frequent pose on the *Ts*Cu/Zn–SOD surface, forms a hydrogen bond between the N atom of its pyrimidine ring and the hydroxyl oxygen of the non-conserved Ser*B*108 (Ser108, chain B). Another hydrogen bond was established between the CO group of the carboxylic ethyl ester moiety of the ligand and the NH group of Met*B*1, also a non-conserved residue. Furthermore, the high predicted stability of the complex resulted also from a good shape complementarity, and also from dipole–dipole and van der Waals interactions with nearby residues: the piperazine moiety is located near Met*A*1, Lys*A*2, Leu*A*103, Ser*A*108, Ile*A*110, and Ile*A*148, while the pyrimidine ring is surrounded by Leu*B*103, Thr*B*104 and Ile*B*110. Good binding poses for compounds 2, 5 and 6 (i.e. docking scores <−7.5) are identified indistinctly in both sites 1 and 2. Compounds **1** and **3** seem to bind exclusively to site 1 as previously described for compound **4**. In Fig. 1, the contact residues (lower than 4.5 Å) in binding site 1 for all active compounds are indicated, and the protein residues which form hydrogen bonds are highlighted. Selectivity might arise from different short and medium distance interactions. Some of the most relevant short-distance contacts include parasite residues: Thr104, and hydrogen bonding to Ser108, Met1, Lys150, Ser151. All these residues in taenia enzyme are different in the human orthologue. Figure 6 shown binding poses of compound 6 in sites 1 and 2 on the surface of *Ts*Cu/Zn–SOD enzyme after docking and the 3-step energy minimization protocol. Schemes of protein–ligand interactions are shown in Figure 1 in Supplementary Material.

It must be considered that docking scores are designed as a fast evaluation of multiple poses of every conformation analyzed from each potential ligand, to select the top scored compounds as an enriched subset of the chemolibrary, and not as an accurate predictor of binding affinity or biological activity. Albeit in some publications certain correlation between IC_{50} and docking scores can be found, it must be considered that for the above reason, a high correlation between docking score and IC_{50} must not be always expected [37].

We found in our case of study that although docking is sometimes seen as an automatic procedure, human intuition to get advantage of robustness and selectivity may still be a good ingredient during the analysis of docking results.

As far as we know, this is the first time that inhibitors have been proposed and tested for this enzyme; specifically, compounds 1–6 can be considered as novel inhibitors of *Ts*Cu/Zn–SOD and could constitute a set of starting points to design more powerful inhibitors opening a new way to tackle infections of *T. solium* and other parasites.

Many enzymes and proteins are regulated by their quaternary structure and/or by their association in homo and/or hetero-oligomer complexes. Thus, these protein–protein interactions can be good targets for blocking or modulating protein function therapeutically [38] Eukaryotic Cu/Zn–SOD has a stable β-barrel fold and a dimer assembly, shows diffusion-limited catalysis and electrostatic guidance of their free-radical substrate. Disruption of the quaternary structure appears to decrease the catalytic activity: Banci and coworkers [39, 40] have replaced two hydrophobic residues (Phe50 and Gly91) at the dimer interface of the human enzyme, producing a soluble monomer with a much lower activity (around 10%) than that of the native dimeric enzyme. Using X-ray diffraction [41] as well as NMR techniques [39], these authors observed changes in the conformation of the loop (residues 120–139) responsible for generating the electrostatic potential for driving superoxide anions to the metallic ions

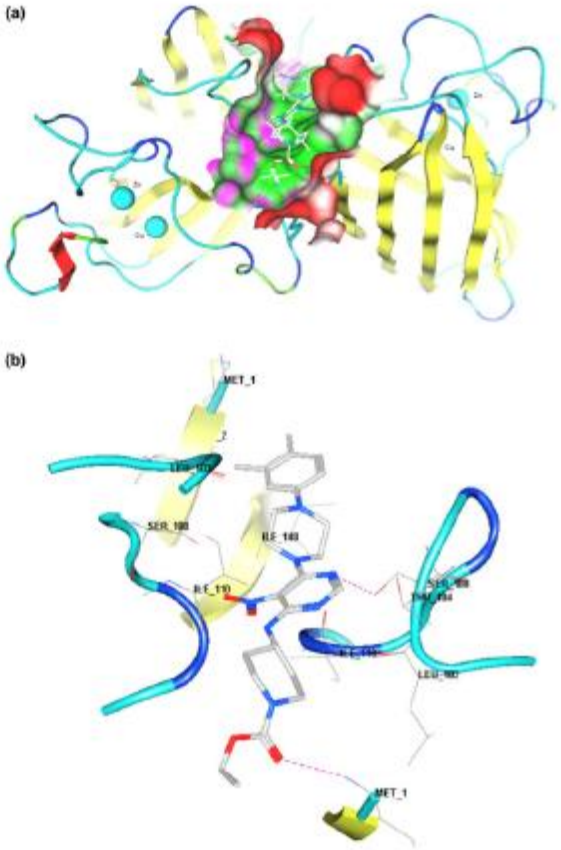

Fig. 5 a Binding pose of compound 4 in the *Tc*Cu/Zn–SOD binding site 1 after docking and the 3-step energy minimization procedure. b Network of hydrogen bonds (*red dashed lines*) between 4 and the amino acids in the *Tc*Cu/Zn–SOD binding site 1. See description in the text

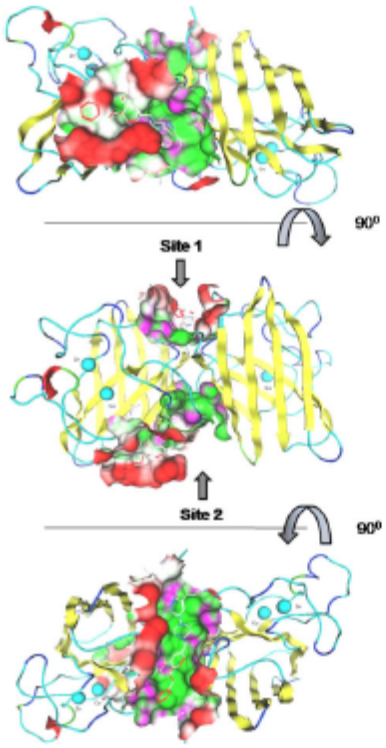

Fig. 6 Binding poses of compound 6 in sites 1 and 2 on the surface of *Tc*Cu/Zn–SOD enzyme after docking and the 3-step energy minimization procedure

at the active site. Also the backbone mobility of the monomeric state was investigated with molecular-dynamics simulations and compared to that of the dimeric species and it was concluded that, as far as motions in the picoseconds to nanoseconds timescale are concerned, the region consisting of residues 131–142 is less mobile in the monomeric mutant than in the dimeric wild-type protein. Structural fluctuations in this region have been suggested to play a role in assisting the superoxide anion in sliding towards the active site [42, 43].

On these bases, we suggest that compounds 1–6 affect the enzyme activity either by disrupting the monomer–monomer interface or by restricting the movements of the loops at each monomer, thus limiting the diffusion of the substrate to the reaction site.

Further studies are being carried out in order to establish the molecular mechanism of the inhibitory action of these compounds.

Conclusion

In summary, six new inhibitors of the *Tc*Cu/Zn–SOD enzymatic activity have been discovered using a methodology developed here which consisted in generating a conformational database from the LeadQuest® database, docking procedures, species selectivity filtering, and finally a proposal of subsequent ligand optimization based on three energy minimization steps over the best protein–ligand complex scores. Three of these compounds showed excellent selectivity to *Tc*Cu/Zn–SOD since they affect the activity of this enzyme at μM range but did not show inhibition against *Hs*Cu/Zn–SOD. Results obtained here are very promising, and now further studies are being carried out to determine the mechanism involved in the inactivation observed against *Tc*Cu/Zn–SOD and *Hs*Cu/Zn–SOD for compounds 1–6.

Acknowledgements This work was partially suported by Consejo Nacional de Ciencia y Tecnología-México (CONACyT, 105532, 80134-M, ECOS M05-901) and the Dirección General de Asuntos del Personal Académico (DEGAPA, IN 207507-3). P.G.-G. and R.P.-U. also thank CONACyT for graduate studies grants.

References

1. Del Brutto OH, Sotelo J, Roman GC (1998) Neurocysticercosis: a clinical handbook. Swets and Zeitlinger Publisher, Lisse, pp 216–222
2. García HH, González AE, Evans CA, Gilman RH (2003) *Taenia solium* cysticercosis. Lancet 362:547–556
3. Wallin MT, Kurtzke JF (2004) Neurocysticercosis in the United States. Review of an important emerging infection. Neurology 63:1559–1564
4. Bern C, García HH, Evans C, González AE, Verastegui M, Tsang VC, Gilman RH (1999) Magnitude of the disease burden from neurocysticercosis in a developing country. Clin Infect Dis 29:1203–1209
5. Carpio A, Escobar A, Hauser WA (1998) Cysticercosis and epilepsy: a critical review. Epilepsia 39:1025–1040
6. Mafojane NA, Appleton CC, Krecek RC, Michael LM, Willingham AL (2003) The current status of neurocysticercosis in Eastern and Southern Africa. Acta Trop 87:25–33
7. Takayanagui OM, Jardim E (1992) Therapy for neurocysticercosis: comparison between albendazole and praziquantel. Arch Neurol 49:290–294
8. Chang MS, Hawkins CP, Cook GC, Hawkes CH, Kozen RS (1991) A resistant case of neurocysticercosis. Postgrad Med J 67:573–578

9. Köhler P (2001) The biochemical basis of anthelminthic action and resistance. Int J Parasitol 31:336–345
10. Stepek G, Behnke JM, Buttle DJ, Duce IR (2004) Natural plant cysteine proteinases as anthelmintics? Trends Parasitol 20:323–327
11. Fridovich I (1998) Oxygen toxicity: a radical explanation. J Exp Biol 201:1203–1209
12. Vaca-Paniagua F, Torres-Rivera A, Unda-Parra R, Landa A (2008) Taenia solium: Antioxidant metabolism enzymes as target for cestocidal drugs and vaccines. Curr Top Med Chem 8:393–399
13. Birnboim HC, Kanabus-Kaminska M (1985) The production of DNA strands breaks in human leukocytes by superoxide anion may involve a metabolic process. Proc Natl Acad Sci USA 82:6820–6824
14. Henkle-Dührsen K, Kampkötter A (2001) Antioxidant enzyme families in parasitic nematodes. Mol Biochem Parasitol 114:129–142
15. Loverde PT (1998) Do antioxidants play a role in schistosoma host parasite interactions? Parasitol Today 4:284–289
16. Monroy-Ostria A, Monroy-Ostria TJ, Gómez G, Hernández MO (1993) Some studies on experimental infection of golden hamsters with *Taenia solium*. Rev Lat Microbiol 35:91–98
17. Sánchez-Moreno M, León P, Salas-Peregrin JM, Osuna A (1988) Superoxide dismutase in trematodes. Arzneimittelforschung 37:903–905
18. Sánchez-Moreno M, García-Ruiz A, García-Rejón L, Valero A, León P (1989) Superoxide dismutase in cestodes. Isoenzymatic characterization and studies of inhibition by series of benzimidazoles and by pyrimidine derivates of recent synthesis. Drug Res 39:759–761
19. Sánchez-Moreno M, Entrala E, Janssen D, Fernández-Becerra C, Salas-Peregrin JM, Osuna A (1996) Inhibition of superoxide dismutase from *Ascaris suum* by benzimidazols and synthesized pyrimidine and glycine derivatives. Pharmacology 52:61–68
20. Castellanos-González A, Jiménez L, Landa A (2002) Cloning, production and characterization of a recombinant Cu/Zn superoxide dismutase from *Taenia solium*. Int J Parasitol 81:541–546
21. Sanz AM, Gómez-Contreras F, Navarro P, Sánchez-Moreno M, Boutaleb-Charki S, Campuzano J, Pardo M, Osuna A, Cano C, Yunta MJR, Campayo L (2008) Efficient inhibition of iron superoxide dismutase and of growth *Trypanosoma cruzi* by benzo[g]phthalazine derivatives functionalized with one or two imidazole rings. J Med Chem 51:1962–1966
22. Temperton NJ, Wilkinson SR, Meyer DJ, Kelly JM (1998) Overexpression of superoxide dismutase in *T. cruzi* results in increased sensitivity to the trypanocidal agents gentian violet and benznidazole. Mol Biochem Parasitol 96:167–176
23. Hernández-Santoyo A, Landa A, González-Mondragón E, Pedraza-Escalona M, Parra-Unda R, Rodríguez-Romero A (2011) Crystal structure of Cu/Zn superoxide dismutase from *Taenia solium* reveals metal-mediated self-assembly. FEBS J (In press)
24. Molecular Operating Environment (MOE). Chemical Computing Group, Inc. CCG, Montreal, Canada. http://www.chemcomp.com. Versions 2005.06 and 2007.09
25. LeadQuest® Compound Library, April 2006, Exelgen, Inc. 1699 South Hanley Road, St. Louis, MO 63144 USA
26. Liang J, Edelsbrunner H, Woodward C (1998) Anatomy of protein pockets and cavities: Measurement of binding site geometry and implications for ligand design. Protein Sci 7:1884–1897
27. Edelsbrunner H Weighted Alpha Shapes. Department of Computer Science, University of Illinois at Urbana-Champaign, Urbana, Illinois 61810
28. This function estimates the enthalpic contribution to the free energy of binding using a linear function: $G = C_{hb}f_{hb} + C_{mc}f_{mc} + C_{metal}f_{metal} + C_{rb}f_{rb} + C_{hp}f_{hp} + C_{aa}f_{aa}$ where the f terms fractionally count atomic contacts of specific types and the Cs are coefficients that weight the term contributions to estimate the docking score
29. Wood ER, Truesdale AT, McDonald OB, Yuan D, Hassell A, Dickerson SH, Ellis B, Pennisi C, Horne E, Lackey K, Alligood KJ, Rusnak DW, Gilmer TM, Shewchuk L (2004) A unique structure for epidermal growth factor receptor bound to GW572016 (Lapatinib): relationships among protein conformation, inhibitor off-rate, and receptor activity in tumor cells. Cancer Res 64:6652–6659
30. Kuntz ID (1993) Structure–base strategies for drug design and discovery. Science 33:107–115
31. Trott O, Olson AJ (2010) AutoDock Vina: improving the speed and accuracy of docking with a new scoring function, efficient optimization, and multithreading. J Comput Chem 31:455–461
32. Sanner MF (1999) Python: a programming language for software integration and development. J Mol Graph Model 17:57–61
33. McCord JM, Fridovich I (1969) Superoxide dismutase. An enzymic function for erythrocuprein (hemocuprein). J Biol Chem 244:6049–6055
34. Perola E, Charifson P (2004) Conformational analysis of drug-like molecules bound to proteins: An extensive study of ligand reorganization upon binding. J Med Chem 47:2499–2510
35. Laurie ATR, Jackson RM (2006) Methods for the prediction of protein–ligand binding sites for structure-based drug design and virtual ligand screening. Curr Protein Pept Sci 7:395–406
36. Molinspiration Property Calculation Service. http://www.molinspiration.com
37. Park MS, Dessal AL, Smrcka AV, Stern HA (2009) Evaluating docking methods for prediction of binding affinities of small molecules to the G protein beta-gamma subunits. J Chem Inf Model 49:437–443
38. Cardinale D, Salo-Ahen OMH, Ferrari S, Ponterini G, Cruciani G, Carosati E, Tochowicz AM, Mangani S, Wade RC, Costi MP (2010) Homodimeric enzymes as drug targets. Curr Med Chem 17:826–846
39. Banci L, Benedetto I, Bertini R, Del Conte M, Piccioli M, Viezzoli MS (1998) Solution structure of reduced monomeric Q133M2 copper, zinc superoxide dismutase. Why is SOD a dimeric enzyme? Biochemistry 37:11780–11791
40. Banci L, Bertini I, Del Conte R, Mangani S, Viezzoli MS, Fadin R (1999) The solution structure of a monomeric reduced form of human copper, zinc superoxide dismutase bearing the same charge as the native protein. J Biol Inorg Chem 4:795–803
41. Ferraroni M, Rypniewski W, Wilson KS, Viezzoli MS, Banci L, Bertini I, Mangani S (1999) The crystal structure of the monomeric human SOD mutant F50/G51E/E133Q at atomic resolution. The enzyme mechanism revisited. J Mol Biol 288:413–426
42. Luty BA, El Amrani S, McCammon JA (1993) Simulation of the bimolecular reaction between superoxide and superoxide dismutase: synthesis of the encounter and reaction steps. J Am Chem Soc 115:11874–11877
43. Banci L, Bertini I, Cramaro F, Del Conte R, Rosato A, Viezzoli MS (2000) Backbone dynamics of human Cu, Zn superoxide dismutase and of its monomeric F50/EG51E/E133Q mutant: The influence of dimerization on mobility and function. Biochemistry 39:9108–9118